Photochemistry of Metal–Metal Bonds

THOMAS J. MEYER* and JONATHAN V. CASPAR

Department of Chemistry, The University of North Carolina, Chapel Hill, North Carolina 27514

Contents

I. Introduction

There is an extensive photochemistry of organometallic compounds.[1] In fact, preparative-scale photolyses have proven to be a most valuable synthetic technique in organometallic chemistry. However, one unfortunate characteristic of much of organometallic photochemistry is a relative absence of detailed mechanistic information. Without such information the systematic and rationally planned use of photochemical

Professor Thomas J. Meyer is M. A. Smith Professor of Chemistry at the University of North Carolina at Chapel Hill. He was born in 1941 and received his B.S. degree from Ohio University in 1963, and the Ph.D. from Stanford University in 1966, the latter under the direction of Professor Henry Taube. In 1967 he was a NATO Postdoctoral Fellow at University College, London where he worked with the late Professor Sir R. S. Nyholm. The research interests of Professor Meyer's research group include photochemistry, oxidation–reduction reactions, redox catalysis, and thermal and photochemical redox processes of metallopolymers and metallopolymeric films.

Jon Caspar was born in Boulder, CO in 1957, obtained his B.S. degree from the Massachusetts Institute of Technology in 1978, and his Ph.D. degree in Chemistry from the University of North Carolina at Chapel Hill in 1982. After postdoctoral studies at the California Institute of Technology he joined the Central Research and Development Department of E. I. du Pont de Nemours and Company as a Research Chemist. His research interests include inorganic and organometallic photochemistry, photophysics, spectroscopy, and theoretical and experimental aspects of electron-transfer reactions.

techniques and the exploitation of photochemical intermediates are left largely to chance.

One exception is the photochemistry of carbonyl-containing metal–metal bonded dimers. In this area sufficient mechanistic information is available that an overall pattern of photoreactivity can be perceived which depends in a systematic way upon such factors
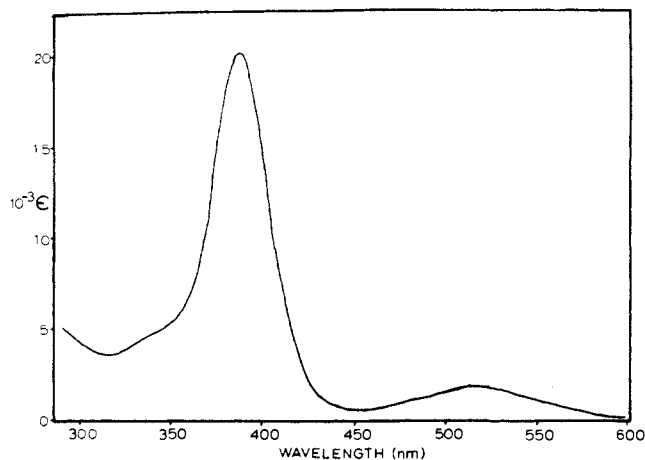
Figure 1. Electronic absorption spectrum of $(\eta^5\text{-}C_5H_5)_2Mo_2(CO)_6$ in cyclohexane.

as electronic and molecular structure. In compounds containing metal–metal bonds, spectroscopic properties are often dominated by electronic transitions localized on the metal–metal bond and the metal–metal bond is usually the site of chemical reactivity in either thermal or photochemical reactions.[1-4]

The impetus here is to review in a critical way the results of mechanistic studies on the photochemistry of compounds containing metal to metal single bonds. In coverage, the content will be restricted to those cases where detailed mechanistic information is available. The results should be of interest both to organometallic chemists and to photochemists, the latter because of the fascinating and diverse photochemical properties that the molecules display.

In Figure 1 is shown the electronic absorption spectrum of the dimer $(\eta^5\text{-}C_5H_5)_2Mo_2(CO)_6$ which contains a Mo–Mo bond. The spectrum of a compound is obviously a key to its photochemistry, if nothing else it dictates appropriate wavelengths to be used for photolysis. However, an additional point arises from the spectrum. Three different features can be clearly discerned—a relatively low-intensity, low-energy band; a well-resolved band at higher energy; and an even higher energy component that appears as a shoulder on the intense band. As noted later, the intense UV band can probably be assigned to a $\sigma \to \sigma^*$ transition localized at the metal–metal bond.[5] However the appearance of the additional bands shows that other excited states are accessible by photolysis. The different bands may have distinctly different electronic origins, and consequently lead to entirely different photochemistries.

In addition, there may be other excited states which are not observable spectroscopically but which play a critical role in the observed photochemistry. Examples could include the "triplet" state analogues of initially populated "singlet" states. Optical absorption by a diamagnetic "singlet" ground state is normally dominated by transitions to states of the same spin multiplicity. However, corresponding "triplet" states having the same electronic configurations lie lower in energy. If the triplet states are populated by singlet → triplet conversion following the initial excitation, they can be the origin of an observed photochemical reaction.

The use of spin-multiplicity terms like "singlet" or "triplet" for excited states having significant transition-metal d character or heavy-atom character in

general is not strictly appropriate because of spin-orbit coupling. The effect of spin-orbit coupling is to mix together the spin character of excited singlet and triplet states. One consequence of such mixing is that optical transitions from a singlet ground state to excited "triplet" states can appear in the absorption spectrum although usually with relatively low intensities.

In addition to triplet states, there may be other excited states for which ground- to excited-state absorption is relatively weak and absorption bands hidden (e.g., dd states) because the magnitudes of the transition moments connecting the ground and excited states are small. In general, any such state can contribute to the observed photochemistry if it is populated from upper excited states following the initial photolysis event.

The photochemistry of a molecule is usually dominated by the lowest lying excited state or states and yet the order in which the absorption bands appear in the absorption spectrum is not always a guaranteed indication of which state lies lowest. Changes in electronic structure between ground and excited states can lead to significant changes in *molecular* structure in an excited state when it reaches thermal equilibrium with its surroundings. An example occurs for dd excited states arising from excitation of an electron from the configuration $(d\pi)^6$ (t_{2g}^6 in O_h symmetry) to $(d\pi)^5(d\sigma^*)$ ($t_{2g}^5 e_g^1$). Excitation of a $d\pi$ electron to an antibonding $d\sigma^*$ level leads to a significant increase in the average metal–ligand bond lengths in the excited state.[6] Transitions to such states may appear at relatively high energies in the absorption spectrum but they can still dominate the observed photochemistry. This fact is a consequence of the Franck–Condon Principle and the fact that light absorption leads to changes in electronic configurations at fixed nuclear coordinates. The optical excitation act gives excited states having the equilibrium intramolecular structure and surrounding orientation of solvent dipoles associated with the electronic configuration of the ground state. It necessarily follows that those excited states which are the most *highly distorted* in the absorption spectrum are also the states which are the most *highly stabilized* following vibrational deactivation and equilibration with the surrounding medium. If sufficient in magnitude, the order of excited states following thermal equilibration may change from the order that appears in the absorption spectrum.

The electronic structures of transition-metal complexes are complex. Excited states can exist whose origins are ligand localized (e.g., $\pi\pi^*$), metal localized (dd), metal to ligand charge transfer (MLCT), or ligand to metal charge transfer (LMCT), or which involve more than one metal center as in the $\sigma \to \sigma^*$ transition associated with a metal–metal bond. Consequently, it should not be surprising if more than one primary photoproduct appears following photolysis or that more than one excited state is involved in the overall photochemistry. In addition, the primary photochemical event or events may produce reactive intermediates which *themselves* undergo subsequent thermal or photochemical reactions. In such cases, the underlying pattern of *initial* photochemical events may become obscured.

Although the list of potential complications cited above is long, it is also relevant. In fact, there is experimental or theoretical evidence available that sug-

TABLE I. Approximate Minimum Time Scales for Various Monitoring Techniques

technique	time scale, s
picosecond spectroscopy	10^{-12}
laser flash photolysis	10^{-9}
conventional flash photolysis (flash lamp)	10^{-6}
conventional spectroscopic monitoring of products	1

gests that many of the entries on the list actually do appear in the photochemistry of metal–metal bonds. They will make an appearance as the story unfolds.

II. Experimental Considerations
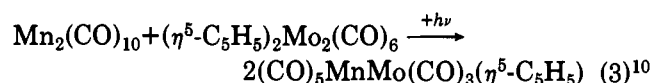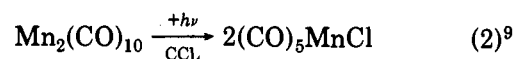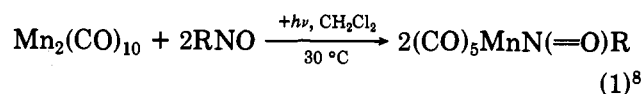
A. Time Scale

In assessing the results of photochemical mechanistic studies it is important to keep in mind the differences in time scales involved for various monitoring techniques in order to avoid the dilemma posed by the fable of the blind men and the elephant. The minimum time scales for different monitoring techniques are summarized in Table I. The time scale for optical excitation is 10^{-15} s. That means that the difference in time for a reacting photochemical system between the instant of excitation and the time needed for the slowest monitoring technique is equivalent to many centuries in the life of the evolving photochemical event. Between the times for excitation and observation a number of following events could have appeared and ended including the appearance and subsequent reactions of a series of secondary intermediates. As a consequence, it is necessary to make observations *throughout the entire time domain* between the excitation act and the appearance of the final products if a photochemical mechanism is to be completely defined. To put the time scales in Table I into a different perspective, the optical excitation act occurs in approximately 10^{-15} s, reorientation of solvent dipoles to an arrangement appropriate to the new electronic distribution of the excited state occurs in 10^{-11}–10^{-13} s, stable, unreactive "singlet" excited states may have lifetimes in the range of 10^{-8}–10^{-10} s, and stable, unreactive "triplet" states may last from 10^{-3} to 10^{-6} s, or even longer for organic excited states.

B. Techniques

The results of a variety of experimental techniques have been applied to the determination of mechanism in the photochemistry of metal–metal bonds.
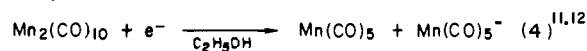
1. Product Studies

In many cases the photochemical products are suggestive of at least some of the features of the photochemical mechanism. Examples are shown in reactions 1–3 in which the products that appear in the presence of radical traps or halocarbon solvents or the observation of interchange products all suggest the appearance of monomeric fragments (e.g., $Mn(CO)_5$) as photochemical intermediates.

$$Mn_2(CO)_{10} + 2RNO \xrightarrow[30\,°C]{+h\nu,\ CH_2Cl_2} 2(CO)_5MnN(=O)R$$

$$(1)^8$$

$$Mn_2(CO)_{10} \xrightarrow[CCl_4]{+h\nu} 2(CO)_5MnCl \qquad (2)^9$$

$$Mn_2(CO)_{10}+(\eta^5\text{-}C_5H_5)_2Mo_2(CO)_6 \xrightarrow{+h\nu}$$
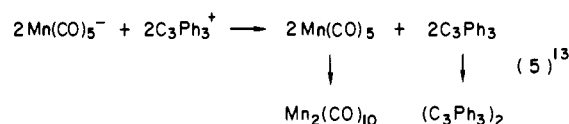$$2(CO)_5MnMo(CO)_3(\eta^5\text{-}C_5H_5) \quad (3)^{10}$$

In some cases, independent nonphotochemical routes have been devised which yield the same intermediates. Examples are shown in eq 4 and 5.

pulse radiolysis

$$Mn_2(CO)_{10} + e^- \xrightarrow{C_2H_5OH} Mn(CO)_5 + Mn(CO)_5^- \quad (4)^{11,12}$$

chemical redox

$$2Mn(CO)_5^- + 2C_3Ph_3^+ \longrightarrow 2Mn(CO)_5 + 2C_3Ph_3$$
$$\downarrow \qquad\qquad \downarrow \qquad (5)^{13}$$
$$Mn_2(CO)_{10} \qquad (C_3Ph_3)_2$$

Obviously, it is appealing to derive mechanistic arguments from the nature of photoproducts which can be isolated and characterized. However, because of the long time span between the initiation of a photochemical event and the appearance of a photoproduct, there is no guarantee that the nature of the final products constitutes a valid picture of the total sequence of events which constitute the photochemical mechanism. The dangers involved in such reasoning will become apparent in later sections. In particular, it is common knowledge that the photochemistry of metal–metal bonds consists of homolysis, e.g.

$$Mn_2(CO)_{12} \xrightarrow{+h\nu} 2Mn(CO)_5$$
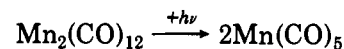
followed by subsequent thermal reactions of the photoproduced monomers.[1] In fact, the creation and subsequent reactions of reactive monomers represent only a part of a sometimes complex photochemical melange. *Under some conditions the monomers appear to play no role in the net photochemistry.*

2. Transient Spectroscopic Techniques

The problems associated with time scale can be addressed by using transient spectroscopic techniques. The techniques utilize excitation by short-lived light pulses and monitor the following sequence of events using UV–visible spectroscopy, and more recently, infrared spectroscopy.

If the systems under study are photochromic, that is if there is no net photochemical change as a consequence of the photolysis, such techniques can provide two results of value. The first is that the kinetic order of a transient event following photolysis can be established. The order of a reaction can be revealing as to the nature of intermediates produced in the photolysis. As examples, consider the generalized cases in eq 6 and 7 where photolysis of the metal–metal bond leads either to an intermediate which returns to the starting dimer by first-order kinetics as in eq 6 or to an intermediate which returns to the starting dimer via second-order, equal-concentration kinetics as in eq 7.

$$M–M \xrightarrow{+h\nu} I \xrightarrow{k} M–M \qquad (6)$$

$$-d[I]/dt = k[I]$$

$$\ln([I]_0/[I]_t) = kt$$

$$\ln (A_0 - A_t) = kt + \ln (A_\infty - A_0)$$

$$M{-}M \xrightarrow{+h\nu} 2M \xrightarrow{k} M{-}M \qquad (7)$$
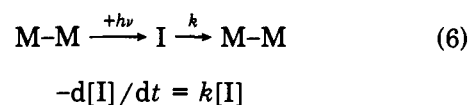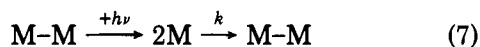
$$-\tfrac{1}{2}(d[M]/dt) = k[M]^2$$

$$(1/[M]_t) - (1/[M]_0) = 2kt$$

$$(1/(A_t - A_\infty)) =$$
$$[2kt/(\epsilon_M + \tfrac{1}{2}\epsilon_{M_2})b + (1/(\epsilon_M + \tfrac{1}{2}\epsilon_{M_2})bA_0]$$

In eq 6 and 7 are given not only the kinetic schemes for each case but also the differential equations which describe the kinetic behavior of the postphotolysis transients, the integrated forms of the differential equations and the integrated forms written in terms of the spectroscopically observable quantities, the absorbance at time t, A_t, the absorbance at time infinity, A_∞, and the absorbance at $t = 0$, A_0. Note that for the case of a bimolecular recombination to form the metal–metal bond (eq 7), the extinction coefficients for the transient intermediate (ϵ_M) and for the metal–metal bond (ϵ_{M_2}) must be known in order to obtain a numerical value for the rate constant. However, for either the first- or second-order cases a simple demonstration of the kinetic order of a transient decay can be revealing as to the details of a photochemical mechanism. An example of second-order kinetics is shown in Figure 2 for transient events that occur following laser or conventional flash photolysis of solutions containing $Mn_2(CO)_{10}$ in cyclohexane.[14,15] In this case the flash-photolysis experiment provides direct evidence for the existence of *both* short- and long-lived transients. As shown in Figure 2, but only for the short-lived transient, both intermediates return to the starting dimer by second-order, equal-concentration kinetics.

The other information of value that can be derived from transient techniques are difference spectra for photointermediates. Difference spectra are obtained by measuring transient absorbance changes at a series of wavelengths at a fixed time. They give spectral differences between the starting dimer and the intermediate and can reveal information concerning the electronic structure of the intermediate. In Figure 3 are shown difference spectra at three different time intervals following flash photolysis of $Mn_2(CO)_{10}$. At the shortest time scale there is clear evidence for the appearance of two transient intermediates, one of which absorbs at approximately 800 nm and the other at approximately 500 nm. The absorbance features observed in the difference spectrum amount to an enhanced absorbance for the intermediates since the difference taken is between the transients after photolysis ($A_t(\lambda)$) and the final solution when the system has returned to the starting dimer ($A_\infty(\lambda)$). When difference spectra are taken as a function of time, it is possible to obtain clear evidence for two distinct intermediates. After 200 μs both intermediates are seen. However, after 50 μs the intermediate absorbing at 800 nm has disappeared leaving only the intermediate which absorbs at ~500 nm. After ~1 s the second intermediate has disappeared as well and only the starting dimer is present in solution.
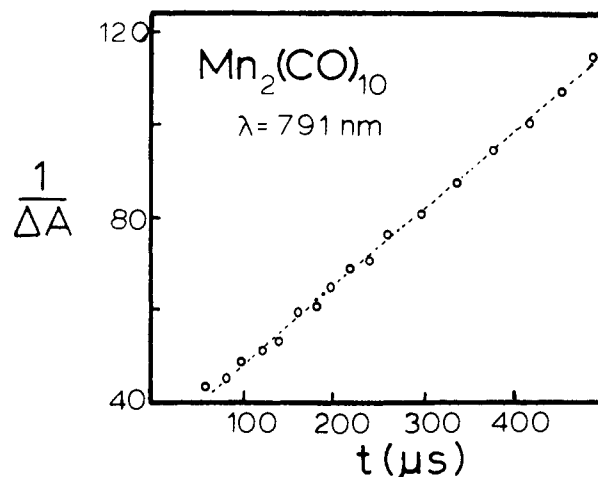
Figure 2. Kinetic plot illustrating the application of eq 7 to the short-lived intermediate following photolysis of $Mn_2(CO)_{10}$ in cyclohexane. $\Delta A = A_0 - A_t$; there is an absorbance *decrease* at 791 nm since the intermediate absorbs and $Mn_2(CO)_{10}$ is transparent.
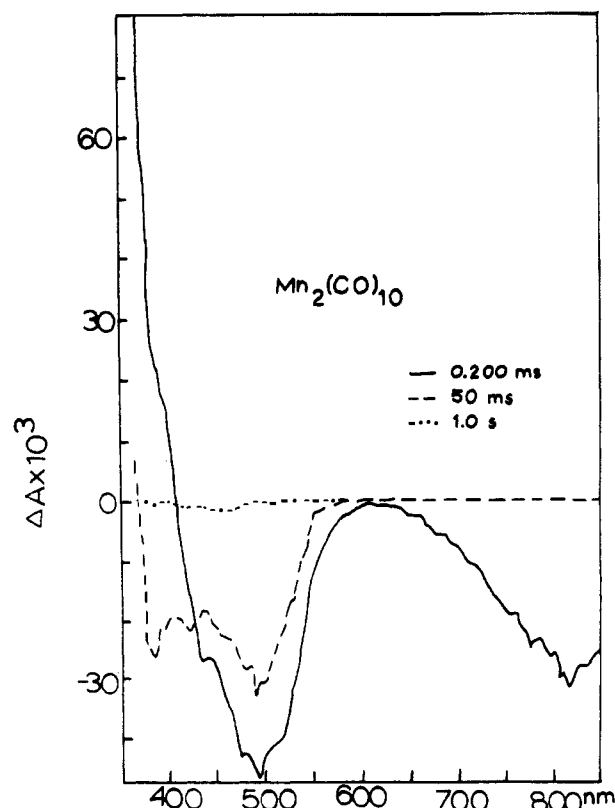
Figure 3. Difference spectra, $A_t(\lambda) - A_\infty(\lambda) = \Delta A$, following conventional flash photolysis of $Mn_2(CO)_{10}$ in cyclohexane.

It is possible to illustrate the power of the transient techniques by combining the result described above for $Mn_2(CO)_{10}$ obtained by conventional or laser flash photolysis with results obtained by picosecond spectroscopy.[16] In the picosecond experiment it was possible to photolyze and monitor the results of the photolysis over the time range 25–250 ns. The observations made are qualitatively the same as those described in Figure 3 in terms of the absorbance characteristics of the two intermediates. This is an important observation since the time scale for the experiment is near that for vibrational relaxation. This means that operationally, the intermediates observed are primary photoproducts and

not secondary intermediates that arise from thermal steps past the initial photolysis. The results of the conventional flash-photolysis experiment show that the primary photoproducts persist unaffected through a time period extending into the microsecond time range at which point they begin the reaction chemistry required to return to the dimer. The combination of the two techniques allows the photochemical reactivity of the system to be traced through the complete time domain necessary to describe the photochemical mechanism in detail.

Transient techniques have their limitations. One is time scale. If only conventional flash photolysis is used, there is no guarantee that an observation made after a microsecond is made on a primary photoproduct. The primary photoproduct could have undergone a thermal reaction to give a secondary intermediate. A second limitation is the lack of easily decipherable information about molecular structure if only electronic spectroscopic monitoring is used. In the past, the difficulty in applying more structure-sensitive techniques like IR or NMR to photochemical transients is that the time response of the detectors has been too slow. However, very recently, fast transient technique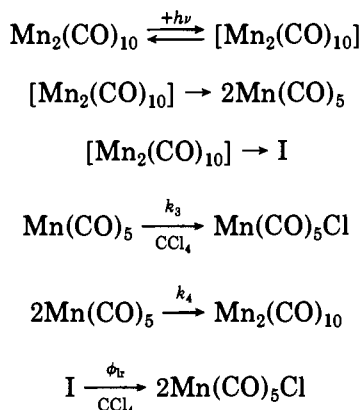s have been extended into the $\nu(CO)$ infrared region using IR-sensitive semiconductor detection[17a,b] and, hopefully, in the future it will be possible to apply techniques such as transient resonance Raman spectroscopy to these problems as well.[17c,d]

3. Kinetic Analysis

Standard techniques of kinetic analysis have been applied to the photochemistry of metal–metal bonds.[18,19] For example, Fox and Poë have proposed the mechanism shown in Scheme I for the photochemical reaction between $Mn_2(CO)_{10}$ and CCl_4 in cyclohexane as solvent.

SCHEME I

$$Mn_2(CO)_{10} \underset{}{\overset{+h\nu}{\rightleftharpoons}} [Mn_2(CO)_{10}]$$

$$[Mn_2(CO)_{10}] \rightarrow 2Mn(CO)_5$$

$$[Mn_2(CO)_{10}] \rightarrow I$$

$$Mn(CO)_5 \xrightarrow[CCl_4]{k_3} Mn(CO)_5Cl$$

$$2Mn(CO)_5 \xrightarrow{k_4} Mn_2(CO)_{10}$$

$$I \xrightarrow[CCl_4]{\phi_{lr}} 2Mn(CO)_5Cl$$

In the scheme it is suggested that there are two photochemical intermediates both of which react with CCl_4. Eq 8 relates the quantum yield for disappearance of $Mn_2(CO)_{10}$ to the concentration of CCl_4 and the incident light intensity, I_a, both of which are experimentally testable variables. ϕ_{lr} is the limiting quantum yield

$$\phi_{obsd} = \phi_{lr} - 4(k_4/k_3{}^2)(\phi_{obsd} - \phi_{lnr})^2 I_a/[CCl_4]^2 + \phi_{lnr} \tag{8}$$

when recombination of $Mn(CO)_5$ is negligible and ϕ_{lnr} the quantum yield for background loss of the second intermediate in the absence of CCl_4. As with any ki-
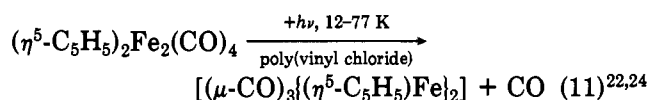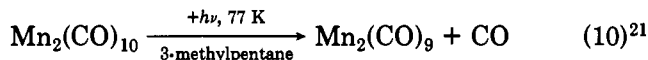
netic analysis, agreement between predictions based on an assumed mechanism and the experimental results does not represent a completely founded proof of the mechanism. However, when combined with transient photolysis techniques, the value of such experiments can be considerable.

4. Photolysis in Low-Temperature Matrices

As in other areas of photochemistry, the application of low-temperature photolysis techniques to the photochemistry of metal–metal bonds has proven to be of great value in generating and identifying possible photochemical intermediates.[20–24] An important example is the photolysis of $HMn(CO)_5$ in a solid CO matrix at 10–20 K to generate $Mn(CO)_5$, eq 9. In addition,

$$HMn(CO)_5 \xrightarrow[10-20\ K]{+h\nu,\ CO(s)} Mn(CO)_5 + HCO \tag{9}^{[20]}$$
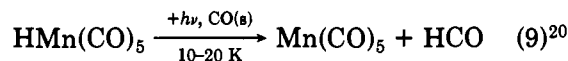
recent work in low-temperature films, frozen-gas matrices, and low-temperature glasses has shown that photolysis leads to the appearance of intermediates whose infrared spectra are consistent with the presence of bridging CO groups, eq 10 and 11. One obvious

$$Mn_2(CO)_{10} \xrightarrow[3-methylpentane]{+h\nu,\ 77\ K} Mn_2(CO)_9 + CO \tag{10}^{[21]}$$

$$(\eta^5\text{-}C_5H_5)_2Fe_2(CO)_4 \xrightarrow[poly(vinyl\ chloride)]{+h\nu,\ 12-77\ K}$$
$$[(\mu\text{-}CO)_3\{(\eta^5\text{-}C_5H_5)Fe\}_2] + CO \tag{11}^{[22,24]}$$

advantage of the low-temperature experiments is that conventional spectroscopic techniques can be applied to the observation of nominally reactive intermediates. For example, for the cases in eq 10 and 11 infrared spectroscopy provides clear evidence for appearance of well-defined $\nu(CO)$ bands at energies consistent with bridging-CO groups.

In addition, the reactivity properties of photogenerated intermediates can be studied by adding potential reactants, such as PPh_3 or CCl_4, to the matrix. When the matrices were warmed up following photolysis, it is possible to observe whether or not reactions occur between the added reactants and the intermediates produced in the photolysis.

C. Additional Experimental Considerations

Although there are a variety of techniques which have been and can be brought to bear on the question of mechanism in the photochemistry of metal–metal bonds, there are some additional experimental considerations which need to be taken into account. For the transient experiments using conventional flash photolysis, it is necessary to use optically dilute solutions so that appreciable amounts of the starting dimers are photolyzed. However, the intermediates produced are generally very reactive and it is absolutely essential that *extreme care* be taken with the purification and degassing of solvents and solutions. The problem does not exist in most net photochemical reactions. If in a photolysis reasonable care is taken with solvent purification and deaeration, the first few percent of the photolysis will suffice to clear the solution of impurities. The remainder of the photolysis can then proceed to give products associated with the inherent photochemistry.

An additional problem arises in attempting to use transient techniques to establish mechanistic details. For photochromic systems it is possible to obtain many independent results simply by carrying out a series of flash photolyses on the same solution. However, in the presence of a potential reactant like CCl_4 or PPh_3, net, irreversible photochemistry can occur as a consequence of the photolysis. Consequently, it may only be possible to observe a few transient events before the solution is largely converted into photoproducts. In such cases, the demands associated with sample preparation can make the acquisition of adequate amounts of data a tedious exercise.

III. Photochemistry of Metal–Metal Bonds

As mentioned above, the emphasis of this account is on the mechanistic details of the photochemistry of metal–metal bonds and, in particular, on the photochemistry of the compounds, $M_2(CO)_{10}$ (M = Mn, Re), $(\eta^5\text{-}C_5H_5)_2M_2(CO)_6$ (M = Mo, W), and $(\eta^5\text{-}C_5H_5)_2Fe_2$-$(CO)_4$. The outline to be followed will be first to summarize the available experimental data and then to discuss and interpret the results in four distinct parts. The first part will be the photolysis step and the nature of the excited states produced. The second part will feature the reactivity and physical properties of photochemically produced monomers, and the third part the reactivity and properties of other intermediates produced photochemically. The fourth part will be a retrospective overview.
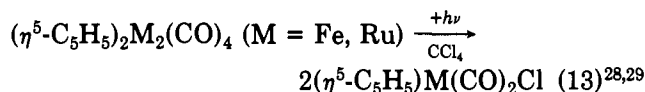
A. Photochemistry of Individual Systems

1. $(\eta^5\text{-}C_5H_5)_2Fe_2(CO)_4$

For $(\eta^5\text{-}C_5H_5)_2Fe_2(CO)_4$, there is infrared and NMR evidence in solution for the existence of cis and trans isomers.[25-28] In organic solvents both isomers are usually present in measurable amounts and undergo a rapid interconversion, eq 12. There is also evidence for a
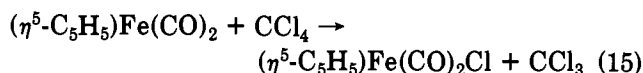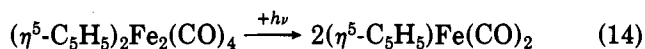

(cis)   (non-bridged)   (trans)

K(25°)~0.36 =[trans]/[cis]
(3:1 $CS_2/C_6D_5CD_3$)
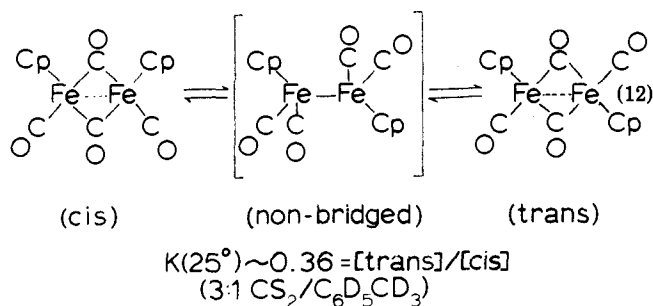
small amount of a nonbridging isomer in solution which is far more important for the analogous ruthenium dimer.[26,27] Qualitatively, the absorption spectrum of the iron dimer has some of the same features as the molybdenum dimer in Figure I in that there are intense bands in the ultraviolet and weaker bands in the visible, although the spectrum of the iron dimer is more complex.[28] It is interesting to note that dramatic spectral shifts are observed for the Ru dimer in the UV when changes are made in temperature or solvent. They have been attributed to the existence of the equilibrium between the bridging and nonbridging isomers.[28]

Photolysis of either the iron or ruthenium dimers in CCl_4 leads to the relatively efficient production of the corresponding chloro compound, eq 13. As has been

$$(\eta^5\text{-}C_5H_5)_2M_2(CO)_4 \text{ (M = Fe, Ru)} \xrightarrow[CCl_4]{+h\nu}$$

$$2(\eta^5\text{-}C_5H_5)M(CO)_2Cl \quad (13)^{28,29}$$

$$\phi \text{ (366 nm)} = 0.23, \text{ M = Fe}$$

stressed repeatedly by Wrighton and co-workers, the photochemistry observed in reactions like eq 13 is consistent with the photochemically induced homolysis of the metal–metal bond to give a reactive intermediate with a d^7 electronic configuration. Once generated photochemically, such monomers are expected to undergo relatively facile halogen-atom abstraction from halocarbons to give the observed photoproduct, eq 14 and 15. However, such a mechanistic conclusion based

$$(\eta^5\text{-}C_5H_5)_2Fe_2(CO)_4 \xrightarrow{+h\nu} 2(\eta^5\text{-}C_5H_5)Fe(CO)_2 \quad (14)$$

$$(\eta^5\text{-}C_5H_5)Fe(CO)_2 + CCl_4 \rightarrow$$
$$(\eta^5\text{-}C_5H_5)Fe(CO)_2Cl + CCl_3 \quad (15)$$

solely on the observation of the nature of the photochemical product is somewhat in doubt because of clear evidence from other techniques for the appearance of an additional photochemically produced intermediate.

Photosubstitutional loss of CO has also been observed in inert solvents, eq 16.[28,30,31,33] Photolysis (λ > 500 nm)

$$(\eta^5\text{-}C_5H_5)_2Fe_2(CO)_4 + P(O\text{-}i\text{-}Pr)_3 \xrightarrow[C_6H_{12}]{+h\nu}$$
$$(\eta^5\text{-}C_5H_5)_2Fe_2(CO)_3(P(O\text{-}i\text{-}Pr)_3) + CO \quad (16)^{31}$$
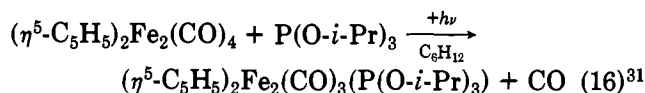
$$\phi \text{ (355 nm)} = 0.11$$

in cyclohexane in the presence of $P(OMe)_3$ results in the quantitative appearance of the disubstituted dimer $(\eta^5\text{-}C_5H_5)_2Fe_2(CO)_2(P(OMe)_3)_2$ with no evidence for the appearance of $(\eta^5\text{-}C_5H_5)_2Fe_2(CO)_3(P(OMe)_3)$ as an intermediate. However, under the same conditions, the monosubstituted dimer is known to undergo efficient photosubstitution to give $(\eta^5\text{-}C_5H_5)_2Fe_2(CO)_2(P\text{-}(OMe)_3)_2$.[31]

The suggestion has been made that the photochemistry observed for the iron dimer can be accounted for by the initial photohomolysis step shown in eq 14.[28] On the other hand, low temperature (–78 °C) photolysis of the iron dimer in THF or ethyl chloride in the presence of $P(O\text{-}i\text{-}Pr)_3$, $P(n\text{-}Bu)_3$, or $P(OMe)_3$ has led to the trapping of a yellow, apparently diamagnetic, dimeric intermediate in which there is a bridging-CO ligand $(\nu(CO) = 1720 \text{ cm}^{-1})$ and, apparently, no iron–iron metal–metal bond, eq 17.
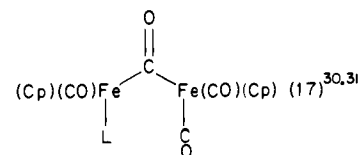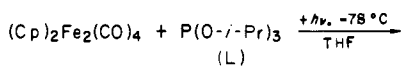
The intermediate is EPR silent down to 15 K and when solutions at –78 °C are warmed to room temperature, the substituted products $(\eta^5\text{-}C_5H_5)_2Fe_2$-

$(CO)_3(L)$ $(L = P(n-Bu)_3$ or $P(O-i-Pr)_3)$ or $(\eta^5-C_5H_5)_2Fe_2(CO)_2(L)_2$ $(L = P(OMe)_3)$ appear in the solution. Addition of CCl_4 at -78 °C followed by warming of the solutions leads to $(\eta^5-C_5H_5)Fe(CO)_2Cl$.

Flash-photolysis studies have been carried out on the iron dimer both under nonphotochemical conditions in cyclohexane and under photochemical conditions in the presence of CCl_4 or PPh_3 and the results are revealing.[32] When spectral changes at a series of wavelengths as a function of time are observed, clear evidence has been obtained for the appearance of two distinct intermediates following photolysis. One intermediate is relatively short lived and is transparent or only weakly absorbing from the low-energy ultraviolet through the visible and undergoes a second-order, bimolecular reaction to give back the starting dimer. The loss of absorbance in the ultraviolet after photolysis is consistent with the loss of the metal–metal bond in the intermediate. The loss of absorbance combined with the second-order nature of the transient decay of the intermediate to return to the iron dimer provides direct evidence for eq 14 followed by the recombination reaction in eq 18, which is what is actually observed in
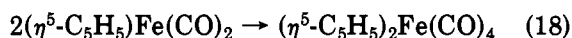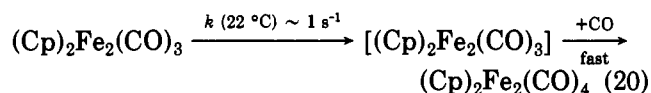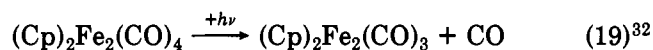
$$2(\eta^5-C_5H_5)Fe(CO)_2 \rightarrow (\eta^5-C_5H_5)_2Fe(CO)_4 \quad (18)$$

$$k \ (25 \ °C \ in \ cyclohexane) = 3 \times 10^9 \ M^{-1} \ s^{-1}$$

the flash-photolysis experiment.

The second intermediate which appears following flash photolysis is quite different in that it absorbs in the visible with $\lambda_{max} = 510$ nm. It also returns to the dimer but through two pathways, one photochemical and one thermal. In contrast to the bimolecular recombination reaction in eq 18, the second intermediate returns to the dimer by a first-order process, eq 19 and 20, Cp is $\eta^5-C_5H_5$.

$$(Cp)_2Fe_2(CO)_4 \xrightarrow{+h\nu} (Cp)_2Fe_2(CO)_3 + CO \quad (19)^{32}$$

$$(Cp)_2Fe_2(CO)_3 \xrightarrow{k \ (22 \ °C) \ \sim \ 1 \ s^{-1}} [(Cp)_2Fe_2(CO)_3] \xrightarrow[\text{fast}]{+CO}$$
$$(Cp)_2Fe_2(CO)_4 \quad (20)$$

It is interesting to note that a recent flash-photolysis experiment with infrared monitoring has provided clear evidence for the appearance of the two intermediates by observing spectral changes in the $\nu(CO)$ region.[17a]

The transient kinetic behaviors observed for $(\eta^5-C_5H_5)Fe(CO)_2$ and $(\eta^5-C_5H_5)_2Fe_2(CO)_3$ are independent of each other showing that one intermediate is *not* the origin of the other. It is tempting to conclude that the intermediates are both primary photoproducts which are coproduced in the photolysis act. However, the point is equivocal since the time window of observation for the iron dimer in the conventional flash-photolysis experiment (10–100 μs) is far longer than the 25 ps time scale data available, for example, for $Mn_2(CO)_{10}$.

Direct evidence as to the nature of the longer lived intermediate has been obtained by visible photolysis of the iron dimer in CH_4 (12 K) and poly(vinyl chloride) film (12–77 K) matrices[22] and by near UV photolysis of the iron dimer and the related dimers, $(\eta^5-C_5H_4CH_2Ph)_2Fe_2(CO)_4$ and $(\eta^5-C_5Me_5)_2Fe_2(CO)_4$ in alkane and 2-methyltetrahydrofuran matrices.[24] The intermediates, monitored by infrared, appear to arise

exclusively from the trans isomer of the starting dimers. Their appearance is signaled both by the appearance of free CO at 2133 cm^{-1} and by the change in the pattern of the $\nu(CO)$ bands in the infrared. The intermediate for the iron dimer produced in the matrices has $\lambda_{max} = 510$ nm.[22] From the appearance of a single $\nu(CO)$ CO band at 1810 cm^{-1} in the infrared it has been concluded that the intermediate contains three bridging-CO groups and probably has structure 1 (Cp = $\eta^5-C_5H_5$).

1
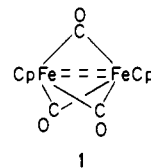
The long-lived intermediate observed by IR monitoring following flash photolysis was found to have $\nu(CO) = 1823$ cm^{-1}.[17a] The fact that the absorption and infrared spectra so closely match between the intermediates produced in the flash photolysis and matrix experiments strongly supports the suggestion that the tricarbonyl-bridged structure is maintained in cyclohexane as well.

It is worth returning to the fact that there are both photochemical and thermal pathways for return of $(\eta^5-C_5H_5)_2Fe_2(CO)_3$ to the starting dimer. The observation provides evidence for the point that if photointermediates are sufficiently long lived and strongly absorbing, they can build up in solution to a sufficient degree to undergo secondary photolytic processes. The secondary processes may in turn contribute to the observed distribution of photoproducts. It should also be appreciated that the importance of such secondary photolytic events can depend critically on the reaction conditions used. For example, at the high concentrations in the initial stages of a photolysis, the dimer effectively acts as an internal light filter because of its high absorptivity which prevents secondary photolysis from occurring. On the other hand, in the dilute solutions used in a transient absorbance experiment, a long-lived intermediate could become a significant light absorber and could play an important role in the observed transient behavior of the system.

With at least inferential evidence as to the nature of the two initial photochemical intermediates, it is of value to return to the observed reactivity when solutions containing the iron dimer and potential reactants such as CCl_4 or PPh_3 are photolyzed. The experimental difficulties associated with the direct observation of net reactions of photointermediates using transient techniques has already been mentioned. Nonetheless, it has been possible to use flash photolysis to assess in a direct way the role of the two intermediates observed in cyclohexane in accounting for the net, overall photochemistry. With added CCl_4 in cyclohexane (0.02–0.002 M) under conditions where the quantum yield for formation of $(\eta^5-C_5H_5)Fe(CO)_2Cl$ is relatively high, *both* intermediates undergo reactions with CCl_4.[32] For $(\eta^5-C_5H_5)_2Fe_2(CO)_3$, the reaction with CCl_4 is first order in both $(\eta^5-C_5H_5)_2Fe_2(CO)_3$ and CCl_4 with k (22 °C) = 4×10^3 M^{-1} s^{-1}. Under the same conditions the reaction between $(\eta^5-C_5H_5)Fe(CO)_2$ and CCl_4 is too rapid to observe but $k > 1.5 \times 10^5$ M^{-1} s^{-1} assuming that the reaction is first order in both $(\eta^5-C_5H_5)Fe(CO)_2$ and CCl_4.

Flash photolysis results have also been obtained in benzene and in cyclohexane in the presence of either phosphines or phosphites under conditions where photochemically induced substitution is known to occur.[32] From the flash results, the observed rate constant for recombination of $(\eta^5\text{-}C_5H_5)Fe(CO)_2$ in cyclohexane is *unaffected* by the presence of added PPh_3 (0.1–0.001 M). The absence of a PPh_3 effect shows that there is *no* reaction between $(\eta^5\text{-}C_5H_5)Fe(CO)_2$ and PPh_3, at least in this concentration range. Under the same conditions, $(\eta^5\text{-}C_5H_5)_2Fe_2(CO)_3$ undergoes a reaction with PPh_3 which is first order in both the intermediate and PPh_3 with k (22 °C) = 1.5×10^5 M^{-1} s^{-1}. The flash results are obviously consistent with the fact that net photosubstitution occurs to give $(\eta^5\text{-}C_5H_5)_2Fe_2(CO)_3(L)$ (L = PPh_3, $P(O\text{-}i\text{-}Pr)_3$,...) as a product under the same conditions.[28,30,31,33]

Clear evidence has also been obtained by flash photolysis for reactions between $(\eta^5\text{-}C_5H_5)_2Fe_2(CO)_3$ and other potential ligands such as Me_2SO or CH_3CN.[32] Although the infrared evidence in hydrocarbon matrices or PVC films suggests a tri(μ-CO)-bridged structure for $(\eta^5\text{-}C_5H_5)_2Fe_2(CO)_3$, it is likely that in potentially corrdinating solvents like Me_2SO or CH_3CN, the dominant form of the intermediate may be $(\eta^5\text{-}C_5H_5)_2Fe_2\text{-}(CO)_3S$ (S = solvent). The observations made by Tyler et al. following low-temperature photolysis (–78 °C) in the presence of phosphines or phosphites may bear directly on this point.[30,31] They propose that intermediate II in eq 21 arises by capture of an earlier intermediate in which one of the iron atoms is coordinatively unsaturated. The subsequent appearance of the final
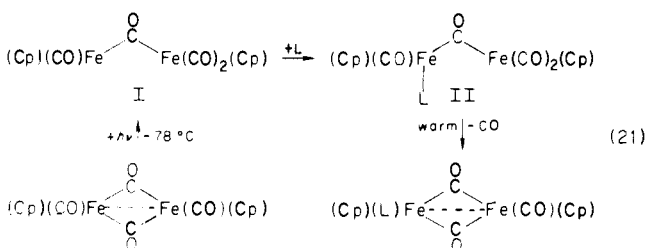
product upon warming was suggested to occur by loss of CO and re-formation of the μ-CO bridging structure. An alternate possibility is that the intermediates observed by Tyler et al. arise from capture of $(\eta^5\text{-}C_5H_5)_2Fe_2(CO)_3$ by L to give an unstable isomer which is converted into the final product by warming.
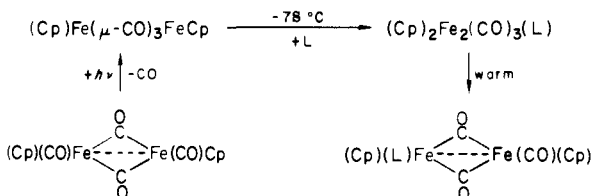
It is also worth noting that in cyclohexane saturated in CO, a reaction occurs between $(\eta^5\text{-}C_5H_5)_2Fe_2(CO)_3$ and CO with k_{obsd} (22 °C) = $k[CO]$ = 280 s^{-1}. In the pres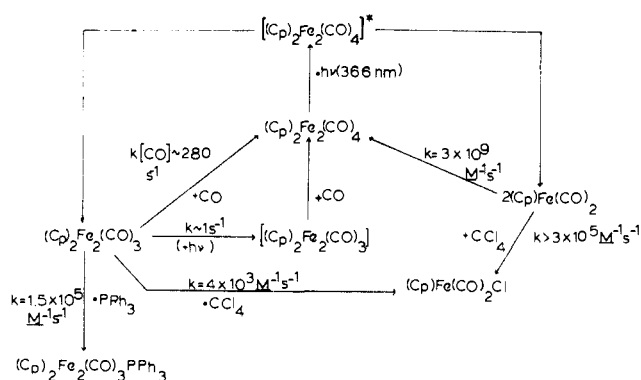ence of added CO, there is a considerable enhancement in the rate of return of $(\eta^5\text{-}C_5H_5)_2Fe_2(CO)_3$ to $(\eta^5\text{-}C_5H_5)_2Fe_2(CO)_4$ ($t_{1/2}$ = 25 ms compared to ~1 s). The enhancement with added CO shows that in addition to the first-order thermal pathway shown in eq 20 for return of $(\eta^5\text{-}C_5H_5)_2Fe_2(CO)_3$ to the starting dimer, a second pathway must also exist. The second pathway

SCHEME II[a]

[a] Cyclohexane, 22 °C.

is analogous to the reactions between the intermediate and PPh_3, CH_3CN, or Me_2SO, in that it is first order in intermediate and at least first order in [CO]. The competitive capture of $(\eta^5\text{-}C_5H_5)_2Fe_2(CO)_3$ by CO when CO is added could clearly account for the lowered quantum yield for photosubstitution by PPh_3 in the presence of added CO reported by Tyler et al.[31]

A summary of the photochemical properties of the iron dimer obtained from a combination of transient absorbance, product studies, and low-temperature photolyses in inert matrices is shown in Scheme II.

The kinetics data mentioned in Scheme II were obtained in cyclohexane at 22 °C. In principle, it should be possible to estimate relative quantum efficiencies for the appearance of $(\eta^5\text{-}C_5H_5)Fe(CO)_2$ and $(\eta^5\text{-}C_5H_5)_2Fe_2(CO)_3$ from available quantum yield data. The basis for the estimation comes from the flash results which show that although *both* intermediates undergo reactions with CCl_4 *only* $(\eta^5\text{-}C_5H_5)_2Fe_2(CO)_3$ reacts with PPh_3 for [PPh_3] ≤ 0.1 M. Consequently, quantum yields obtained by photolysis of the iron dimer in the presence of added CCl_4 at high, limiting concentrations of CCl_4 should provide an estimate for the sum of the appearance efficiencies of $(\eta^5\text{-}C_5H_5)Fe(CO)_2$ and $(\eta^5\text{-}C_5H_5)_2Fe_2(CO)_3$ while ϕ values for substitution by PPh_3 should give only the appearance efficiency for $(\eta^5\text{-}C_5H_5)_2Fe_2(CO)_3$. Unfortunately, although quantum yield data are available for the two types of processes, they are only available in different media—neat CCl_4 and hydrocarbon solutions containing added PPh_3. As a consequence, direct comparisons can not be made since, as noted later, the efficiencies for the appearance of the two intermediates appear to be dependent on the medium.

2. $(\eta^5\text{-}C_5H_5)_2M_2(CO)_6$ (M = Mo, W)

One of the most interesting features to emerge from photochemical studies on the η^5-cyclopentadienyl-molybdenum and -tungsten dimers is the diversity of the photochemistry. Based on product studies, a number of different types of photochemical reactions have been identified including the expected halogen abstraction chemistry in the presence of halocarbons
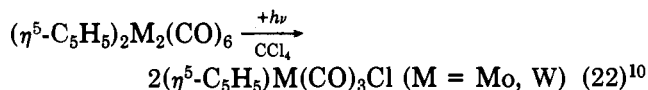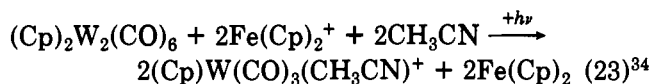
$$(\eta^5\text{-}C_5H_5)_2M_2(CO)_6 \xrightarrow[CCl_4]{+h\nu}$$

$$2(\eta^5\text{-}C_5H_5)M(CO)_3Cl \ (M = Mo, W) \ (22)^{10}$$

outer-sphere electron transfer

$$(Cp)_2W_2(CO)_6 + 2Fe(Cp)_2^+ + 2CH_3CN \xrightarrow{+h\nu}$$
$$2(Cp)W(CO)_3(CH_3CN)^+ + 2Fe(Cp)_2 \quad (23)^{34}$$

photosubstitutional loss of CO

$$(\eta^5\text{-}C_5H_5)_2Mo_2(CO)_6 + 2PPh_3 \xrightarrow{+h\nu}$$
$$(\eta^5\text{-}C_5H_5)_2Mo_2(CO)_4(PPh_3)_2 + 2CO \quad (24)^{35-37}$$

disproportionation in the presence of good σ bonding ligands

$$(\eta^5\text{-}C_5H_5)_2Mo_2(CO)_6 + 2X^- \xrightarrow{+h\nu}$$
$$2(\eta^5\text{-}C_5H_5)Mo(CO)_3X \quad (25)^{38-40}$$

$$X = Cl, Br, NCS$$

or donor solvents

$$(\eta^5\text{-}C_5H_5)_2M_2(CO)_6 \xrightarrow[\text{pyridine}]{+h\nu}$$
$$(\eta^5\text{-}C_5H_5)M(CO)_3^- + M(II) \quad (M = Mo, W) \quad (26)^{41}$$

loss of CO to give a triple bond between the two metal atoms

$$(Cp)_2M_2(CO)_6 \xrightarrow[\text{M = Cr, Mo, W}]{+h\nu}$$
$$(Cp)(CO)_2M\equiv M(CO)_2(Cp) + 2CO \quad (27)^{42}$$
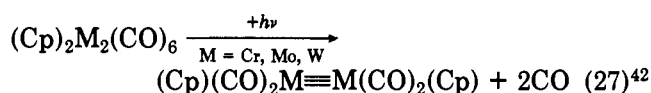
and in unsymmetrical dimers, metal–metal cleavage to give symmetrical metal–metal bonded products.

$$2(CO)_5Mn\text{-}Mo(CO)_3(Cp) \xrightarrow[\text{isooctane}]{+h\nu}$$
$$Mn_2(CO)_{10} + (Cp)_2Mo_2(CO)_6 \quad (28)^{43}$$
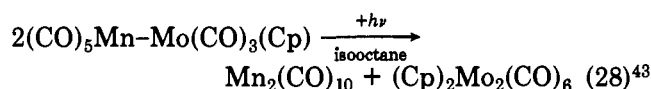
The kinetic details of the photochemical reaction between the tungsten dimer, $(\eta^5\text{-}C_5H_5)_2W_2(CO)_6$, and halocarbons have been studied by Laine and Ford.[18] By measuring disappearance quantum yields for the dimer in THF solution as a function of added CCl_4 and incident light intensity they were able to fit their kinetics data to the mechanism shown in Scheme III. In the

SCHEME III

$$(Cp)_2W_2(CO)_6 \overset{+h\nu}{\rightleftharpoons} [(Cp)_2W_2(CO)_6] \begin{cases} 2CpW(CO)_3 \\ \xrightarrow{-CO} I \end{cases}$$

$$2(Cp)W(CO)_3 \longrightarrow (Cp)_2W_2(CO)_6$$

$$(Cp)W(CO)_3 \xrightarrow{+CCl_4} (Cp)W(CO)_3Cl$$
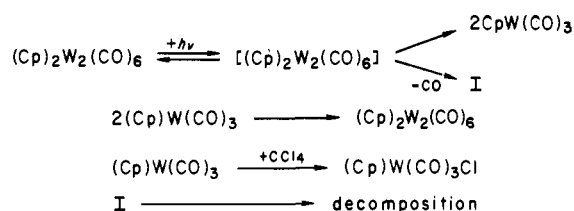
$$I \longrightarrow \text{decomposition}$$

mechanism two intermediates were involved (η^5-C_5H_5)W(CO)$_3$, and a CO-loss intermediate, I. It was suggested that the minor photodecomposition observed occurs through I and the reaction with CCl_4 through $(\eta^5\text{-}C_5H_5)W(CO)_3$.

As was the case for the iron dimer, conventional flash photolysis of solutions containing the molybdenum dimer under nonphotochemical conditions in degassed cyclohexane solution gives evidence for two distinct intermediates which are produced during the lifetime of the flash.[44] Both intermediates return to the starting dimer by relatively rapid second-order processes, but because of the difference in time scales involved the two processes are separable kinetically. The difference spectrum obtained for the more facile of the two processes shows that the products of the photolysis are transparent in the near UV–visible in regions usually

associated with strong absorption by the metal–metal bond. The observation of second-order kinetics for the reappearance of the metal–metal bond and the relative transparency of the intermediate both suggest that at least one of the processes observed is a photochemically induced homolysis followed by recombination to reform the metal–metal bond, eq 29 and 30. At 22 °C

$$(\eta^5\text{-}C_5H_5)_2Mo_2(CO)_6 \xrightarrow{+h\nu} 2(\eta^5\text{-}C_5H_5)Mo(CO)_3 \quad (29)$$

$$2(\eta^5\text{-}C_5H_5)Mo(CO)_3 \rightarrow (\eta^5\text{-}C_5H_5)_2Mo_2(CO)_6 \quad (30)^{44}$$
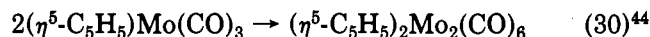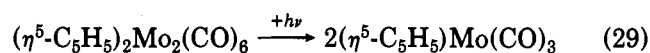
in cyclohexane, the rate constant for the recombination reaction is 3.1×10^9 M^{-1} s^{-1}. For the dimer (η^5-$C_5H_5)_2W_2(CO)_6$, $k = 1.9 \times 10^9$ M^{-1} s^{-1} under the same conditions.

However, as noted above, a second intermediate is also formed in the photolysis. From the difference spectrum between the intermediate and the starting dimer it is clear that the second intermediate absorbs light relatively strongly in the ultraviolet in a region associated with metal–metal bond localized $\sigma \rightarrow \sigma^*$ transitions. The appearance of the ultraviolet absorption suggests that the metal–metal bond remains intact in the intermediate. That fact plus the observation that the second intermediate returns to the starting dimer via second-order kinetics suggests that it is a CO-loss product and that the process observed by flash photolysis is recombination with CO as shown in eq 32. The

$$(\eta^5\text{-}C_5H_5)_2Mo_2(CO)_6 \xrightarrow{+h\nu} (\eta^5\text{-}C_5H_5)_2Mo_2(CO)_5 + CO \quad (31)^{44}$$

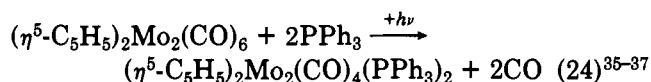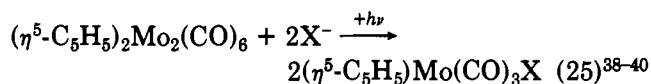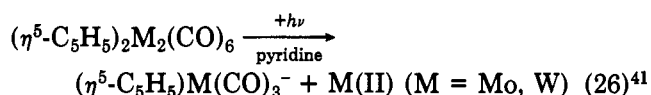$$(\eta^5\text{-}C_5H_5)_2Mo_2(CO)_5 + CO \rightarrow (\eta^5\text{-}C_5H_5)_2Mo_2(CO)_6 \quad (32)^{44}$$
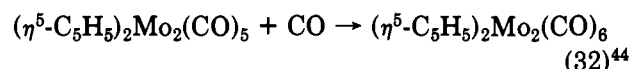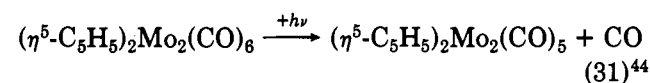
rate constant for the suggested recapture of CO by the intermediate is 1.8–2.3×10^7 M^{-1} s^{-1} in cyclohexane at 22 °C. The uncertainty in the value is a consequence of the fact that the molar extinction coefficient for the intermediate is unknown, note eq 7.

Within the time limits of the conventional flash-photolysis experiment both the dimeric and monomeric intermediates are present in the solution immediately after photolysis and their subsequent behaviors are independent of each other. As a consequence, the intermediates are either primary photoproducts or arise from different primary photoproducts which were in the solution at an earlier time.

Similar observations were made for the Mo dimer in THF and CH_3CN, although noticeable decomposition was observed to occur after a series of flashes.[44] The decomposition chemistry observed is, no doubt, disproportionation as described below. The W dimer is photochemically more stable. Although some evidence was obtained with this system for a long-lived, presumably CO-loss intermediate, the efficiency of its appearance is low and reliable kinetics data for its transient decay were unobtainable.[45]

Additional information concerning the probable nature of the relatively long-lived intermediate (η^5-$C_5H_5)_2Mo_2(CO)_5$ has been obtained for both the molybdenum and tungsten dimers by infrared monitoring following photolysis of the dimers in low-temperature matrices.[23,24] In poly(vinyl chloride) film matrices at 12 or 77 K either visible or near-ultraviolet excitation

leads to a decrease in intensity for the infrared bands associated with the terminal CO groups and new bands appear at lower energies. Analogous observations were made in CH_4, Ar, or CO matrices at 12 K. The photolysis produces free CO and when a PVC film containing the photolysis product is warmed to 180 K the starting dimers reappear. The photolysis product of the molybdenum dimer has an intense ultraviolet absorption band at λ_{max} = 330 nm (PVC matrix) and for the tungsten dimer at λ_{max} = 300 nm (PVC matrix). On the basis of the observed pattern of CO bands in the infrared and reasoning by analogy from the pattern of ν(CO) bands for previously reported compounds, it has been suggested that the structures of the photointermediates contain a four-electron donor, bridging-CO ligand and two semibridging CO ligands.

Both the molybdenum and tungsten dimers have been investigated in cyclohexane solution at room temperature by using picosecond emission techniques.[46] Following photolysis at 354 nm, two transient emissions were observed from the molybdenum dimer, one at λ_{max} ~ 440 nm with τ = 10 ± 3 ps and one at λ_{max} ~ 560 with τ = 4–5 ns.[46] A low-energy emission was also observed for the tungsten dimer. Visible photolysis of the Mo dimer at 530 nm gave no evidence for either of the two transients.

Flash-photolysis experiments have been carried out on the molybdenum dimer under photochemical conditions in THF solution in the presence of Br⁻, eq 33.

$$(\eta^5\text{-}C_5H_5)Mo_2(CO)_6 + Br^- \xrightarrow[\text{THF}]{+h\nu}$$
$$(\eta^5\text{-}C_5H_5)Mo(CO)_3^- + (\eta^5\text{-}C_5H_5)Mo(CO)_3Br \quad (33)^{45}$$

In solutions dilute in Br⁻ (10^{-4} M), the second-order-decay characteristics of $(\eta^5\text{-}C_5H_5)Mo(CO)_3$ remain second order and the rate constant is unaffected showing that the monomer does not undergo a reaction with Br⁻. Apparently, in dilute Br⁻, return to $(\eta^5\text{-}C_5H_5)_2Mo_2(CO)_6$ is too rapid for capture by Br⁻ to be competitive. Under the same conditions, $(\eta^5\text{-}C_5H_5)_2Mo_2(CO)_5$ appears to be completely captured by Br⁻ since the only relatively long-lived transient process observed follows first-order kinetics and there is no evidence for the recapture of $(\eta^5\text{-}C_5H_5)_2Mo_2(CO)_5$ by CO. The flash-photolysis results suggest the sequence of events shown in eq 34. Although the initial photochemical intermediate in eq 34 is written as the electron-deficient pentacarbonyl, in a potentially coordinating solvent like THF, the dominant form of the dimer may well be the solvento complex.

$(Cp)_2Mo_2(CO)_5 + Br^- (10^{-4} M) \xrightarrow{\text{fast}} [(Cp)_2Mo_2(CO)_5Br^-]$

$h\nu \big|{-CO} \qquad\qquad k \sim 10^2 s^{-1}\big|$ (34)

$(Cp)_2Mo_2(CO)_6 \qquad (Cp)Mo(CO)_3^- + (Cp)Mo(CO)_2Br(?)$

$\big|{+CO}$ (35)

$(Cp)Mo(CO)_3^- + (Cp)Mo(CO)_3Br$

e.g., $(\eta^5\text{-}C_5H_5)_2Mo_2(CO)_5(THF)$.

When spectral changes before and after flash photolysis are used, it is possible to estimate that the relative ratio of the monomeric and dimeric photointermediates which appear as a consequence of the flash is ~4/1 in favor of the monomer. In THF solution in the presence of $CHBr_3$, both intermediates appear to react to give $(\eta^5\text{-}C_5H_5)Mo(CO)_3B$ as the photoproduct. Under limiting conditions of a relatively high concentration of $CHBr_3$ in THF (8.8 × 10^{-2} M) the limiting quantum yield for disappearance of the molybdenum dimer is 0.57.[45] With the two numbers in hand it is possible to estimate that the quantum efficiencies for production of the two intermediates in THF solution under conditions where the starting dimer is completely photolyzed are ~0.4 for the monomer and ~0.1 for the intermediate.

At higher concentrations of Br⁻, capture of $(\eta^5\text{-}C_5H_5)Mo(CO)_3$ by Br⁻ becomes competitive with recombination. For example, the quantum efficiency for the disproportionation in eq 33 increases from 0.10 at [Br⁻] = 1.0 × 10^{-3} M to 0.32 at [Br⁻] = 12.7 × 10^{-3} M.[45] Presumably, at even higher Br⁻ concentrations the same limiting yield would be reached as in the experiment at high $CHBr_3$.

The photochemically induced disproportionation of $(\eta^5\text{-}C_5H_5)_2Mo_2(CO)_6$ and/or of $(\eta^5\text{-}CH_3C_5H_4)_2Mo_2(CO)_6$ has been studied in further detail under a variety of conditions by Stiegman and Tyler.[3,36,50,51] UV (290 nm) or visible (405 nm) photolysis of $(\eta^5\text{-}CH_3C_5H_4)_2Mo_2$-$(CO)_6$ in benzene or cyclohexane in the presence of a series of phosphines or phosphites leads to monosubstitution, $(\eta^5\text{-}CH_3C_5H_4)_2Mo_2(CO)_5(L)$, or disubstitution, $(\eta^5\text{-}C_5H_5)_2Mo_2(CO)_4(L)_2$, and/or to the disproportionation products, $(\eta^5\text{-}CH_3C_5H_4)Mo(CO)_2(L)_2^+$ and $(\eta^5\text{-}CH_3C_5H_4)Mo(CO)_3^-$.[36,37] Qualitatively, the appearance of the disproportionation products depends critically on both the steric and electronic properties of the added ligand. Through a range of ligands like $P(OCH_3)_3$, $P(n\text{-}Bu)_3$, PPh_3, etc., the appearance of disproportionation products is favored by good electron-donating ligands and disfavored by ligands that are sterically bulky. The appearance of mono- vs. disubstituted products is also dependent upon the steric properties of the added ligand with disubstitution being limited to ligands with cone angles τ < 140°. Where they both occur, the importance of substitution relative to disproportionation is dependent both upon the steric properties and the concentration of the added ligand. Disproportionation is favored for large ligands at high concentrations.

Mechanistic insight into the disproportionation chemistry was gained by 405 nm photolysis of $(\eta^5\text{-}CH_3C_5H_4)_2Mo_2(CO)_6$ in benzene in the presence of the chelating ligand $Ph_2PCH_2CH_2PPh_2$(dppe).[36] Under these conditions, only disproportionation occurs, eq 36.

$(Cp)_2Mo_2(CO)_6 + dppe \rightarrow$
$(Cp)Mo(CO)_3^- + (Cp)Mo(CO)_2(dppe)^+$ (36)

The results of quantum-yield studies were revealing in that irreproducible disproportionation quantum yields of up to 11.8 were obtained with a general trend toward increasing yields as the concentration of added ligand was increased. In order to explain values of ϕ_{dis} > 1 it was necessary to invoke a radical-chain mechanism

similar to the mechanism proposed earlier by McCullen and Brown to explain the photoinduced disproportionation of $Mn_2(CO)_{10}$ in pyridine and substituted pyridines[47] and thermal disproportionation of $Co_2(CO)_8$[48] and $Cl_3SnCo(CO)_4$[49] in the presence of bases. In the mechanism it was suggested that the first step involves photohomolysis of the metal–metal bond followed by substitution of L for CO (eq ii in Scheme IV) and addition of L to the substituted monomer to give the 19-electron reducing agent $CpMo(CO)_2(L)_2$ (eq iii in Scheme IV). The existence of such an intermediate

SCHEME IV

(i) $(Cp)_2Mo_2(CO)_6 \xrightarrow{+h\nu} 2(Cp)Mo(CO)_3$

(ii) $(Cp)Mo(CO)_3 + L \rightleftharpoons (Cp)Mo(CO)_2L + CO$

(iii) $(Cp)Mo(CO)_2(L) + L \rightleftharpoons (Cp)Mo(CO)_2(L)_2$

(iv) $(Cp)Mo(CO)_2(L)_2 + (Cp)_2Mo_2(CO)_6 \rightarrow$
$(Cp)Mo(CO)_2(L)_2^+ + (Cp)_2Mo_2(CO)_6^-$

(v) $(Cp)_2Mo_2(CO)_6^- \rightarrow$
$(Cp)Mo(CO)_3^- + (Cp)Mo(CO)_3$

(Cp is η^5-C_5H_5 or η^5-$CH_3C_5H_4$)[36]
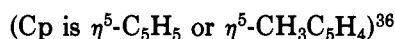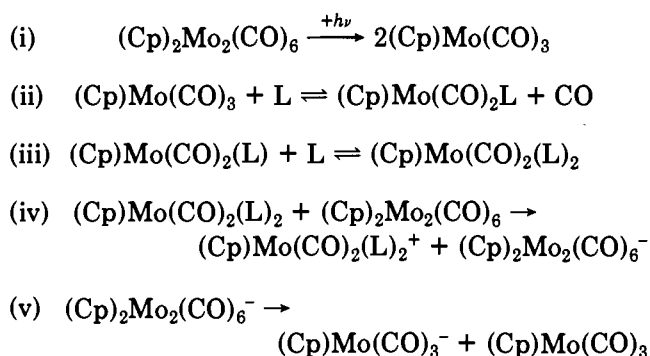
is suggested both by the appearance of $CpMo(CO)_2(L)_2^+$ as a product and by disproportionation as the sole reaction with added dppe. In the latter case, substitution followed by chelate ring closure would lead directly to the chelated equivalent of $CpMo(CO)_2(L)_2$, $CpMo(CO)_2(dppe)$. In order to complete the mechanism and account for the observed products it was suggested that $CpMo(CO)_2(L)_2$ undergoes outer-sphere electron transfer with $Cp_2Mo_2(CO)_6$ (eq iv) to give $CpMo(CO)_2(L)_2^+$ and $Cp_2Mo_2(CO)_6^-$, which is presumably unstable and decomposes to give $CpMo(CO)_3^-$ and $CpMo(CO)_3$, eq v in Scheme IV. The latter two reactions provide the basis for the radical chain and $\phi_{dis} > 1$ since disproportionation is accompanied by the regeneration of $CpMo(CO)_3$ which can reenter the cycle via eq ii and iii in Scheme IV. Electron transfer between $CpMo(CO)_2(L)_2$ and $CpMo(CO)_3$ would also lead to the disproportionation products via eq 37. In the

$(Cp)Mo(CO)_2(L)_2 + (Cp)Mo(CO)_3 \rightarrow$
$(Cp)Mo(CO)_2(L)_2^+ + (Cp)Mo(CO)_3^-$ (37)
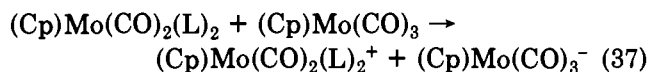
context of the radical chain in Scheme IV, the electron-transfer reaction in eq 37 represents a chain-termination step.

As suggested by Stiegman et al., under conditions where mono- and/or disubstitution is also occurring, photohomolysis of the substituted dimers $(Cp)_2Mo_2(CO)_5(L)$ or $(Cp)_2Mo_2(CO)_4(L)_2$ is potentially an additional source of the intermediate, $(Cp)Mo(CO)_2L$ in Scheme IV.[36] In fact, a possible origin for the formation of the substituted dimers is via recombination pathways involving the substituted and unsubstituted monomers

$(Cp)Mo(CO)_3 + (Cp)Mo(CO)_2(L) \rightarrow$
$(Cp)_2Mo_2(CO)_5(L)$ (38)

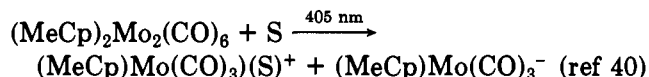$2(Cp)Mo(CO)_2L \rightarrow (Cp)_2Mo_2(CO)_4(L)_2$ (39)
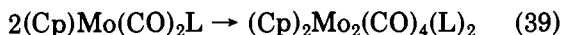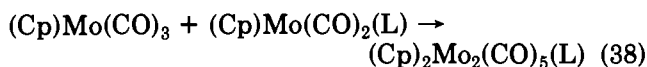
Including eq 38 and 39 provides a basis for the competition between disproportionation and substitution. The substituted dimers do undergo photochemically induced disproportionation in the presence of added L, but for the disubstituted dimers only if $Cp_2Mo_2(CO)_6$ is also present.

Although the reactions proposed to account for the observed photochemistry are reasonable, it is important to realize that there are no *direct* observations in support of the proposed steps. The failure to find a role for the CO-loss intermediate, $Cp_2Mo_2(CO)_5$, may be justifiable since its contribution could be negligible under conditions where $\phi_{dis} \gg 1$. However, under different conditions, $Cp_2Mo_2(CO)_5$ may play an important role, as it obviously also may in helping to account for the appearance of the monosubstituted products, $Cp_2Mo_2(CO)_5L$.

An observation in support of the importance of monomeric intermediates in substitution and disproportionation comes from 405-nm photolysis of (η^5-$CH_3C_5H_4)_2Mo_2(CO)_6$ in cyclohexane with added P(OCH$_3)_3$ (0.25 M).[50] Under these conditions substitution is favored over disproportionation as the incident light intensity is increased.[50] A possible origin for the effect is that at higher light intensities, the steady-state concentration of $CpMo(CO)_2(L)$ is higher which favors recombination because recombination is a second-order process, eq 39.

Of the 11 phosphines and phosphites studied by Stiegman, et al.,[36] photodisproportionation was strongly wavelength dependent for the sole case of PPh.[51] In hexane or cyclohexane, UV or visible photolysis of $Cp_2Mo_2(CO)_6$ (Cp = η^5-$CH_3C_5H_4$ or η^5-C_5H_5) in the presence of PPh$_3$ leads to monosubstitution and $Cp_2Mo_2(CO)_5(PPh_3)$. However, efficient photodisproportionation to give $CpMo(CO)_2(PPh_3)_2^+$ and $CpMo(CO)_3^-$ occurs only with UV photolysis. Again, without any direct evidence, it was suggested that UV photolysis may lead to a CO-bridged intermediate, $Cp(CO)_3Mo(\mu$-$CO)Mo(CO)(L)Cp$, via a higher excited state which is responsible for disproportionation. Another suggestion, which will be returned to later, was that UV photolysis leads to direct ionic dissociation via population of high vibrational levels of the $^1(\sigma\sigma^*)$ state of the Mo–Mo bond.

The photochemically induced (405 nm) disproportionation of (η^5-$CH_3C_5H_4)_2Mo_2(CO)_6$ by the anions Cl$^-$, Br$^-$, and I$^-$ (note eq 33) has been studied in the polar organic solvents acetone, Me_2SO, and acetonitrile.[40] Quantum-yield and photolysis studies at 405 nm have revealed several important features about these reactions. Quantum yields for disproportionation are independent of the nature of the anion (Cl$^-$, Br$^-$, I$^-$) and of the concentration of the anion. In the coordinating solvents Me_2SO and CH_3CN, disproportionation occurs even in the absence of added anions. Disproportion-

$(MeCp)_2Mo_2(CO)_6 + S \xrightarrow{405\ nm}$
$(MeCp)Mo(CO)_3(S)^+ + (MeCp)Mo(CO)_3^-$ (ref 40)
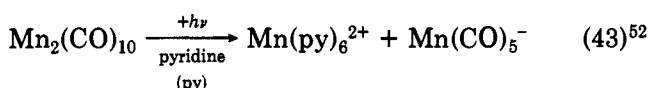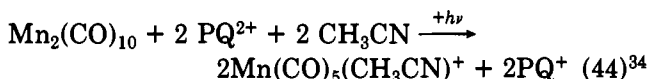
S is Me_2SO or CH_3CN

ation also occurs in acetone, but in acetone, the disproportionation products are observed at $-78\ ^\circ C$ but not at room temperature because re-formation of the metal–metal bond is too rapid.
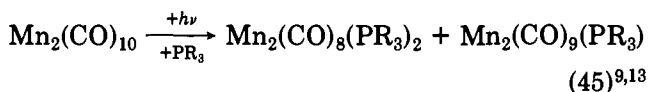
$(MeCp)Mo(CO)_3(S)^+ + (MeCp)Mo(CO)_3^- \rightarrow$
$$(MeCp)_2Mo_2(CO)_6 + S$$

$$S = \text{acetone}$$

The appearance of the products $(MeCp)Mo(CO)_3X$ in polar organic solvents occurs by anation of the initially formed solvento complexes

$$(MeCp)Mo(CO)_3(S)^+ + X^- \rightarrow (MeCp)Mo(CO)_3X$$

The disproportionation quantum yield varies linearly with $I^{-1/2}$ where I is the incident light intensity. At sufficiently low intensities, ϕ_{dis} values as high as 2.4 ± 1.0 were observed.

On the basis of the intensity dependence and values of $\phi_{dis} > 1$, it was proposed that the reactions in polar organic solvents proceed via the electron-transfer chain mechanism shown in Scheme V. With regard to the

SCHEME V

(i) $(MeCp)_2Mo_2(CO)_6 \xrightarrow{405 \text{ nm}} 2(MeCp)Mo(CO)_3$

(ii) $2(MeCp)Mo(CO)_3 \rightarrow (MeCp)_2Mo_2(CO)_6$

(iii) $(MeCp)Mo(CO)_3 + S \rightleftharpoons (MeCp)Mo(CO)_3(S)$

(iv) $(MeCp)Mo(CO)_3(S) + (MeCp)_2Mo_2(CO)_6 \rightarrow$
$(MeCp)Mo(CO)_3(S)^+ + (MeCp)Mo(CO)_3^- +$
$$(MeCp)Mo(CO)_3$$

(v) $(MeCp)Mo(CO)_3S + (MeCp)Mo(CO)_3 \rightarrow$
$$(MeCp)Mo(CO)_3(S)^+ + (MeCp)Mo(CO)_3$$

MeCp is η^5-$CH_3C_5H_4$, S is solvent

disproportionation chemistry, the first feature of note in Scheme V is the binding of S to $(MeCp)Mo(CO)_3$ in eq iii which, as noted later, is expected to greatly enhance the reducing ability of the monomer. The second is the proposed competition for $(MeCp)Mo(CO)_3(S)$ by the electron acceptors $(MeCp)_2Mo_2(CO)_6$ (eq iv) and $(MeCp)Mo(CO)_3$ (eq v). The dimer is present at higher concentration but, as noted later, the monomer is thermodynamically a better oxidant and is expected to react more rapidly. The variation in ϕ_{dis} with I—ϕ_{dis} = 0.64 ± 0.09 at I = 1540 × 10⁹ einsteins/min to ϕ_{dis} = 2.4 ± 1.0 at I = 3.35 × 10⁹ einsteins/min for $(MeCp)_2Mo_2(CO)_6$ (1.2 × 10⁻³ M) in acetone 0.1 M in $[N(n\text{-Bu})_4]Cl$—is consistent with comparable contributions for the two processes.[40]

When taken together, the results with halides obtained in THF compared to the results obtained in acetone, Me_2SO, or acetonitrile, point to an important role for the nature of the solvent. The absence of an X^- dependence for ϕ_{dis} in the polar organic solvents suggests that solvent binding leads to an enhanced electron-donating ability which triggers the capacity to undergo disproportionation. In THF where there is an anion dependence, the equilibrium in eq iii, Scheme V may lie to the left, or $(Cp)Mo(CO)_3(THF)$ may be less strongly reducing than are the complexes with Me_2SO, etc. However, the appearance of $(Cp)Mo(CO)_3Br^-$, either by binding of Br^- to $(Cp)Mo(CO)_3$ or by displacement of THF in $(Cp)Mo(CO)_3(THF)$, would be expected to lead to disproportionation because of the

ᵃ In THF at 22 ± 2 °C.

expected enhanced reducing abilities of $(Cp)Mo(CO)_3Br^-$.

In Scheme VI is provided a mechanistic summary of the events that occur after photolysis of $(\eta^5$-$C_5H_5)_2Mo_2(CO)_6$ in THF solution.

The suggestion has been made[42] that the triply bonded metal-metal dimer $(\eta^5$-$C_5H_5)(CO)_2Mo\equiv Mo(CO)_2(\eta^5$-$C_5H_5)$ appears via CO loss from $(\eta^5$-$C_5H_5)Mo(CO)_3$, followed by dimerization. A problem with

$$(\eta^5\text{-}C_5H_5)Mo(CO)_3 \rightarrow (\eta^5\text{-}C_5H_5)Mo(CO)_2 + CO$$

$$2(\eta^5\text{-}C_5H_5)Mo(CO)_2 \rightarrow (\eta^5\text{-}C_5H_5)_2Mo_2(CO)_4 \quad (40)$$

this mechanism is the experimental observation that at room temperature $(\eta^5$-$C_5H_5)_2Mo_2(CO)_4$ undergoes a rapid reaction with CO to return to $(\eta^5$-$C_5H_5)_2Mo_2(CO)_6$. If the mechanism above were correct, from microscopic reversibility, the reaction with CO would occur by initial cleavage of the triple bond, $(\eta^5$-$C_5H_5)(CO)_2Mo\equiv Mo(CO)_2(\eta^5$-$C_5H_5) \rightarrow 2(\eta^5$-$C_5H_5)Mo(CO)_2$, followed by capture of $(\eta^5$-$C_5H_5)Mo(CO)_2$ by CO. Kinetics data are apparently not available to test this mechanism but it seems unlikely that cleavage of the triply bonded dimer could be sufficiently facile at room temperature to accommodate the reaction with CO.

An alternate possibility is that $(\eta^5$-$C_5H_5)_2Mo_2(CO)_4$ arises from secondary photolysis of $(\eta^5$-$C_5H_5)_2Mo_2(CO)_5$ or $(\eta^5$-$C_5H_5)_2Mo_2(CO)_5(S)$ (S = solvent), eq 41. Recall

$$(\eta^5\text{-}C_5H_5)_2Mo_2(CO)_5 \xrightarrow{+h\nu} (\eta^5\text{-}C_5H_5)_2Mo_2(CO)_4 + CO \quad (41)$$

from the flash-photolysis results that $(\eta^5$-$C_5H_5)_2Mo_2(CO)_5$ absorbs light relatively strongly in the near UV and visible.

3. M₂(CO)₁₀ (M = Mn, Re)

The third type of metal-metal bonded system which has been studied in mechanistic detail is $M_2(CO)_{10}$ (M = Mn, Re). In the compounds, there is a direct metal-metal bond and no bridging-CO groups. As for the molybdenum and tungsten dimers there is an extensive net photochemistry for these compounds. The photochemical reactions observed include halogen abstraction

$$Mn_2(CO)_{10} \xrightarrow[CCl_4]{+h\nu} 2Mn(CO)_5Cl \quad (42)^9$$

disproportionation

$$Mn_2(CO)_{10} \xrightarrow[\substack{pyridine \\ (py)}]{+h\nu} Mn(py)_6^{2+} + Mn(CO)_5^- \qquad (43)^{52}$$

outer-sphere electron transfer

$$Mn_2(CO)_{10} + 2\ PQ^{2+} + 2\ CH_3CN \xrightarrow{+h\nu}$$
$$2Mn(CO)_5(CH_3CN)^+ + 2PQ^+ \quad (44)^{34}$$

$(PQ^{2+} = 1,1'\text{-dimethyl-4,4'-bipyridinium ion})$

and substitution

$$Mn_2(CO)_{10} \xrightarrow[+PR_3]{+h\nu} Mn_2(CO)_8(PR_3)_2 + Mn_2(CO)_9(PR_3)$$
$$(45)^{9,13}$$

In addition, trapping by radical scavengers, eq 1, and photochemically induced interchange, eq 3, have already been mentioned.

The mechanism of the photochemical reaction between $Mn_2(CO)_{10}$ and CCl_4 in cyclohexane has been studied in kinetic detail by Fox and Poe and found to be consistent with the pattern of reactions shown in Scheme I.[19] From their results they were able to derive quantum efficiencies for the production of both $Mn(CO)_5$ ($\phi = 0.30$) and a second intermediate ($\phi = 0.11$), and to obtain the rate constant ratio for the recombination of $Mn(CO)_5$ to give $Mn_2(CO)_{10}$ relative to the reaction between $Mn(CO)_5$ and CCl_4 ($k_3/k_4^{1/2}$) = 2.13 $M^{-1/2}$.

The results of a series of conventional[12,15,53-55] and laser-flash-photolysis[14] studies have been reported for $Mn_2(CO)_{10}$ and $Re_2(CO)_{10}$. In the laser experiments, 10-ns 337-nm light pulses from a N_2 laser were used to excite $Mn_2(CO)_{10}$ in cyclohexane.[14] Clear evidence was obtained for the appearance of two intermediates following the flash. The extent of formation of the two intermediates was linearly dependent on the incident light intensity showing that both were produced in a single photon process.

The shorter lived of the two intermediates absorbs in the low-energy visible with λ_{max} at 815 nm and returns to $Mn_2(CO)_{10}$ by second-order, equal-concentration kinetics with k = 1.9 × 10⁹ M^{-1} s^{-1}.[15] The results are in good agreement with those found by pulse radiolysis of $Mn_2(CO)_{10}$ in ethanol. In the pulse-radiolysis experiment, $Mn(CO)_5$ is produced with λ_{max} = 830 nm (ϵ = 800 cm⁻¹ M⁻¹), eq 46.

$$Mn_2(CO)_{10} \xrightarrow[C_2H_5OH]{e^-(solv)} Mn(CO)_5 + Mn(CO)_5^-$$

$$2Mn(CO)_5 \rightarrow Mn_2(CO)_{10} \qquad (46)$$
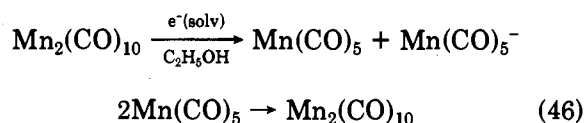
For the analogous Re dimer conventional flash photolysis also produces a short-lived intermediate with λ_{max} = 550 nm (cyclohexane)[15] or 535–540 nm (isooctane)[12] which also returns to the parent dimer by second-order, equal-concentration kinetics.[12,15,54] The recombination rate constants are k = 2.7 × 10⁹ M^{-1} s^{-1} (isooctane)[12] and k(22 °C) = 1.9–2.0 × 10⁹ M^{-1} s^{-1} in hexane[54] or cyclohexane.[15]

The flash-photolysis results suggest that the monomers $M(CO)_5$ (M = Mn, Re) appear upon photolysis. $Mn(CO)_5$ has been generated independently by photolysis of $HMn(CO)_5$,[20] in a CO matrix at 10–20 K, eq 9.

In the matrix, λ_{max} = 798 nm.[20] $Re(CO)_5$ has also been generated independently both by depositing Re atoms in a CO/Ar matrix at 10 K[56] and by pulse radiolysis of $Re(CO)_5X$ (X = Br, CH_3SO_3) in ethanol where for $Re(CO)_5$, λ_{max} = 535 nm (ϵ = 1000 ± 100 M^{-1} cm^{-1}).[12]

An interesting point of note is the use of the flash-photolysis kinetics data for $Mn_2(CO)_{10}$ to estimate the strength of the Mn–Mn bond.[53] The estimate was made by combining the rate constant and energy of activation obtained by flash photolysis for recombination, $2Mn(CO)_5 \rightarrow Mn_2(CO)_{10}$, with rate parameters obtained for thermal decomposition of $Mn_2(CO)_{10}$ in decalin.[57] Extrapolation of the thermal data to 25 °C gave for the metal–metal bond equilibrium in eq 47 the thermodynamic parameters indicated.

$$(CO)_5Mn-Mn(CO)_5 \rightarrow 2Mn(CO)_5 \qquad (47)$$
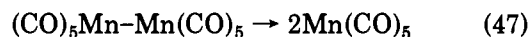
$$K(25\ °C) = 10^{-20}$$

$$\Delta H = 36\ kcal\ mol^{-1}$$

$$\Delta S(25\ °C) = 32\ eu$$

In addition to photochemically induced homolysis of the metal–metal bond, clear evidence is also obtained for additional intermediates based on the transient behavior following flash photolysis.[14,15] In particular, for the Mn_2 dimer the difference spectra in Figure 3 provide direct evidence for the existence of a relatively long-lived intermediate having λ_{max} 495 nm which, as noted later, appears to be $Mn_2(CO)_9$ The long-lived intermediate returns to $Mn_2(CO)_{10}$ with $k \leq 1.2 \times 10^5$ M^{-1} s^{-1} in cyclohexane.[14] The reappearance kinetics are clearly reminiscent of the situation observed for (η^5-$C_5H_5)_2Mo_2(CO)_6$ suggesting that photochemically induced loss of CO occurs followed by its thermal recapture by CO, eq 48. Recall also from the results of picosecond experiments in ethanol that the two intermediates are present in solution after 25 ps.

$$Mn_2(CO)_{10} \xrightarrow{+h\nu} Mn_2(CO)_9 + CO$$

$$Mn_2(CO)_9 + CO \rightarrow Mn_2(CO)_{10} \qquad (48)$$
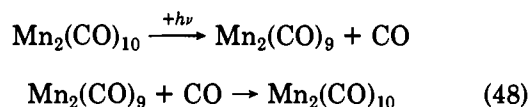
The situation for $Re_2(CO)_{10}$ is more complicated.[12,15] For the Re_2 dimer, intermediates analogous to both the short- and long-lived transients for $Mn_2(CO)_{10}$ are observed having $\lambda_{max} \sim 550$ nm and $\lambda_{max} \sim 500$ nm, respectively, and both return to $Re_2(CO)_{10}$.[15] The short-lived intermediate, $Re(CO)_5$, returns to $Re_2(CO)_{10}$ by second-order, equal-concentration kinetics with k(22 °C) = 2 × 10⁹ M^{-1} s^{-1} in hydrocarbon solvents.[12,15,54] For the longer lived intermediate, return to $Re_2(CO)_{10}$ occurs with $t_{1/2} \sim 100$ ms. In fact, a third, relatively unimportant intermediate having $\lambda_{max} \sim 375 \pm 10$ nm may also exist which returns to the starting dimer but on a time scale long compared to 5 s.[15] Possible evidence for a third, long-lived intermediate for $Mn_2(CO)_{10}$ has also been obtained by flash photolysis but it is clear that if the intermediate is present, it represents a miniscule component of the overall photochemical events at least in terms of the efficiency of its appearance on a per photon basis. In later work by Yesaka, et al.,[14] the importance of purging by dry N_2 before freeze-pump–thaw cycles is noted and it is suggested that the long-lived transient could only be observed when cy-

clohexane was insufficiently deoxygenated before dissolution. In another report, flash photolysis of the manganese dimer in a vacuum-degassed solution led to a complex transient behavior.[54] Intermediates were observed which absorb strongly in the 350–500-nm region and grew in and disappeared in the time interval 50–100 ms. The pattern of absorbance vs. time change was complex and a partly successful but complicated mechanistic scheme was proposed involving photochemically induced homolysis followed by loss of CO from $Mn(CO)_5$ and recombination to give dimeric species deficient in CO. However, more recent work suggests that the origin of the complex absorbance–time changes can be attributed to an experimental artifact.[55]

Flash photolysis of $Mn_2(CO)_{10}$ in cyclohexane in the presence of CCl_4 or potential ligands like nitriles or phosphines has provided direct evidence for the details of the photochemical reaction mechanisms.[14,15] For example, the results show that reactions occur between CCl_4 and *both* $Mn(CO)_5$ and $Mn_2(CO)_9$ in cyclohexane.[15] The reaction between $Mn(CO)_5$ and CCl_4 is first order in both reactants. For $Mn_2(CO)_9$, the evidence for a reaction with CCl_4 in cyclohexane is indirect. At low concentrations of CCl_4 where recombination of $Mn(CO)_5$ to give $Mn_2(CO)_{10}$ is sufficiently rapid that its reaction with CCl_4 is not competitive, net photochemistry with CCl_4 continues to occur.

In solutions which are dilute in added PPh_3 $(10^{-3} M)^{15}$ or $P(n\text{-}Bu)_3$, the rate constant for recombination of $Mn(CO)_5$ to give $Mn_2(CO)_{10}$ is unaffected showing that under these conditions there is no reaction between $Mn(CO)_5$ and the phosphines. However, direct observation by laser-flash photolysis shows that $Mn_2(CO)_9$ does react with added phosphines to give $Mn_2(CO)_9$-(PR_3). With $P(n\text{-}Bu)_3$ as the added phosphine, $k = (1.0 \pm 0.1) \times 10^9 M^{-1} s^{-1}$. Additional evidence that $Mn_2(CO)_9$ is involved in net photosubstitution comes from a variety of experiments: (1) When hydrocarbon matrices at 77 K containing $Mn_2(CO)_9$ and PPh_3 $(10^{-2} M)$ are warmed to room temperature, $Mn_2(CO)_9(PPh_3)$ appears as a product.[21] (2) Near ultraviolet photolysis of $Mn_2(CO)_{10}$ in hydrocarbon solvents in the presence of $10^{-2} M$ PPh_3 results in the production of *both* mono-, $Mn_2(CO)_9(PPh_3)$, and disubstituted, $Mn_2(CO)_8(PPh_3)_2$, dimers.[21] (3) Photolysis of $Mn_2(CO)_{10}$ in acetonitrile solution gives only the monosubstituted product, $Mn_2(CO)_9(CH_3CN)$.[21] (4) The independent generation of $Mn(CO)_5$ in acetonitrile by the one-electron, outer-sphere oxidation of $Mn(CO)_5^-$ by $Fe(\eta^5\text{-}C_5H_5)_2^+$ gives only $Mn_2(CO)_{10}$ as a product showing that $Mn(CO)_5$ does *not* undergo substitution of CH_3CN for CO.[21]

The results described above show that in hydrocarbon solutions dilute in PPh_3 or nitriles, or in CH_3CN solution, photochemical substitution appears to occur *solely* through the longer lived intermediate, $Mn_2(CO)_9$. However, at higher phosphine concentrations in cyclohexane—$[PPh_3] = 0.1 M^{15}$ or $[(P(n\text{-}Bu)_3] = 2 \times 10^{-2} M$—where the major photochemical product is $Mn_2\text{-}(CO)_8(PR_3)_2$, direct evidence for a reaction between $Mn(CO)_5$ and PR_3 has been obtained by laser- and conventional-flash photolysis.[14,15] Under these conditions the bimolecular recombination of $Mn(CO)_5$ to give $Mn_2(CO)_{10}$ is quenched. It is replaced by a first-order transient process with $k(22 °C) = 205 s^{-1}$, $[(PPh_3)] = 0.1 M^{15}$. Difference spectral studies near 800 nm where $Mn(CO)_5$ absorbs show that a new intermediate is

produced which absorbs in the same region.

From these observations, at $10^{-1} M$ PPh_3 $Mn(CO)_5$ must be captured by PPh_3, at least in part, before recombination to give $Mn_2(CO)_{10}$ can occur, eq 49. In

$$Mn(CO)_5 + PPh_3 \underset{k=1.9\times10^9 M^{-1} s^{-1}}{\overset{k>2\times10^5 M^{-1} s^{-1}}{\rightleftharpoons}} Mn(CO)_5PPh_3$$

(49)
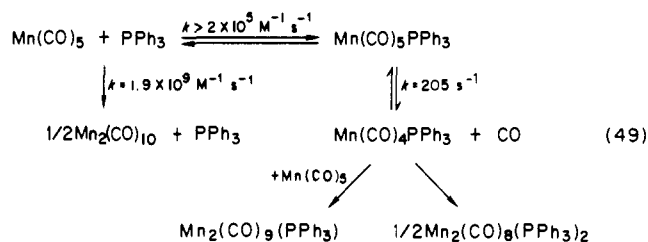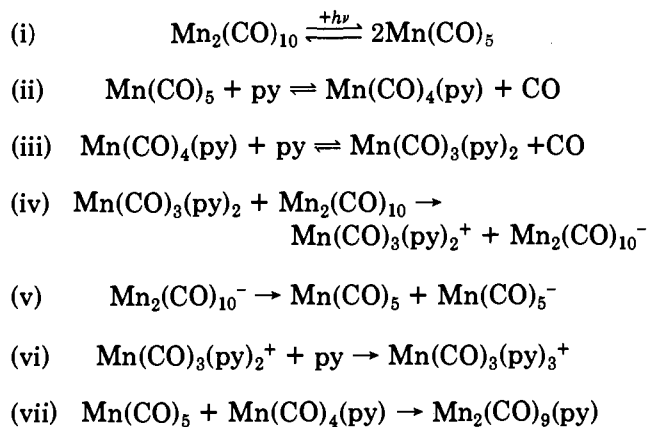
order to be consistent with the experimental observations, the initial reaction between $Mn(CO_5$ and PR_3 must be associative in nature giving the six-coordinate intermediate, $Mn(CO)_5PR_3$.[14,15] Presumably, the first-order transient process observed by flash photolysis involves loss of CO from $Mn(CO)_5(PPh_3)$ to give $Mn(CO)_4(PPh_3)$. Once formed, $Mn(CO)_4(PPh_3)$ is known to undergo rapid dimerization with $Mn(CO)_4(PPh_3)$ to give $Mn_2(CO)_8(PPh_3)_2^{55}$ and, no doubt, with $Mn(CO)_5$ as well to give $Mn_2(CO)_9(PPh_3)$. In the presence of 1 atm of CO, there is no evidence for $Mn(CO)_6$ since the rate constant for recombination of $Mn(CO)_5$ is unaffected.[15] However, this could be a consequence of the limited quantity of dissolved CO under these conditions.

The rate constant for the reaction between $Mn(CO)_5$ and PPh_3 in eq 49 was estimated by assuming that $[Mn(CO)_5] = 2[Mn_2(CO)_{10}] = 10^{-5} M$ after the flash, that the ratio of PPh_3 capture to recombination is >0.9; the values $[PPh_3] = 0.1 M$ and $k = 1.9 \times 10^9 M^{-1} s^{-1}$ for the recombination reaction were also used.

The photochemically induced disproportionation of $Mn_2(CO)_{10}$ in pyridine (py) and substituted pyridines[47] and by four amine bases in hexane[58] has been studied. Photolysis (366 nm) of $Mn_2(CO)_{10}$ in pyridine leads to the concurrent formation of $Mn_2(CO)_9(py)$ and equal amounts of $Mn(CO)_3(py)_3^+$ and $Mn(CO)_5^-$. The cation $Mn(CO)_3(py)_3^+$ is unstable under these conditions and with extended photolysis gives $Mn(py)_6^{2+}$. The relative amount of $Mn_2(CO)_9(py)$ formed initially is enhanced in the presence of CO. Disproportionation in the presence of the radical trap galvinoxyl is somewhat inhibited. Based on these observations, the mechanism in Scheme VII was proposed in which photochemically induced Mn–Mn bond cleavage is followed by substi-

SCHEME VII[58]

(i) $Mn_2(CO)_{10} \overset{+h\nu}{\rightleftharpoons} 2Mn(CO)_5$

(ii) $Mn(CO)_5 + py \rightleftharpoons Mn(CO)_4(py) + CO$

(iii) $Mn(CO)_4(py) + py \rightleftharpoons Mn(CO)_3(py)_2 + CO$

(iv) $Mn(CO)_3(py)_2 + Mn_2(CO)_{10} \rightarrow$
$\qquad\qquad\qquad Mn(CO)_3(py)_2^+ + Mn_2(CO)_{10}^-$

(v) $Mn_2(CO)_{10}^- \rightarrow Mn(CO)_5 + Mn(CO)_5^-$

(vi) $Mn(CO)_3(py)_2^+ + py \rightarrow Mn(CO)_3(py)_3^+$

(vii) $Mn(CO)_5 + Mn(CO)_4(py) \rightarrow Mn_2(CO)_9(py)$

tution of py for CO to give $Mn(CO)_3(py)_2$. In the scheme the disubstituted monomer was suggested to be a sufficiently strong electron donor to reduce $Mn_2(CO)_{10}$ to $Mn(CO)_5 + Mn(CO)_5^-$, presumably through $Mn_2(CO)_{10}^-$.
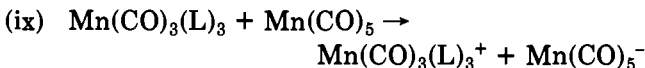
The substitutional steps in eq ii and iii in Scheme VII were originally written as occurring via initial dissociative loss of CO from $Mn(CO)_5$, e.g., $Mn(CO)_5 \rightarrow Mn(CO)_4 + CO$, as suggested in earlier work.[59,60] However, the results cited above[14,15] and additional results obtained from kinetic studies based on $Mn(CO)_5$ and $Re(CO)_5$, suggest that the reactions occur via associative mechanisms.[61-63] This is an important point when electron-transfer steps are involved as they are in Scheme VII, as noted in a later section, based on energetic considerations it is very likely that preassociation of a third pyridine group to $Mn(CO)_3(py)_2$ to give $Mn(CO)_3(py)_3$ occurs prior to electron transfer.

McCullen and Brown note that an interesting aspect of the photochemistry is the absence of the disubstituted product $Mn_2(CO)_8(py)_2$ and speculate that steric effects prevent recombination of $Mn(CO)_4(py)$.[47] However, this explanation seems unlikely given the appearance of disubstituted products in the presence of phosphines.[9,13,14] Given the observed photochemistry of $Mn_2(CO)_{10}$ in the presence of nitriles, an alternate possibility is that the initial step in the photolysis scheme involves pyridine capture of $Mn_2(CO)_9$ to give $Mn_2(CO)_9(py)$.

The importance of a radical chain component in the disproportionation chemistry has been demonstrated by photolysis (366 nm) of $Mn_2(CO)_{10}$ in hexane in the presence of added nitrogen bases.[58] Although quantum yields are low for unidentate bases ($\phi = 0.1$ for pyridine), they are enhanced for the bidentate chelate trimethylethylenediamine ($\phi = 1.2$) and for the potential terdentate ligand diethylenetriamine (dien, $NH_2CH_2CH_2NHCH_2CH_2NH_2$), they exceed 1 by a considerable degree ($\phi = 6-19$). Given their results, Stiegman and Tyler propose that Scheme VII should be modified by replacing the key electron-transfer step in eq iv by

(viii) $Mn(CO)_3(L)_3 + Mn_2(CO)_{10} \rightarrow$
$$Mn(CO)_3(L)_3^+ + Mn_2(CO)_{10}^-$$
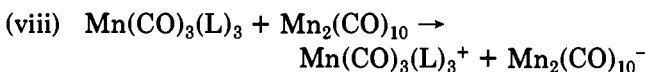
and including the chain-termination step

(ix) $Mn(CO)_3(L)_3 + Mn(CO)_5 \rightarrow$
$$Mn(CO)_3(L)_3^+ + Mn(CO)_5^-$$

The authors also note that the disproportionation chemistry is induced in solutions containing $Mn_2(CO)_{10}$ and dien to which sodium dispersed in mineral oil had been added. The authors propose that in their experiment $Mn_2(CO)_{10}$ is reduced to $Mn_2(CO)_{10}^-$ which enters the disproportionation cycle through eq v in Scheme VII. However, for completeness it should be noted that in neither the experiments in pyridine nor the experiments in hexane with added base was a role assumed for $Mn_2(CO)_9$.

The results of low-temperature photolyses of $Mn_2(CO)_{10}$ (at 77 K in frozen methylcyclohexane or 3-methylpentane) have provided evidence for the appearance and structure of $Mn_2(CO)_9$.[21] Free CO ($\nu(CO)$ = 2132 cm^{-1}) appears as does a new intermediate with modified $\nu(CO)$ frequencies in the terminal-CO region

SCHEME VIII[a]
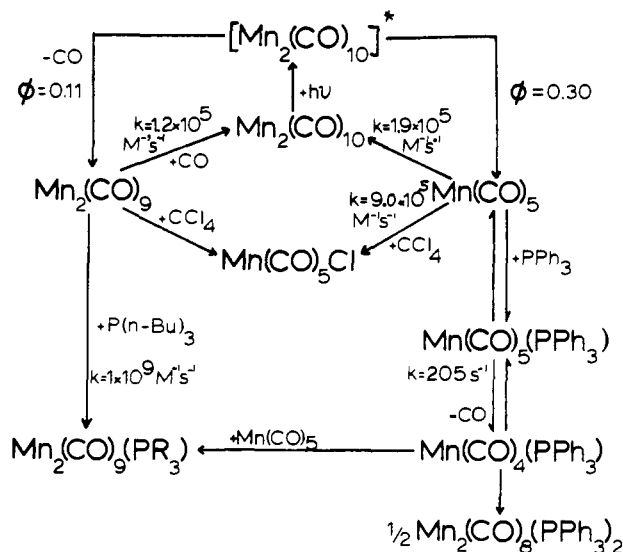
^{a} Cyclohexane at 22 °C

and a new band in the bridging CO region at 1760 cm^{-1}. The photointermediate is thought to be $Mn_2(CO)_9$ in which there is a bridging-CO group. Photolysis of $Mn_2(CO)_{10}$ in 2-methyltetrahydrofuran (2-MeTHF) at 77 K gives a photoproduct in which there are no bridging-CO groups and whose infrared spectrum is consistent with the 2-MeTHF-substitution product, $Mn_2(CO)_9(2\text{-MeTHF})$.[21]

When hydrocarbon matrices containing $Mn_2(CO)_9$ and PPh_3 are warmed to room temperature, the product is $Mn_2(CO)_9(PPh_3)$. However, the reaction between $Mn_2(CO)_9$ and CCl_4 is apparently relatively slow compared to capture by nucleophiles. When hydrocarbon matrices with CCl_4 added, or with both CCl_4 and PPh_3 added, are warmed, the products are $Mn_2(CO)_{10}$ and $Mn_2(CO)_9(PPh_3)$. Apparently, capture of $Mn_2(CO)_9$ by CO released in the matrix is competitive with capture by CCl_4 in the first experiment, but PPh_3 is an effective competitor with CO in the second.[21] It has been possible to estimate that $Mn_2(CO)_9$ is formed in 30 ± 5% of the yield of $Mn(CO)_5$ by observing product ratios following photolysis of $Mn_2(CO)_{10}$ in hydrocarbon solvents to which CCl_4 and PPh_3 or CH_3CN had been added. The analysis was based on the relative amounts of $Mn(CO)_5Cl$ and $Mn_2(CO)_9(L)$ (L = PPh_3 or CH_3CN) which formed and took advantage of the fact that CCl_4 is not a competitive scavenger for $Mn_2(CO)_9$ under these conditions.

The mechanistic details associated with the photochemistry of $Mn_2(CO)_{10}$ in cyclohexane at 22 °C are summarized in Scheme VIII. One of the notable features of the scheme is the evidence from the picosecond experiment that both $Mn(CO)_5$ and $Mn_2(CO)_9$ are probably primary photoproducts. Another is a happy coincidence between results obtained from the kinetic analysis of Fox and Poë[19] and the matrix experiments of Hepp and Wrighton.[21] From their data, Fox and Poë derived quantum efficiencies for the appearances of $Mn(CO)_5$ ($\phi = 0.30$) and $Mn_2(CO)_9$ ($\phi = 0.11$) which are in the ratio 3:1 as predicted from the competition studies of Hepp and Wrighton. ϕ values obtained by direct observation using laser-flash photolysis gave ϕ = 0.3 for both intermediates.[14] However, the product

SCHEME IX
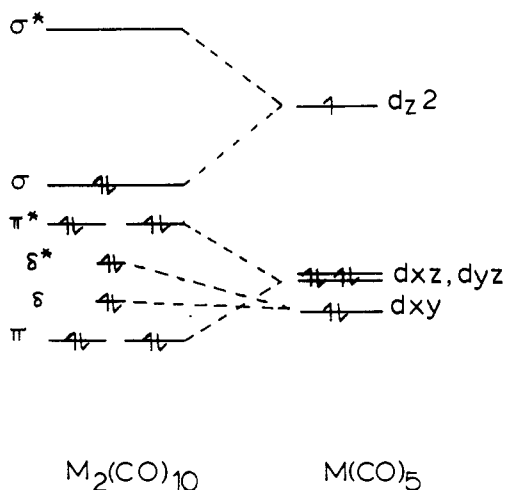
ratio of 1:3 for $Mn_2(CO)_9(P(n\text{-Bu})_3)$ compared to $Mn_2(CO)_8(P(n\text{-Bu})_3)_2$ obtained by photolysis of Mn_2-$(CO)_{10}$ in the presence of excess $P(n\text{-Bu})_3$ also suggests a ratio of 1:3 for the two efficiencies.[14] On the other hand, Fox and Poë also derived the ratio of rate constants for the recombination of $Mn(CO)_5$ relative to its reaction with CCl_4 to be $k_3/k_4^{1/2} = 2.1$. The same ratio but obtained by direct measurement of each of the rate constants in hexane by conventional flash photolysis gives $k_3/k_4^{1/2} = 31.$[64] At least part of the discrepancy may arise from the failure of Fox and Poë to account for the reaction between $Mn_2(CO)_9$ and CCl_4 and the fact that their data were extended to very low concentrations leading to large experimental uncertainties.

B. The Photolysis Step

1. Photolysis and Electronic Structure

$Mn_2(CO)_{10}$. The electronic structures of the dimers $M_2(CO)_{10}$ (M = Mn, Re) have been studied both theoretically[5,65] and by photoelectron spectroscopy (PES).[66] The schematic molecular-orbital energy diagram in Scheme IX for $Mn_2(CO)_{10}$ is based on the results of these studies. In the scheme a relative ordering of the levels, which are significantly metal based, is indicated. The labels σ, π, and δ refer to the symmetries of the various metal-based molecular orbitals with regard to the metal-to-metal bond. The combinations of d orbitals on each metal atom used to construct the molecular orbitals are also indicated.

For the dimers $M_2(CO)_{10}$ (M = Mn, Re) intense bands appear in the ultraviolet which have been assigned to optical excitation of an electron from the σ to the σ^* orbitals of the metal-to-metal bond.[5] For example, for $Mn_2(CO)_{10}$ in cyclohexane a band appears at $\lambda_{max} = 324$ nm with $\epsilon = 21\,400$. The electronic structural details associated with excitations of this kind can be considered, at least in qualitative detail, based on calculated results for the excited states of H_2 by Coulson and Fischer.[67] In their calculations, Coulson and Fischer determined the relative energies of the ground (σ^2) and ($\sigma\sigma^*$) excited states for H_2 as a function of the H–H normal coordinate. Their results are illustrated in a schematic way in Figure 4 but using as the example $Mn_2(CO)_{10}$ and energy variations along a normal coordinate largely Mn–Mn in character. It is
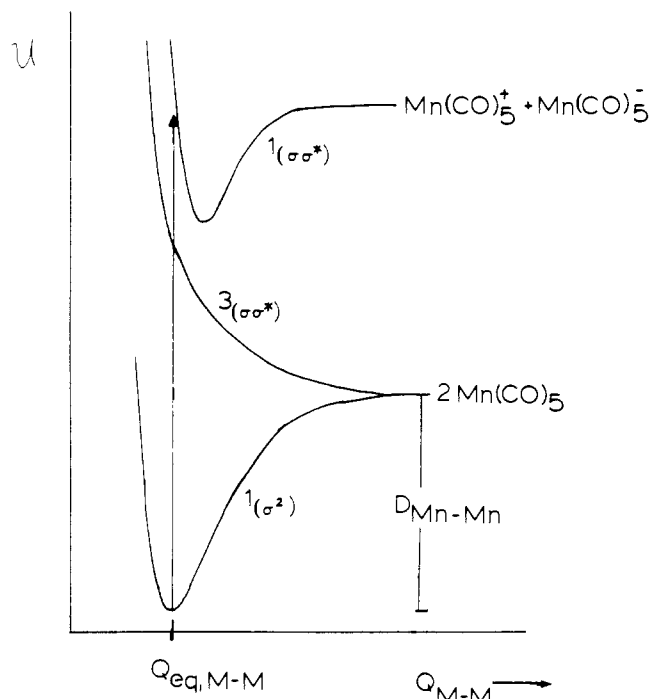
Figure 4. Schematic energy–normal coordinate diagram for the ground, σ^2, and $\sigma\sigma^*$ excited states of $Mn_2(CO)_{10}$ along a normal coordinate largely Mn–Mn in character.

dangerous to extrapolate results for H_2 to multielectron atoms but similar features exist in the excited state structure of analogous but electronically more complex diatomic molecules. The diagram in Figure 4 is only qualitative but the result is of value in suggesting the origins of electronic absorption bands and the possible photochemical consequences of optical photochemical excitation.

From Figure 4, the intense absorption band in the ultraviolet can be assigned to the transition, $^1(\sigma^2) \rightarrow {}^1(\sigma\sigma^*)$. Electronically, the resulting "singlet" excited state correlates with the disproportionation products $Mn(CO)_5^+$ and $Mn(CO)_5^-$. In the disproportionation products, the electron pair of the metal–metal bond is localized on one of the atoms at infinite separation. An important feature of the diagram is the fact that the excited singlet state is predicted not to be dissociative in character but that the lower lying "triplet" state is.

Electronically, the triplet state, $^3(\sigma\sigma^*)$, correlates with the isolated neutral monomers with unpaired spins aligned, $(CO)_5Mn(\uparrow)...$, $(\uparrow)Mn(CO)_5$. In the formation of the $^1(\sigma^2)$ ground state, the unpaired spins become paired in the formation of the metal–metal bond. The excited singlet state is nondissociative, although higher in energy than the isolated monomers, because of attractive ionic terms associated with its electronic distribution. The ionic terms arise because in the configuration $\sigma(\uparrow)\sigma^*(\downarrow)$ both electrons are somewhat localized on a single Mn atom given the nodal properties of the σ^* orbital. The resulting $M^+...M^-$ interactions lead to the minimun in the potential curve.

The triplet state, $\sigma(\uparrow)\sigma^*(\uparrow)$, is always lower in energy than the excited singlet state because electron–electron correlation tends to keep electrons with parallel spins as separated in the isolated atoms as possible in order to minimize electron–electron repulsion.[68] At the same time, the triplet state is dissociative because of the antibonding nature of σ^* and the absence of attractive ionic terms. As shown in Figure 4 for $^3(\sigma\sigma^*)$, for a

dissociative state there is no internuclear separation distance at which a minimum appears in the potential curve and the interaction between initial atoms is always repulsive. The potential curve in Figure 4 for $^3(\sigma\sigma^*)$ is overly simplistic. In fact, in solutions a shallow minimum or minima are expected to exist at M–M internuclear separations past the M–M bond distance because of ·Mn(CO)$_5$/·Mn(CO)$_5$ van der Waals interactions and because of the necessity of the Mn(CO)$_5$ fragments to escape from the surrounding solvent cage before their translational and rotational motions become uncorrelated.

In Figure 4, the relative energies associated with the absorption maximum for Mn$_2$(CO)$_{10}$ in cyclohexane (324 nm, 88 kcal/mol) and the metal–metal bond dissociation energy estimated kinetically ($\Delta H \sim 36$ kcal/mol)[53] are indicated. In the gas phase, the dissociation energy for the Mn–Mn bond is 24.9 ± 0.7 kcal/mol.[69] It is not possible to estimate the energy of the disproportionation products above the isolated monomers. However, the appearance of photochemically induced disproportionation could clearly depend profoundly on the solvent both in providing a solvation energy for the ionic products, and ultimately, a sixth ligand for the cationic fragment, e.g., Mn(CO)$_5^+$ + CH$_3$CN → Mn(CO)$_5$(CH$_3$CN)$^+$.

For metal–metal bonds between transition metals, the model on which Figure 4 is based is obviously too simplistic. For example, spin-orbit coupling can cause considerable mixing of pure "singlet" and "triplet" states. The resulting states of mixed spin character and how they vary with the M–M separation distance could well be more complicated than suggested in Figure 4. Nonetheless, as noted above, if the ideas illustrated are at least qualitatively correct, they provide a convenient rationale for many of the features which appear in the spectroscopy and photochemistry of metal–metal bonds.

The energy-coordinate diagram in Figure 4 shows the $^1(\sigma\sigma^*)$ state as *not* being dissociative, but heretofore, no evidence has been obtained for its existence, for example, from emission studies. The inability to observe such a state is not too surprising since with spin-orbit coupling, interconversion between the singlet and triplet states $^{1,3}(\sigma\sigma^*)$ could be quite facile. Since the triplet state is predicted to be dissociative once formed, it has available an efficient mechanism for the dissipation of the excess energy of excitation by dynamic M–M bond cleavage to give 2Mn(CO)$_5$ and vibrational excitation of Mn–C modes in the resulting fragments.[70] The excess energy must ultimately appear in the low-frequency, collective modes of the solvent following dynamic interchange with surrounding solvent molecules.

The results of gas-phase molecular beam experiments on M$_2$(CO)$_{10}$ (M = Mn, Re) are consistent with the predictions of Figure 4.[70] Photolysis of a molecular beam of Re$_2$(CO)$_{10}$ molecules with 300-nm (95.2 kcal/mol) light results in the appearance of Re(CO)$_5$ monomers. The lifetime of the initial state is shorter than a few picoseconds. Translationally, the monomers produced are polarized along the metal–metal bond axis, eq 50, consistent with the assignment of the intense absorption band to the $^1(\sigma^2) \rightarrow {}^1(\sigma\sigma^*)$ transition which is also polarized along the metal–metal axis.[65] On the basis of a Re–Re bond energy of 51.1 kcal/mol the excess energy in the photolysis beam (44 kcal/mol)

SCHEME X
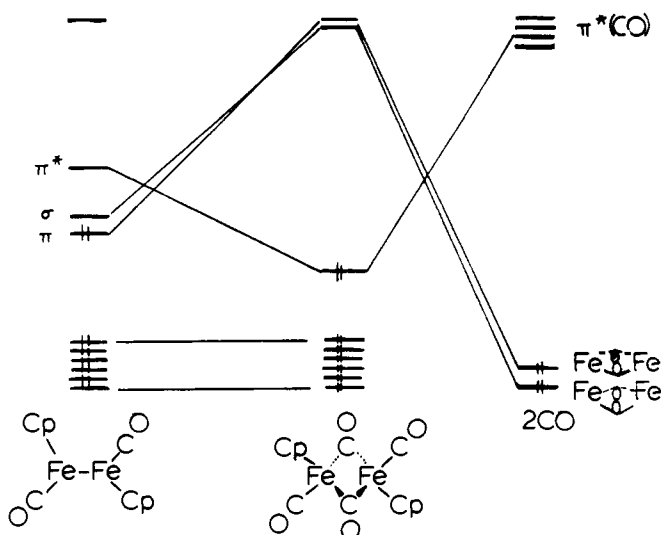
appears as $\sim 1/3$ translational energy and $\sim 2/3$ vibrational energy, eq 50.

$$\text{Re}_2(\text{CO})_{10}(g) \xrightarrow{+300 \text{ nm}} [\text{Re}_2(\text{CO})_{10}(g)]^* \rightarrow$$
$$2\text{Re}(\text{CO})_5(g) \text{ (Re–Re polarized)}$$

$$\tau < 1\text{–}2 \text{ ps} \tag{50}$$
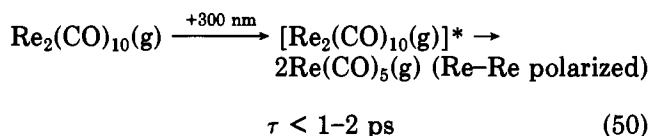
Although the gas-phase photolysis experiment shows evidence only for metal–metal bond dissociation, it should be recalled that, in solution and low-temperature matrices, good evidence is available for both metal–metal dissociation and loss of CO. The point is worth noting since it suggests that the appearance of primary photoproducts and the nature of the initial photochemical act may well be different in detail between the gas phase and solution.

(η^5-C$_5$H$_5$)$_2$M$_2$(CO)$_4$ (M = Fe, Ru). As mentioned in an earlier section, the η^5-cyclopentadienyl iron dimer exists in solution largely as CO-bridged cis and trans isomers. For the ruthenium dimer, the non-CO-bridged isomer is an important contributor. For the non-CO-bridged isomer, the d configurations at the individual metal atoms, d^7, and coordination numbers, counting the η^5-C$_5$H$_5$ ligand as occupying three coordination sites, are formally the same as for the dimers M$_2$(CO)$_{10}$ (M = Mn, Re). Consequently, a related pattern of electronic levels may exist leading to the assignment of intense bands in the ultraviolet to the $^1(\sigma^2) \rightarrow {}^1(\sigma\sigma^*)$ transition of the metal–metal bond.

However, for the CO-bridged isomers, the situation appears to be quite different. The results of a low-temperature X-ray study suggest that there is *no* significant, direct through-space bonding between the iron atoms at least in the trans isomer of the iron dimer.[71] Bonding schemes for the dimer have been derived[72,73] which give rise to the ordering of levels shown in Scheme X.[72] The bonding scheme is derived from a combination of molecular orbitals appropriate for the fragment *trans*-(η^5-C$_5$H$_5$)$_2$Fe$_2$(CO)$_2$ and combinations arising from overlap between orbitals localized on the bridging-CO ligands. When the CO-based orbitals are mixed with the metal-based levels of the dimeric fragment, the orbitals which originally carried the σ and π interactions between metals are destabilized and become largely antibonding in character. In addition,

mixing between the nominally π^* level of the metal–metal bond and higher energy $\pi^*(CO)$ orbitals localized on the CO ligands stabilize the $\pi^*(M–M)$ level to such a degree that it becomes the highest occupied level in the CO-bridged structure. In the final scheme the molecular orbitals are strongly mixed combinations of metal- and CO-based orbitals. An interesting feature of the scheme is that it predicts that the intense, ultraviolet absorption band in the CO-bridged isomer has its origin in a $\pi \rightarrow \pi^*$ transition localized on the bridging framework where the molecular orbitals involved are of a mixed, metal-bridging ligand character. Regardless of the precise composition of the orbitals, the electronic nature of the transition is presumably $^1(\pi^2) \rightarrow {}^1(\pi\pi^*)$ and the lower lying, largely triplet states, $^3(\pi\pi^*)$, could well be dissociative or slightly bonding with regard to the bridge, leading to fragmentation. However, once again, the flash photolysis and low-temperature matrix photolysis evidence for the appearance of both $(\eta$-$C_5H_5)Fe(CO)_2$ and $(\eta$-$C_5H_5)_2Fe_2(CO)_3$ upon photolysis should be recalled. Further, the observed pattern of photochemistry occurs whether photolysis is carried out either in the ultraviolet or in the visible where there are absorption bands of lower intensity. Although the rationale offered above for the electronic structure may account for homolysis and the appearance of $(\eta^5$-$C_5H_5)Fe(CO)_2$, the origin of the CO-loss intermediate remains obscure.

$(\eta^5$-$C_5H_5)_2M_2(CO)_6$ (M = Mo, W). The molybdenum and tungsten cyclopentadienyl dimers have non-CO-bridged structures and spectra which are reminiscent of the spectrum of $Mn_2(CO)_{10}$ in that there are both intense bands in the ultraviolet and bands of lower intensity in the visible, note Figure 1. Although detailed calculational or experimental information on the electronic structure of these dimers is not available, it seems reasonable, at least qualitatively, that the ultraviolet bands are the expected $^1(\sigma^2) \rightarrow {}^1(\sigma\sigma^*)$ transitions localized at the M–M bond. One basis for such assignments is that the intense bands in the ultraviolet appear only for the dimers and not for related monomers like $(\eta^5$-$C_5H_5)Mo(CO)_3Cl$ or $(\eta^5$-$C_5H_5)Mo(CO_3^-$. If the electronic structures are analogous to those for $M_2(CO)_{10}$ (M = Mn, Re), optical excitation to $^1(\sigma\sigma^*)$ followed by conversion to $^3(\sigma\sigma^*)$ would be expected to lead to the photochemically induced homolysis of the metal–metal bonds. However, recall that there is also clear evidence from flash photolysis and photochemical matrix isolation photolysis experiments for the presence of the CO-loss intermediate, $(\eta^5$-$C_5H_5)_2Mo_2(CO)_5$.

There is also direct evidence from the picosecond emission experiments of Morgante and Struve[46] for the intervention of higher excited states when photolysis is carried out in the ultraviolet. The higher energy states may have different electronic origins. One possibility is that they are metal-to-ligand charge transfer (MLCT) in character involving optically induced charge transfer between metal $d\pi$ levels and π^* levels localized on either the CO or $(\eta^5$-$C_5H_5)$ ligands. Based on such an assignment, the initially observed state with $\tau < 10 \pm 3$ ps could be the largely "singlet" partner of a longer lived "triplet" state with $\tau \sim 4$–5 ns (M = Mo) with both states having the same orbital origin.

2. Appearance Efficiencies, Solvent Cage Effects

Appearance efficiencies and subsequent reactivities

of the photochemically produced intermediates can depend upon the nature of the surrounding medium. Consider as an example the data in eq 51.[18] The data

$$(\eta^5\text{-}C_5H_5)_2W_2(CO)_6 \xrightarrow[+CCl_4]{+h\nu} 2(\eta^5\text{-}C_5H_5)W(CO)_3Cl \quad (51)$$
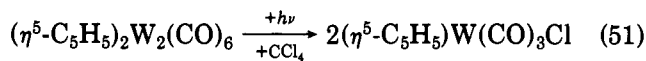
medium	ϕ
CCl$_4$	0.34
THF, 0.083 M in CCl$_4$	0.49

show that the efficiency of loss of the dimer is actually higher in a dilute solution of CCl$_4$ in THF than in the neat solvent.

Given the nature of the initial photochemical act, the existence of such effects is not surprising. They can be discussed in the context of the outline of reactions in Scheme XI which uses $Mn_2(CO)_{10}$ as the example.

SCHEME XI
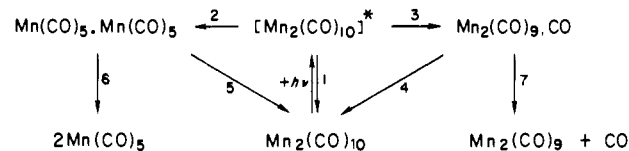

The initial optical excitation occurs on a time scale of $\sim 10^{-15}$ s and for $Mn_2(CO)_{10}$ two intermediates are observed in the solution after 25 ps. Even before the appearance of the free intermediates, there exist a series of medium-dependent, competitive processes which can influence appearance efficiencies and through them, photochemical quantum yields. For example, the initially populated electronic excited state could undergo nonradiative decay processes via energy loss through intramolecular vibrations and dynamic interchange with the solvent (reaction 1 in Scheme XI) in competition with the dynamic processes necessary to produce the intermediates (reactions 2 and 3). For the CO-loss intermediate the surrounding solvent could conceivably play a role both in assisting the loss of the CO group (reactions 3 and 7) and, in a coordinating solvent, by capturing the coordinatively deficient intermediate $Mn_2(CO)_9$ before recapture by CO (reaction 4). An important consideration determining the efficiency of production of the separated monomers is the competition between separation by translation out of the surrounding solvent cage (reaction 6) and recombination (reaction 5). The importance of such effects is shown by the fact that low temperature photolyses in frozen solutions, polymer films or glasses fail to provide evidence for the appearance of the monomeric intermediates.[21-24] This is hardly surprising given the much longer translational correlation times in such media compared to fluid solutions at room temperature. Apparently, in a rigid medium, separation can not compete with recombination.
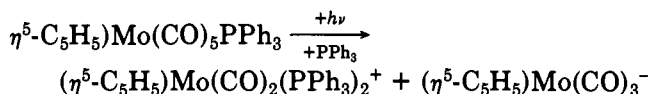
3. Intervention of Other Excited States

As presented so far, the photochemistry of metal–metal bonds has centered on the appearance of intermediates arising from metal–metal bond cleavage or loss of CO following photolysis of low-energy ultraviolet or visible absorption bands. By their natures the intermediates are suggestive of photochemistry arising from $\sigma\sigma^*$ and $d\pi$–σ^* or dd excited states as discussed below. However, in certain cases there is either photochemical

or photophysical evidence for the intervention of additional excited states and it is important to take them into account.

One example is the appearance of emission following ultraviolet photolysis of $(\eta^5\text{-}C_5H_5)_2M_2(CO)_6$ (M = Mo, W).[46] Another is the existence of wavelength-dependent quantum yields. For example, photolysis of the iron dimer in CCl_4

$$(\eta^5\text{-}C_5H_5)_2Fe_2(CO)_4 \xrightarrow{+h\nu} 2(\eta^5\text{-}C_5H_5)Fe(CO)_2Cl$$
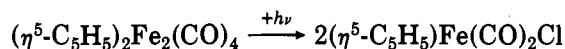
occurs with quantum efficiencies for loss of the dimer of 505 nm = 0.067;[31] 450 nm = 0.11;[31] 436 nm = 0.21;[28] 366 nm = 0.42,[31] 0.23;[28] 313 nm = 0.38.[28] More striking is the report that the monosubstituted dimer, $(\eta^5\text{-}C_5H_5)_2Mo_2(CO)_5(PPh_3)$, undergoes photodisproportionation

$$\eta^5\text{-}C_5H_5)Mo(CO)_5PPh_3 \xrightarrow[+PPh_3]{+h\nu}$$
$$(\eta^5\text{-}C_5H_5)Mo(CO)_2(PPh_3)_2{}^+ + (\eta^5\text{-}C_5H_5)Mo(CO)_3{}^-$$

but only at wavelengths shorter than 290 nm.[51]

Given these observations, it is worthwhile to consider the possible intervention of higher excited states and of excited states other than $\sigma\sigma^*$ states and the role they might play in the observed photochemistry.

(A) Charge Transfer. For cases like the wavelength-dependent photochemistry found for the iron dimer in CCl_4, the higher energy photolyses could lead to the direct or indirect sensitization of states which are largely charge transfer to solvent CTTS in character. An example of such photochemistry is shown in eq 52

$$(\eta^5\text{-}C_5H_5)_4Fe_4(CO)_4, CCl_4 \xrightarrow{+h\nu}$$
$$(\eta^5\text{-}C_5H_5)_4Fe_4(CO)_4{}^+, CCl_4{}^- \quad (52)^{74}$$
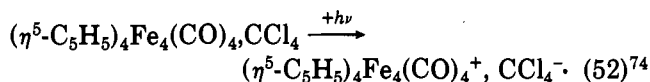
where photolysis of the cluster $(\eta^5\text{-}C_5H_5)_4Fe_4(CO)_4$ leads to the cluster cation which is stable.[75] Once formed, halocarbon radical anions are known to undergo rapid loss of halide, e.g., $CCl_4{}^- \rightarrow CCl_3 + Cl^-$,[76] to give products which are derived from the organic radical which is produced.

Such pathways could play a role in the photochemistry of the dimers. For example, photolysis of $(\eta^5\text{-}C_5H_5)_2Mo_2(CO)_6$ in THF in the presence of $CHBr_3$ to give $(\eta^5\text{-}C_5H_5)Mo(CO)_3Br$ reaches a limiting quantum yield of 0.57 with photolysis at 546 nm but in the neat solvent the quantum yield rises to 1.[45] It is conceivable that a contribution to the observed photochemistry exists from net charge transfer to solvent, eq 53.

$$(\eta^5\text{-}C_5H_5)_2Mo_2(CO)_6, CHBr_3 \xrightarrow{+h\nu}$$
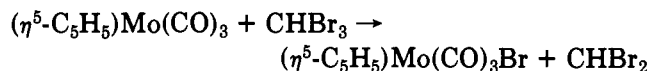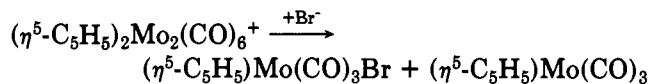$$(\eta^5\text{-}C_5H_5)_2Mo_2(CO)_6{}^+, CHBr_3{}^- \quad (53)$$
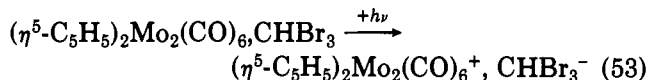
In mechanistic detail such pathways could either involve sensitization of CTTS states as suggested above, or capture of the initially formed excited state $[(\eta^5\text{-}C_5H_5)_2Mo_2(CO)_6]^*$ by oxidative quenching

$$[(\eta^5\text{-}C_5H_5)_2Mo_2(CO)_6]^*, CHBr_3 \rightarrow$$
$$(\eta^5\text{-}C_5H_5)_2Mo_2(CO)_6{}^+, CHBr_3{}^-$$
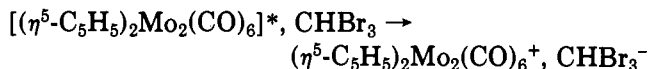
The $^1(\sigma\sigma^*)$ state produced by optical excitation, is both a strong reducing agent and a strong oxidizing agent since it contains an excited electron in a σ^* orbital and an electron hole in the σ orbital. Conceivably, outersphere electron transfer to an adjacent solvent molecule

or other electron acceptor could compete with excited-state decay and decomposition. Given the results of chemical and electrochemical redox studies on related dimeric systems,[4] the results of one-electron oxidation of the metal–metal bond would be expected to give products of the type $(\eta^5\text{-}C_5H_5)Mo(CO)_3Br$ via steps like

$$(\eta^5\text{-}C_5H_5)_2Mo_2(CO)_6{}^+ \xrightarrow{+Br^-}$$
$$(\eta^5\text{-}C_5H_5)Mo(CO)_3Br + (\eta^5\text{-}C_5H_5)Mo(CO)_3$$

$$(\eta^5\text{-}C_5H_5)Mo(CO)_3 + CHBr_3 \rightarrow$$
$$(\eta^5\text{-}C_5H_5)Mo(CO)_3Br + CHBr_2$$

(B) dd States. In classical coordination complexes having the d^6 electronic configuration, e.g., $Ru(NH_3)_5$-$(pyX)^{2+}$,[77,78] $Fe(CN)_5(pyX)^{3-}$,[79] $W(CO)_5(pyX)$[80] (pyX is a substituted pyridine), clear evidence for the presence of low-lying dd states has been obtained as evidenced by the appearance of ligand-loss photochemistry. Ligand-loss photochemistry is also observed for d^6 compounds like, $Re(CO)_5Cl$ [81] or $(\eta^5\text{-}C_5H_5)Fe(CO)_2Br$,[82] which are clearly related chemically to the metal–metal-bonded compounds of interest here. The possible role of dd states in the photochemistry of metal–metal bonds will be considered in a later section.

(C) MLCT. In compounds of the type (phen)Re-$(CO)_3Cl$ (phen is 1,10-phenanthroline) or (bpy)Re-$(CO)_3Cl$ (bpy is 2,2'-bipyridine) absorption and excited-state properties are dominated by metal-to-ligand charge-transfer (MLCT) excited states. Visible light absorption occurs by optical transitions to MLCT states largely singlet in character e.g.

$$(phen)Re^I(CO)_3Cl \xrightarrow{+h\nu} {}^1[(phen^-)Re^{II}(CO)_3Cl]^*$$
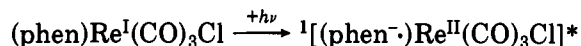
and emission from states having the same electronic configuration but largely ^{3}MLCT in character.[83–85] The electronic configurations involved in the MLCT excited states are analogous to those of related polypyridyl complexes of Ru(II) and Os(II) whose electronic structures and radiative and nonradiative decay rates are reasonably well understood in the context of available theoretical models including the energy-gap law.[86–89]

In a clever experiment, Morse and Wrighton introduced a MLCT excited state into the excited-state manifold of a metal–metal bond by displacement of bound-CO groups in $Re_2(CO)_{10}$ by 1,10-phenanthroline to give the dimer $(CO)_3ReRe(CO)_3(phen)$.[90] In addition to the usual transitions assignable to the metal–metal bond, a new, relatively intense absorption band appears in the substituted dimer at λ_{max} = 502 nm (19 900 cm^{-1}) which arises from a MLCT transition of the type

$$(phen)Re^I \xrightarrow{+h\nu} (phen^-)Re^{II*}$$
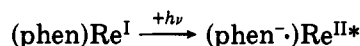
In an EPA glass at 77 K, excitation of the dimer leads to an emission at λ_{max} = 694 nm (14 400 cm^{-1}) with a radiative efficiency of $\phi_r \sim 10^{-2}$ and a lifetime of τ = 95 μs.

However, photolysis of the dimer in a 1:1 mixture of CH_2Cl_2 and CCl_4 leads to typical metal–metal bond cleavage products as shown in eq 54. It is interesting
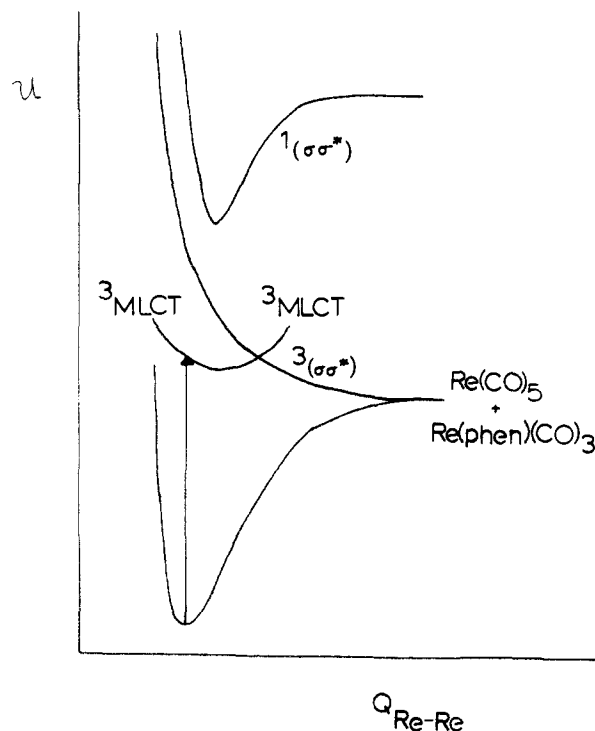
$$(CO)_5ReRe(CO)_3(phen) \xrightarrow[CCl_4]{+h\nu}$$
$$Re(CO)_5Cl + (phen)Re(CO)_3Cl \quad (54)^{90}$$
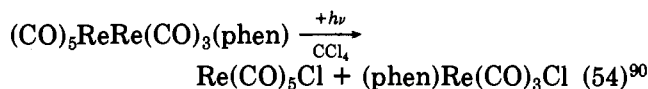
Figure 5. Schematic potential energy–coordinate diagram for $(CO)_5ReRe(CO)_3(phen)$ showing the presumed intersection between $(\sigma\sigma^*)$ and ^3MLCT states.

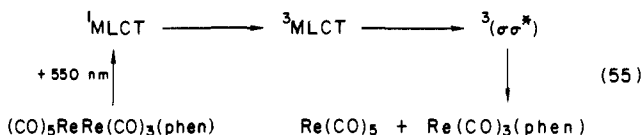that the quantum yield for appearance of the cleavage products is relatively insensitive to photolysis wavelength—ϕ (313 nm) = 0.15, ϕ (366) = 0.22, ϕ (436) = 0.19, ϕ (550) = 0.13. The appearance of metal-metal-bond photochemistry continues to persist even when photolysis is carried out in the visible region where the origin of light absorption is in the MLCT chromophore. A possible qualitative disposition of the various excited states in the substituted dimer is illustrated in Figure 5.

Figure 5 follows from Figure 4 but includes a low-lying ^3MLCT state largely localized on the 1,10-phenanthroline half of the dimer. It should be recalled that because of the extent of spin-orbit coupling for the third-row transition-metal rhenium, significant mixing must exist between the ^3MLCT state and low-lying ^1MLCT excited states. As in Figure 4, it is assumed in Figure 5 that the low lying $^3(\sigma\sigma^*)$ state correlates with homolysis products and that the $^1(\sigma\sigma^*)$ state correlates with disproportionation products. It is expected that variations in the energy of the ^3MLCT state along a normal coordinate largely Re–Re in character should be small and this is illustrated by the shallow potential well for this state in Figure 5. On the other hand, the dissociative $^3(\sigma\sigma^*)$ state is strongly dependent upon Q_{M-M} and an intersection between the states may occur along Q_{M-M} as suggested in Figure 5.
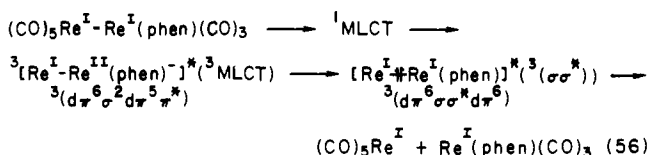
Morse and Wrighton have suggested that the origin of the observed photochemistry may lie in the fact that the lowest MLCT state is $\sigma(M-M)-\pi^*$(phen) in character.[90] The formation of such an excited state via the transition $(\sigma)^2 \rightarrow (\sigma)(\pi^*(phen))$ would lead to depopulation of σ and, potentially, to a labilization of the Re–Re bond.

However, the proposed intersection between MLCT and $\sigma\sigma^*$ states in Figure 5 suggests an alternate explanation of how low-energy, visible photolysis into the

MLCT chromophore could lead to cleavage of the metal-metal bond. The process envisioned is an "intramolecular sensitization" in which initial excitation to give ^1MLCT is followed by a series of excited-state interconversions as shown in eq 55. The key event in

$$^1MLCT \xrightarrow{\hspace{1.5cm}} {}^3MLCT \xrightarrow{\hspace{1.5cm}} {}^3(\sigma\sigma^*)$$

$$\uparrow {+550 \text{ nm}} \hspace{5cm} \downarrow \hspace{1cm} (55)$$

$$(CO)_5ReRe(CO)_3(phen) \hspace{1.5cm} Re(CO)_5 + Re(CO)_3(phen)$$

the proposed sequence is the surface crossing between the ^3MLCT and $^3(\sigma\sigma^*)$ states. Notice that electronically speaking, this transition involves intramolecular energy transfer between the Re–phen-localized MLCT state and the $^3(\sigma\sigma^*)$ state of the metal-metal bond, eq 56.

$$(CO)_5Re^I\text{-}Re^I(phen)(CO)_3 \xrightarrow{\hspace{1cm}} {}^1MLCT \xrightarrow{\hspace{1cm}}$$

$$\underset{^3(d\pi^6\sigma^2 d\pi^5\pi^*)}{^3[Re^I\text{-}Re^{II}(phen)^-]^*(^3MLCT)} \xrightarrow{\hspace{1cm}} \underset{^3(d\pi^6\sigma\sigma^* d\pi^6)}{[Re^I\text{+}Re^I(phen)]^*(^3(\sigma\sigma^*))} \xrightarrow{\hspace{1cm}}$$

$$(CO)_5Re^I + Re^I(phen)(CO)_3 \hspace{0.5cm} (56)$$

Related processes involving intramolecular sensitization of low-lying dd states following MLCT excitation are known to be of importance for d^6 systems.[77-80,91] If the interpretation of the photochemical quantum-yield data given here is correct, it leads to the estimate that the minimum energy for the appearance of the monomers $Re(CO)_5$ and $Re(CO)_3(phen)$ is <550 nm (51.9 kcal/mol). It follows that this value would also represent the minimum energy for bond dissociation of the Re–Re bond.

(D) High Energy Chemical States. In addition to the possible intervention of multiple excited states, it is conceivable that nonspectroscopic but closely related chemical states may also play a role as high-energy intermediates. An example is illustrated in Figure 6 which also follows from Figure 4 but deals specifically with $(\eta^5\text{-}C_5H_5)_2Mo_2(CO)_6$ which is known to undergo photochemically induced disproportionation in the presence of halide ions, eq 26.[38-40]

In Figure 6 the same electronic structural details with regard to the metal–metal bond are assumed as in Figure 4 but the presence of Br^- is included. Under these conditions photochemically induced disproportionation to give $(\eta^5\text{-}C_5H_5)Mo(CO)_3Br$ and $(\eta^5\text{-}C_5H_5)\text{-}Mo(CO)_3^-$ occurs. The disproportionation products, $(\eta^5\text{-}C_5H_5)Mo(CO)_3^+$ and $(\eta^5\text{-}C_5H_5)Mo(CO)_3^-$, which correlate with the $^1(\sigma\sigma^*)$ state, are at high energy because they involve the formation of the coordinatively unsaturated d^6 cation $(\eta^5\text{-}C_5H_5)Mo(CO)_3^+$. It is the same high-energy intermediate which would be involved in the dissociative loss of Br^- from $(\eta^5\text{-}C_5H_5)Mo(CO)_3Br$. As suggested in Figure 6, the disproportionation products, $(\eta^5\text{-}C_5H_5)Mo(CO)_3Br + (\eta^5\text{-}C_5H_5)Mo(CO)_3^-$, must be more stable than the homolysis products, $2(\eta^5\text{-}C_5H_5)Mo(CO)_3 + Br^-$. Otherwise, electron transfer

$$(\eta^5\text{-}C_5H_5)Mo(CO)_3^- + (\eta^5\text{-}C_5H_5)Mo(CO)_3Br \rightarrow$$
$$2(\eta^5\text{-}C_5H_5)Mo(CO)_3 + Br^-$$
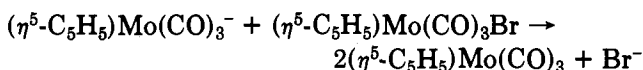
followed by recombination would provide what should be a reasonably facile pathway for return to the starting dimer. In fact, as noted later, the *reverse* reaction may play an important role in the photochemically induced disproportionation of the dimer in THF with added
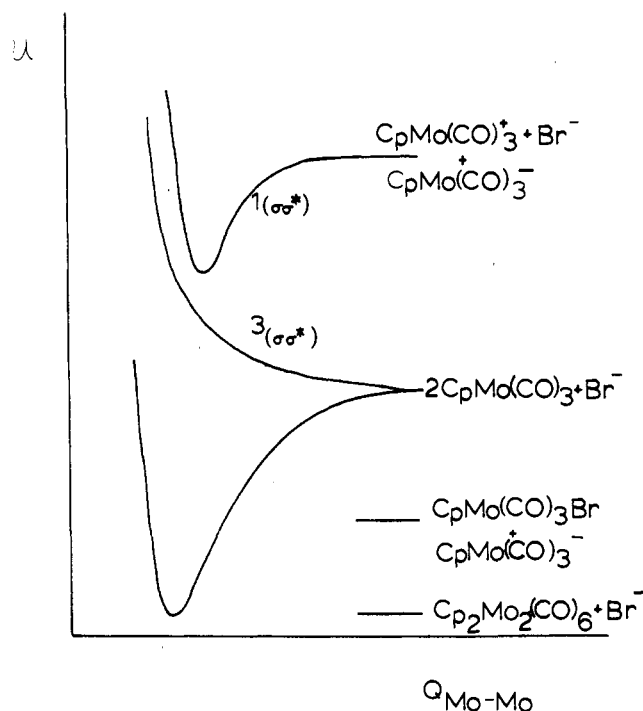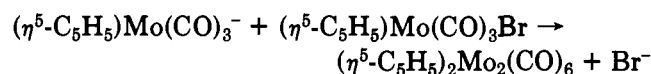
Figure 6. Schematic potential energy–coordinate diagram for the system $(\eta^5\text{-}C_5H_5)_2Mo_2(CO)_6 + Br^-$.

halide ions. A reaction does occur between $(\eta^5\text{-}C_5H_5)Mo(CO)_3^-$ and $(\eta^5\text{-}C_5H_5)Mo(CO)_3Br$ but only at elevated temperatures or after long reaction times and probably occurs by nucleophilic displacement

$$(\eta^5\text{-}C_5H_5)Mo(CO)_3^- + (\eta^5\text{-}C_5H_5)Mo(CO)_3Br \rightarrow$$
$$(\eta^5\text{-}C_5H_5)_2Mo_2(CO)_6 + Br^-$$

rather than by electron transfer.[39]

Obviously, the intervention of a low-lying chemical state like the disproportionation products in Figure 6 could also occur in potentially coordinating solvents where the cation, $(\eta^5\text{-}C_5H_5)Mo(CO)_3S^+$ (S = solvent) would be formed. Recall that the dimer is unstable toward disproportionation in polar organic solvents.[40] The importance that such chemical states play photochemically could be highly solvent dependent since the nature of the solvent would help dictate whether the disproportionation products are more or less stable than the homolysis products. It should also be noted that if the disproportionation products are stable with respect to the monomers, it necessarily follows that a possible route to disproportionation is by electron transfer

$$2(\eta^5\text{-}C_5H_5)Mo(CO)_3 + S \rightarrow$$
$$(\eta^5\text{-}C_5H_5)Mo(CO)_3^- + (\eta^5\text{-}C_5H_5)Mo(CO)_3(S)^+$$
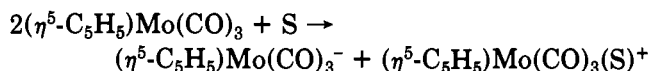
4. Origin of the Two Intermediates

As noted above, a common feature in the photochemistry of the metal–metal-bonded dimers is the appearance of intermediates arising from metal–metal-bond cleavage or loss of CO. From their transient decay properties, the intermediates are independent of each other kinetically, and at least for $Mn_2(CO)_{10}$, they are primary photoproducts in that they are in the solution 25 ps after photolysis.

In terms of electronic structure, the origin of the
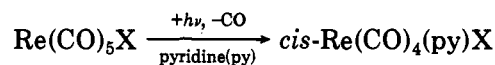
cleavage products can be accounted for by the sequence

$$Mn_2(CO)_{10}(\sigma^2) \xrightarrow{+h\nu} {}^1(\sigma\sigma^*) \rightarrow {}^3(\sigma\sigma^*) \rightarrow 2Mn(CO)_5$$
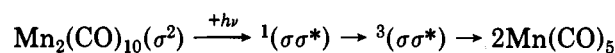
as suggested by Figure 4. From the electronic spectral assignments, metal–metal bond cleavage is an expected consequence of UV excitation into the $\sigma \rightarrow \sigma^*$ transition. However, an excited-state electronic origin for the CO-loss intermediate remains to be established.

For the metal–metal-bonded compounds, relatively low intensity bands appear in electronic spectra at lower energies than the $\sigma \rightarrow \sigma^*$ transitions, note Figure 1. A possible origin for the bands is in $d\pi^* \rightarrow \sigma^*$ transitions which involve optical excitation of an electron from an orbital with $d\pi^*$ type symmetry with regard to the metal–metal bond to σ^*, note Scheme IX. One justification for the assignment is the experimental observation that metal–metal bond cleavage occurs following both UV *and* visible photolysis. As has been noted by several authors, since such an excitation leads to partial electronic population of $\sigma^*(M-M)$, it could lead to labilization of the M–M bond.

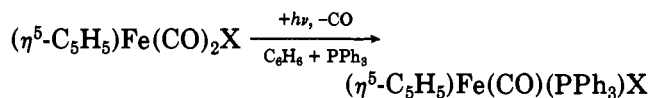PES data on $Mn_2(CO)_{10}$[66] suggest that the $d\pi^*$ levels lie *below* σ while the assignment of the absorption bands as $(\sigma \rightarrow \sigma^*) > (d\pi^* \rightarrow \sigma^*)$ requires the ordering $d\pi^* > \sigma$. Nonetheless, the PES experiment involves a "vertical" ionization on the time scale for changes in electronic and nuclear coordinates. In the relaxed ion, the ordering of levels could be inverted.

If the visible absorption bands have their origins in $d\pi^* \rightarrow \sigma^*$ transitions, the resulting $d\pi^*d\sigma^*$ excited states could also conceivably account for the loss of CO. Compared to the ground state, which has the configuration $(d\pi^*)^4$, optical excitation to give $(d\pi^*)^3\sigma^*$ would lead to an electronic deficiency in the $d\pi^*$ levels, a decrease in metal–CO backbonding by $d\pi$–$\pi^*(CO)$ mixing, and conceivably, to labilization of CO.
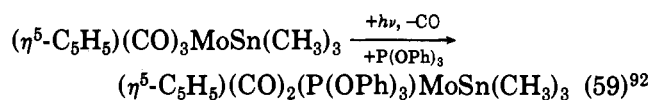
However, there is another interpretation for the origin of the low-energy absorption bands which is consistent with, and, in fact, suggested by the appearance of CO loss products. The other interpretation is that the bands have their origins in $d \rightarrow d$ transitions given the propensity of dd excited states in related systems to undergo ligand loss photochemistry.[77–82] In closely related complexes, photolysis of visible absorption bands is known to lead to efficient loss of CO, e.g., eq 57–59. The examples in eq 57 and 58 are of monomeric d^6 complexes which are closely related to the corresponding metal–metal-bonded dimers and the example in eq 59 of CO loss from a heteronuclear metal–metal bond

$$Re(CO)_5X \xrightarrow[\text{pyridine(py)}]{+h\nu, -CO} cis\text{-}Re(CO)_4(py)X$$

$$\phi_{366} = 0.30 \text{ (Cl)}; 0.34 \text{ (Br)}; 0.10 \text{ (I)} \qquad (57)^{81}$$

$$(\eta^5\text{-}C_5H_5)Fe(CO)_2X \xrightarrow[\text{C}_6\text{H}_6 + \text{PPh}_3]{+h\nu, -CO}$$
$$(\eta^5\text{-}C_5H_5)Fe(CO)(PPh_3)X$$

$$\phi_{366} = 0.087 \text{ (Br)}; 0.071 \text{ (I)} \qquad (58)^{82}$$

$$(\eta^5\text{-}C_5H_5)(CO)_3MoSn(CH_3)_3 \xrightarrow[\text{+P(OPh)}_3]{+h\nu, -CO}$$
$$(\eta^5\text{-}C_5H_5)(CO)_2(P(OPh)_3)MoSn(CH_3)_3 \quad (59)^{92}$$

In addition *to* the observation of dd-like photochem-

TABLE II. Spectral Data in Cyclohexane

compd	λ_{max}, nm (ϵ)
$Mn_2(CO)_{10}$	390 (4000), 324 (21 400)
$Mn(CO)_5I$	425 (300)
$[(\eta^5\text{-}C_5H_5)Mo(CO)_3]_2$	509 (1700), 306 (19 000)
$(\eta^5\text{-}C_5H_5)Mo(CO)_3Br$	476 (490)

istry, there are clear spectral similarities in the visible region between dimers and related monomers as shown by the data in Table II. A significant point to arise from the data in Table II is that in the monomeric d^6 complexes, the ultraviolet band assigned to the $\sigma \to \sigma^*$ transition of the metal–metal bond is missing but low-energy bands do appear. The apparent molar extinction coefficients are lower for the monomers but, in part, because of the tailing of the intense $\sigma \to \sigma^*$ bands into the visible for the dimers.

The appearance of the lower energy absorption bands in related monomers and metal–metal-bonded dimers suggests that the bands may have a common origin and, given the observed photochemistry, that they may arise from d $\to$ d transitions. d $\to$ d transitions are nominally LaPorte forbidden since they involve electronic excitations among levels having the same orbital angular momentum quantum number. However, dd bands can gain significant intensity through metal–ligand mixing which has the effect of introducing charge-transfer and/or ligand-localized character into the transitions.

One way of viewing comparisons between the monomers and dimers is that in a localized sense, the manganese atom in $(CO)_5Mn–Mn(CO)_5$, for example, sees a group $(Mn(CO)_5^-)$ whose electronic characteristics are not totally different from those of the iodide ion in $(CO)_5Mn–I$. If so, it should not be too surprising if certain elements of the electronic character of the metal–metal bond are retained in the d^6 monomer and vice versa.

The effect on the energy-ordering scheme for Mn_2-$(CO)_{10}$ of assigning the low-energy bands to d $\to$ d transitions is shown in Scheme XII as is an ordering scheme for the monomer, $Mn(CO)_5I$. Compare with Scheme IX and note the inclusion of the $d\sigma^*$ orbitals, $d_{x^2-y^2}$ which lie along the Mn–CO bonds in the plane perpendicular to the Mn–Mn or Z axis. These levels were calculated to be well above σ^*_{M-M} by Levenson and Gray.[5]

The $\sigma \to \sigma^*$ transition is labeled as 1 in Scheme XII and the d $\to$ d transition as 2. Given the D_{4h} symmetry of the metal sites in the dimer and at the manganese atom in $Mn(CO)_5I$, relatively low-energy, ligand-field-based absorption bands might be expected to appear arising from the transitions, $^1T_1 \leftarrow {}^1A_1$ and $^1T_2 \leftarrow {}^1A_1$, given the appearance of such bands for complexes of the type $Co(NH_3)_5X^{2+}$.[93] If so, the low-energy visible component observed for the metal–metal bond would be the lower of the two d $\to$ d transitions, $^1T_1 \leftarrow {}^1A_1$, with the second transition and possibly the $d\pi^* \to \sigma^*$ transition as well, hidden beneath the intense $\sigma \to \sigma^*$ absorption band in the ultraviolet.

A reasonable case can be built for the assignment of the absorption bands in the metal–metal-bonded dimers as d $\to$ d and $\sigma \to \sigma^*$ in origin. The assignments are appealing in that with $\sigma \to \sigma^*$ excitation, labilization of the M–M bond along metal–metal or Z axis to give monomers is an expected result. Further, electronic occupation of $d\sigma^*$ $(d_{x^2-y^2})$ following $d\pi,d\delta \to d\sigma^*$ exci-

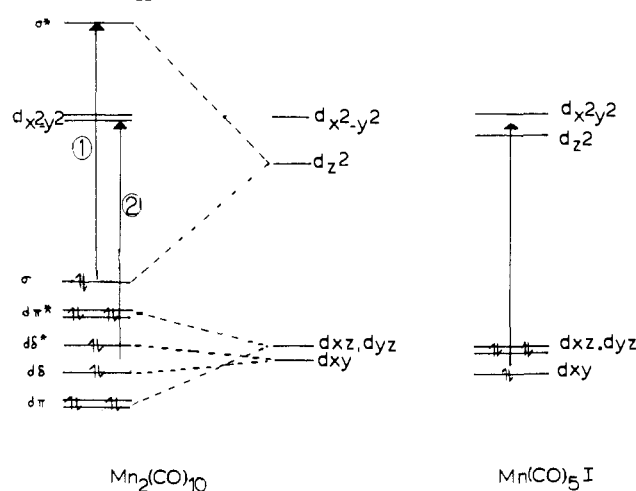**SCHEME XII**

$Mn_2(CO)_{10}$ $\qquad\qquad$ $Mn(CO)_5I$

TABLE III. Quantum Yield Data Relating to the Origins of the Two Photochemical Intermediates

compd	$\phi_M{}^b$	$\phi_D{}^b$	$\phi_{CCl_4}{}^a$ (λ_{excit}, nm)	ref
$Cp_2Fe_2(CO)_4$			0.21 (436)	28
			0.23 (366)	28
$Cp_2Mo_2(CO)_6$	0.4^c	0.1^c	0.35 (550)	10
			0.42 (405)	10
			0.45 (366)	10
$Mn_2(CO)_{10}$	0.3^d	0.11^d	0.41 (366)	9
			0.48 (313)	9

^{a} ϕ_{CCl_4} is the disappearance quantum yield for the dimer in CCl_4 solution. ^{b} ϕ_M and ϕ_D are the quantum yields for the appearance of monomeric (e.g., $Mn(CO)_5$) and dimeric (e.g., $Mn_2(CO)_9$) intermediates. ^{c} In THF by visible flash photolysis, ref 45. ^{d} In cyclohexane at 436 nm, ref 19.

tation is predicted to lead to labilization of CO groups in the XY plane because of increased electron–electron repulsion at the M–CO bonds thus explaining the appearance of the CO-loss intermediates. In fact, such a reactive dd state might be expected to be largely triplet in character, ^{3}(dd).[94]

However, there is an additional point to consider. If the two types of intermediates have their electronic origins in different excited states and different absorption bands, why, as shown in Table III, are photochemical quantum yields usually largely wavelength independent?

Also listed in Table III are approximate quantum efficiencies for the appearance of both the monomeric (ϕ_M) and CO-loss, dimeric (ϕ_D) intermediates following *visible* photolysis. The question naturally arises, if homolytic cleavage is a consequence of UV, $\sigma \to \sigma^*$ excitation, how can *visible* photolysis lead to the appearance of monomers?

There are at least two reasonable explanations. The first is that the visible absorption bands do arise from $d\pi \to \sigma^*$ (M–M) transitions and that the resulting $(d\pi^*\sigma^*)$ excited states are the origin of both types of photochemistry. In this interpretation, loss of CO and M–M bond cleavage are competitive processes from the *same* excited state. A wavelength-independent product distribution would be expected as long as the transition, $^{1,3}(\sigma\sigma^*) \to (d\pi^*\sigma^*)$, occurs with high (>0.5) efficiency.

The second explanation is more intricate and relies on an intersection between the $^3(\sigma\sigma^*)$ and dd states as proposed in Figure 7. Figure 7 also follows from Figure 4 in showing the variations in energy for the $^1(\sigma^2)$, $^3(\sigma\sigma^*)$,
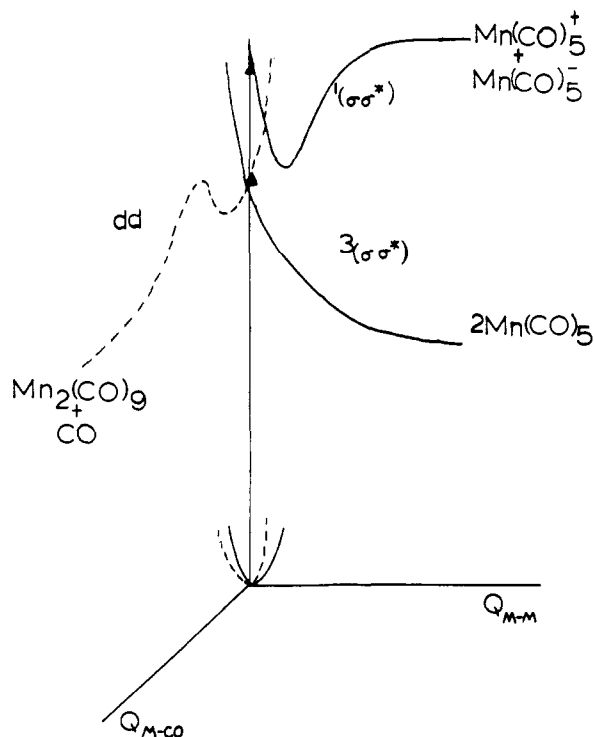
Figure 7. Potential energy–coordinate curves showing the possible crossing between dd and $^3(\sigma\sigma^*)$ states.

and $^1(\sigma\sigma^*)$ states as a function of $Q_{\text{M-M}}$. However, a dd state is also included and its variation in energy along a normal coordinate largely M–CO in character is also shown by the dashed curve. The ultraviolet $(\sigma \to \sigma^*)$ and proposed visible $d\pi,d\delta \to d\sigma^*$ transitions are illustrated as vertical arrows. The reactive dd state is shown as correlating with the CO loss products, $Mn_2(CO)_9$ + CO.

Given their electronic configurations, (1) the $^3(\sigma\sigma^*)$ state is expected to be dissociative along $Q_{\text{M-M}}$ but stable with regard to CO loss and (2) the dd state is expected to have a large restoring force along $Q_{\text{M-M}}$ but be unstable with regard to loss of CO along $Q_{\text{M-CO}}$. The feature in Figure 7 which may provide the clue for explaining the wavelength-independent photochemistry is the possibility of a transition between the reactive dd and $^3(\sigma\sigma^*)$ states. If the intersection between states falls *below* the energies of the two optical transitions, photolysis into either transition could give the same photoproducts. $\sigma \to \sigma^*$ excitation in the ultraviolet followed by crossing to $^3(\sigma\sigma^*)$ and vibrational relaxation would lead to the intersection between dd and $^3(\sigma\sigma^*)$. At the intersection the system would either cross to dd, followed by loss of CO, or would stay on the $^3(\sigma\sigma^*)$ potential curve with continued vibrational relaxation until the separated monomers are formed. Visible photolysis to give $^1(dd)$ followed by relaxation and crossing to $^3(dd)$ could lead to the same intersection or intersections. As long as the processes which occur at the intersection are independent of how the intersection is reached, the same photoproducts would appear following either visible or ultraviolet photolysis.

C. Reactivity and Properties of the Photochemically Produced Monomers

In previous sections a fairly detailed account has evolved of the mechanistic details of the photochemistry

TABLE IV. Recombination Rate Constants in Cyclohexane at 22 ± 2 °C

reaction	$10^{-9}k_{\text{obsd}}$, M^{-1} s^{-1}	$10^{-9}k_{\text{act}}$, M^{-1} s^{-1}	ref
$2Mn(CO)_5 \to Mn_2(CO)_{10}$	1.9	3.9	14, 15, 53–55
$2Re(CO)_5 \to Re_2(CO)_{10}$	2.0	4.4	12, 15, 54
$2(Cp)Mo(CO)_3 \to$ $(Cp)_2Mo_2(CO)_6$	3.1	19	44, 45
$2(Cp)W(CO)_3 \to (Cp)_2W_2(CO)_6$	19	3.9	44, 45
$2(Cp)Fe(CO)_2 \to (Cp)_2Fe_2(CO)_4$	3.2	24	32
$2Co(CO)_4 \to Co_2(CO)_8$	0.42^a		

^{a} In hexane at room temperature, ref 29 in Wegman, R. W.; Brown, T. L. *Inorg. Chem.* **1983**, *22*, 183.

of metal–metal bonds. In order to complete the story of photochemical mechanism for these compounds, it is necessary to consider the properties and chemical reactivities of the initial intermediates that appear after photolysis.

1. Molecular and Electronic Structures

From metal-atom deposition studies in CO/Ar matrices at 15 K[56] and photolysis of $HMn(CO)_5$ in a CO matrix,[20] it has been concluded by infrared $(\nu(CO))$ studies that the structure of $M(CO)_5$ (M = Mn, Re) is square pyramidal having C_{4v} symmetry.[49] That the structure in the matrix at low temperature is maintained in fluid solution at room temperature is suggested by the similarities between electronic spectra in the two media. It has already been noted that $Mn(CO)_5$ and $Re(CO)_5$ have noticeable visible absorbances at λ_{max} = 830 nm (ϵ = 800 M^{-1} cm^{-1}) and λ_{max} = 535 nm (ϵ = 1000 ± 100 M^{-1} cm^{-1}), respectively in ethanol,[11,12,16] and that similar results have been obtained in cyclohexane.[14,15] It is interesting to note that for the electronically related d^7 ion $Co^{II}(CN)_5^{3-}$, which has the square-pyramidal structure and C_{4v} symmetry in the solid state,[95] a low-energy absorption band is observed at 966 nm (ϵ = 233 M^{-1} cm^{-1}) which has been assigned to the transition $^2A \to {}^2B$ ($d_{z^2} \to d_{x^2-y^2}$).[95] The absorption bands for the intermediates $Mn(CO)_5$ and $Re(CO)_5$ could have a related electronic origin[96] with the shift to higher energy being consistent with the greater degree of metal–ligand mixing with the CO ligands in the lower formal oxidation state.

2. Recombination Rate Constants

From flash-photolysis studies it has been possible to obtain recombination rate constants for the various monomers, in some cases in a series of solvents. Data in cyclohexane at 22 ± 2 °C are collected in Table IV. It should be realized that the experimentally derived values include contributions both from the chemical step (k_{act}) and from diffusional effects.[97] The two contributions can be separated by using eq 60. The

$$1/k_{\text{obsd}} = 1/k_{\text{D}} + 1/k_{\text{act}} \tag{60}$$

corrections for diffusional effects become necessary as k_{act} approaches the diffusion-controlled limit (k_{D}). Note that in the limit, $k_{\text{act}} \gg k_{\text{D}}$, $k_{\text{obsd}} = k_{\text{D}}$ and the reaction reaches the diffusion-controlled limit. k_{D} for chemically equivalent, spherical reactants is given by eq 61 where η is the viscosity of the solvent. For cyclohexane at 22 °C, $k_{\text{D}} = 3.7 \times 10^9$ M^{-1} s^{-1}.

$$k_D \sim 4RT/3000\eta \qquad (61)$$

Both k_{obsd} and k_{act} values calculated using eq 60 are listed in Table IV. Because of the relative imprecision of the data and the approximations involved, the k_{act} values should only be regarded as symptomatic of trends in reactivity. It is apparent from the data that the recombination rate constants are near the diffusion-controlled limit. It should be noted that a temperature dependence is expected for the recombination reactions even in the diffusion-controlled limit if only from the temperature dependence of the viscosity which appears in eq 61.

For carbon-based radicals, the less than diffusion-controlled recombination rate constants found experimentally have been attributed in part to statistical effects arising from electron-spin considerations.[98] For the spatially isolated monomers there are three different components of a spin triplet state with spins aligned ($\alpha\alpha$, $\beta\beta$, and $1/2^{1/2}/(\alpha\beta + \beta\alpha)$) and one singlet component ($1/2^{1/2}(\alpha\beta - \beta\alpha)$). For noninteracting monomers, all of the spin states are at the same energy and all are equally populated. However, as the monomers approach, electron–electron interactions lift the singlet–triplet degeneracy. The three triplet components correlate with the $^3(\sigma\sigma^*)$ state which, as shown in Figure 4, is dissociative, and if populated does not lead to M–M bond formation. Population of $^1(\sigma^2)$ does lead to M–M bond formation but if spin effects were important, the recombination rate would be decreased by a statistical factor of $1/(1 + 3)$ or $^1/_4$. In fact, such effects can only play a role if the interconversion between singlet and triplet states is slow on the diffusional time scale. For the transition-metal-based, paramagnetic monomers in Table IV, the combination of significant spin-orbit coupling which mixes the spin character of the states, and the nearness in energy of the $^3(\sigma\sigma^*)$ and $^1(\sigma^2)$ states as the two monomers approach, should ensure appreciable mixing between the two states and rapid transition rates between the "triplet" and "singlet" states. As a consequence, spin effects are not expected to play an important role in the recombination reactions.

Although the data in Table V are limited, they do suggest that the recombination process may be somewhat solvent dependent at least for $(\eta^5\text{-}C_5H_5)Mo(CO)_3$. A detectable decrease in the ratio k_{obsd}/k_D exists in the potentially coordinating solvents THF and acetonitrile suggesting the possible existence of at least weak monomer–solvent interactions.

The importance of steric effects on recombination has been demonstrated by Walker, et al., by conventional flash photolysis of hexane solutions containing the disubstituted dimers $Mn_2(CO)_8(L)_2$ ($L = CO$, $P(n\text{-}Bu)_3$, $P(i\text{-}Bu)_3$, $P(i\text{-}Pr)_3$, $P(OPh)_3$, and PPh_3.[55] Through the series, they found that recombination rate constants varied from 9×10^8 M^{-1} s^{-1} to 4×10^6 M^{-1} s^{-1} with a trend toward lower values existing as the cone angle of the phosphine increases.

3. Reactions with Halocarbons

Oxidation by net halogen-atom abstraction from reactive halocarbons appears to be a ubiquitous photochemical reaction for the metal–metal-bonded compounds which have been investigated to date. In some cases rate constants are available; the data are presented in Table VI.

TABLE V. Variations in Recombination Rate Constants with Solvent for the reaction $2(Cp)Mo(CO)_3 \rightarrow (Cp)_2Mo_2(CO)_6$ at 22 ± 2 °C[44]

solvent	$10^{-9}k_{obsd}$, M^{-1} s^{-1}	$10^{-9}k_D$, M^{-1} s^{-1}	k_{obsd}/k_D
cyclohexane	3.1	3.7	0.84
CH$_3$CN	3.2	9.0	0.36
THF	1.6	6.0	0.27

TABLE VI. Rate Constants for Reactions between Monomeric Intermediates and Halocarbons at Room Temperature

monomer	reactant	medium	k, M^{-1} s^{-1}	ref
$(Cp)W(CO)_3$	CCl$_4$	THF	1.3×10^9	18
	CHCl$_3$	THF	~ 21	18
	PhCH$_2$Cl	THF	<0.6	18
Mn(CO)$_5$	CCl$_4$	hexane	$(1.4 \pm 0.1) \times 10^6$	64
	CCl$_4$	C$_2$H$_5$OH	6.1×10^5	11, 12
	CCl$_4$	CCl$_4$	$(9.1 \pm 0.8) \times 10^5$	14
Re(CO)$_5$	CCl$_4$	C$_2$H$_5$OH	3.9×10^7	12

Based on the results of competition experiments, Wrighton and Abrahamson were able to order the reactivities of a series of monomeric intermediates toward halocarbons based on the results of product studies following photolysis in either CCl$_4$ or 1-iodopentane.[99] The experiments were carried out by photolyzing mixed-metal dimers like $(\eta^5\text{-}C_5H_5)(CO)_3MoMn(CO)_5$ in halocarbon solvents and observing the relative amounts of symmetrical metal–metal bond formation, e.g., to give $(\eta^5\text{-}C_5H_5)_2Mo_2(CO)_6$ and $Mn_2(CO)_{10}$, compared to the amount of oxidized products, e.g., $(\eta^5\text{-}C_5H_5)Mo(CO)_3X$ and $Mn(CO)_5X$ ($X = Cl$, I). Their results suggested the reactivity order: $Re(CO)_5 > Mn(CO)_5 > (\eta^5\text{-}C_5H_5)W(CO)_3 > (\eta^5\text{-}C_5H_5)Mo(CO)_3 > (\eta^5\text{-}C_5H_5)Fe(CO)_2 > Co(CO)_4$.

That reactions should occur between the monomers and halocarbons is not surprising. Once again, a useful analogy is with $Co^{II}(CN)_5^{3-}$, this time in its reactivity with methyl iodide as shown in eq 62. Presumably, the

$$Co(CN)_5^{3-} + CH_3I \rightarrow (CN)_5CoI^{3-} + CH_3 \qquad (62)^{100}$$

$$CH_3 + Co(CN)_5^{3-} \rightarrow (CN)_5Co\text{-}CH_3^{3-}$$
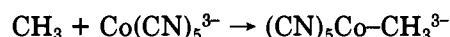
reactions between the monomeric intermediates and halocarbons occur by the same initial redox step, eq 63.

$$Mn(CO)_5 + CCl_4 \rightarrow (CO)_5MnCl + CCl_3 \qquad (63)$$

The inclination of the lower coordinate monomers to undergo inner-sphere, atom-transfer reactions is expected since in the redox products the coordination number is increased by one. The point is illustrated in Figure 8 for the reaction between $Co(CN)_5^{3-}$ and CH_3I using a schematic energy-coordinate diagram along a normal coordinate largely Co–I in character. The diagram is necessarily qualitative because the Co^{III}/Co^{II} and CH_3I/CH_3 couples are chemically irreversible and thermodynamic redox potentials are not known. As shown by the potential curve for $Co^{II}(CN)_5^{3-} + CH_3I$, the interaction between $Co^{II}(CN)_5^{3-}$ and CH_3I in the absence of atom transfer is assumed to be dissociative although at least a weak-bonding interaction probably exists. The basis for the assumption is the preference of $Co^{II}(CN)_5^{3-}$ to be five-coordinate, and the expected weak interaction between Co^{II} and CH_3I arising from $p(I) \rightarrow Co^{II}$ lone pair donation. The latter point is a natural consequence of the inability of CH_3I
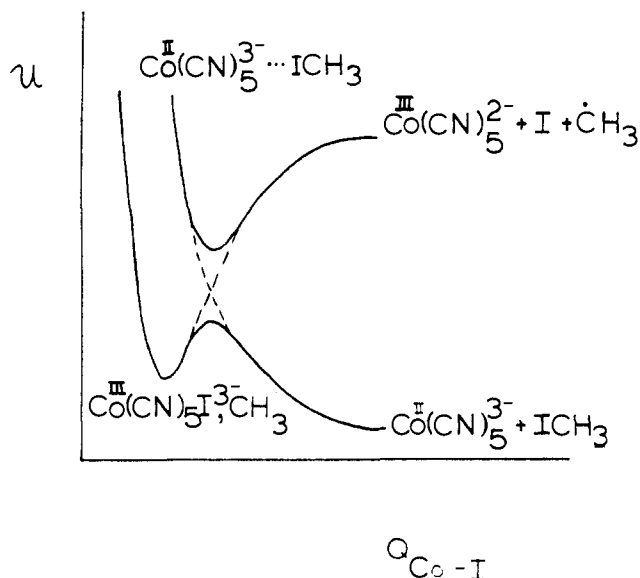
Figure 8. Schematic energy–coordinate diagram for the reaction between $Co^{II}(CN)_5^{3-}$ and CH_3I along a normal coordinate largely Co–I in character.

to function as a good donor ligand.

The potential curve for $(Co^{III}(CN)_5{}^{2-} + I + CH_3)$ describes the dissociative, substitutional loss of I^- from $Co(CN)_5I^{3-}$ to give the five-coordinate, d^6 intermediate, $Co(CN)_5{}^{2-}$. The difference in energy between the bottom $(Co(CN)_5I^{3-} + CH_3)$ and flat $(Co(CN)_5{}^{2-} + I^- + CH_3)$ portions of the curve is the energy of activation for the substitutional process. The "avoided crossing"[101] in the region of intersection between the potential curves for $(Co^{II}(CN)_5{}^{3-} + ICH_3)$ and $(Co^{III}(CN)_5I^{3-} + CH_3)$ is a consequence of significant, Q_{Co-I}-dependent electronic coupling between Co^{II} and CH_3I. The electronic configuration of $Co^{II}(CN)_5{}^{3-}$ is $(d_{xy}{}^2d_{xz}{}^2d_{yz}{}^2d_{z^2}{}^1)$ where the Z axis is taken to lie along the axis perpendicular to the plane of the square pyramid. The orbital basis for the electronic interaction is through d_{z^2} mixing with the vacant σ^* orbital of the C–I bond. Note that d_{z^2}–σ^*(C–I) mixing leads to metal-to-ligand charge transfer and redox product formation while $p(I) \rightarrow d\sigma^*(Co^{II})$ donation leads to net ligand-to-metal bond formation and the weak, interaction between Co^{II}-$(CN)_5{}^{3-}$ and ICH_3 suggested in Figure 8.

Because of strong electronic coupling and the avoided crossing, atom transfer for $Co^{II}(CN)_5{}^{3-}$ and related d^7 monomers like $Mn(CO)_5$ or $(\eta^5$-$C_5H_5)Fe(CO)_2$ can proceed by the concerted, synchronous process, $[(CN)_5Co^{II}\cdots I\text{-}CH_3]^{3-} \rightarrow [(CN)_5Co\cdots I\cdots CH_3]^{3-} \rightarrow [(CN)_5Co^{III}\text{-}I\cdots CH_3]^{3-}$, illustrated in Figure 8. Notice that simple outer-sphere electron transfer from Co^{II}-$(CN)_5{}^{3-}$ would necessarily give the lower coordinate, high-energy intermediate $Co^{III}(CN)_5{}^{2-}$. Outer-sphere electron transfer is a nonadiabatic process since it involves a transition from the lower state in Figure 8 to the upper. It is also a high energy process because of the profound change in coordinative preference which accompanies oxidation of Co(II) to Co(III). As a consequence, if atom transfer is an electronically allowed process, *it will always be more easily accessible by thermal activation* than will outer-sphere electron transfer.

Outer-sphere electron-transfer pathways may appear in potentially coordinating solvents. In coordinating

solvents even weak metal–solvent interactions may lead to monomer–solvent binding, e.g.

$$(\eta^5\text{-}C_5H_5)Mo(CO)_3 + S \rightleftharpoons (\eta^5\text{-}C_5H_5)Mo(CO)_3S$$
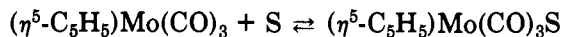
or at least to a kinetically significant concentration of the solvent-bound complex if five-coordination is favored. For such cases, the energetic dilemma associated with formation of a lower coordinate cation can be avoided and the appearance of outer-sphere electron transfer may be signalled by the appearance of the solvent-containing product $(\eta^5\text{-}C_5H_5)Mo(CO)_3S^+$.

It is worthwhile pursuing the analogy with $Co^{II}(CN)_3{}^{3-}$ even one step further. For this ion and related isonitrile complexes, the dimeric compounds, which contain or are thought to contain metal–metal bonds, Co_2-$(CN)_{10}{}^{6-\,102}$ and $Co_2(CNCH_3)_{10}{}^{4+},{}^{103}$ are isolable as solids. However, the monomeric species are the dominant forms in solutions. Most likely, in the relatively high formal oxidation state Co(II), decreased d-orbital extension leads to relatively weak metal–metal bonding and a shift in the monomer–dimer equilibrium toward the monomer in solution. The formation of monomers is favored entropically. For the metal–metal bonded dimers of interest here, the metal–metal bonds are apparently considerably stronger, ΔH (Mn–Mn) $\sim$ 36 kcal/mol for $Mn_2(CO)_{10}$ in hydrocarbon solution,[53] and the monomer–dimer equilibrium lies in favor of the dimer. However, it is important to realize that the monomers themselves are discrete chemical species with their own characteristic properties. Although they are somewhat reactive, it is conceivable that they could be quite stable in inert solvents except for the inherent dilemma associated with the thermodynamically favored coupling process to form the metal–metal bond.

The point is illustrated very nicely by the observations by Brown et al. on the formation of persistent, paramagnetic monomers.[96,104,105] Photolysis of substituted phosphine- or phosphite-containing dimers in hydrocarbon solvents in the presence of excess ligand with degassing leads to monomers as shown in eq 64 and 65. The resulting products were characterized by

$$Mn_2(CO)_8(PBu_3)_2 + PBu_3 \xrightarrow{+h\nu,\,-CO} Mn(CO)_3(PBu_3)_2 \quad (64)$$

$$Mn_2(CO)_7(P(OEt)_3)_3 + P(OEt)_3 \xrightarrow{+h\nu,\,-CO} Mn(CO)_3(P(OEt)_3)_2 \quad (65)$$
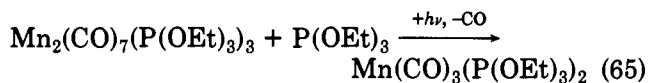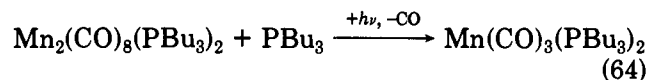
solution measurements and assigned square-pyramidal structures with mutually trans PR_3 or $P(OR)_3$ groups based on EPR spectral fitting.[96,104,105] The monomers absorb in the low-energy visible (600–1500 nm) and react with CO to return to the disubstituted dimers, $Mn_2(CO)_8(L)_2$. There is evidence that a measurable monomer–dimer equilibrium may exist for some systems at 0 °C, eq 66.

$$Mn_2(CO)_6(P(O\text{-}i\text{-}Pr)_3)_4 \rightleftharpoons 2Mn(CO)_3(P(O\text{-}i\text{-}Pr)_3)_2 \quad (66)$$
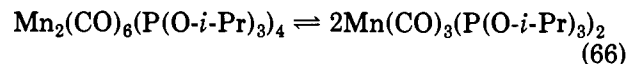
4. Disproportionation

Metal–metal bonds are prone to undergo disproportionation reactions in polar solvents, e.g., eq 67. The

$$Co_2(CO)_8 + C_5H_{10}NH \rightarrow Co(CO)_4(pip)^+, Co(CO)_4^-$$
$$(67)^{106}$$

$$C_5H_{10}NH = pip = piperidine$$
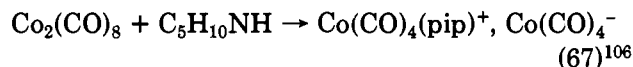
driving force for disproportionation appears to come from coordination of the added base to the higher oxidation state and solvation of the two ions once disproportionation has occurred.[4] Thermodynamically, disproportionation becomes spontaneous when the factors stabilizing the products are sufficient to overcome the strength of the metal–metal bond. For the case of the cobalt carbonyl dimer in eq 66, the metal–metal bond is relatively weak and the chemistry illustrated occurs under thermal conditions. For the dimers $Mn_2(CO)_{10}$ and $(\eta^5-C_5H_5)_2Mo_2(CO)_6$, disproportionation also occurs but under photochemical conditions, eq 26 and 43 occur. In contrast to $Co_2(CO)_8$, the disproportionation products produced photochemically are probably thermodynamically unstable, as suggested for $(\eta^5-C_5H_5)_2Mo_2(CO)_6$ in Figure 6, since they return to the metal–metal bond when solutions are heated or held at room temperature for extended periods, at least for the molybdenum dimer.[39]

As mentioned earlier, for the molybdenum dimer there is evidence from flash photolysis that both the monomeric and dimeric intermediates are involved in photodisproportionation. In solutions containing 10^{-3} M or greater Br^-, capture of $(\eta^5-C_5H_5)Mo(CO)_3$ by Br^- competes with recombination leading to the disproportionation products $(\eta^5-C_5H_5)Mo(CO)_3Br$ and $(\eta^5-C_5H_5)Mo(CO)_3^-$. From the experimental evidence cited in earlier sections, it is possible to write out plausible mechanisms by which disproportionation occurs. As shown in eq 68, in a first step association with an added ligand, or in a polar solvent like acetonitrile, of a solvent molecule occurs. The association step is not too surprising since the lower coordinate intermediates are expected to be somewhat electron deficient. In this regard, the associative substitution of PR_3 for CO in $Mn(CO)_5$ comes to mind. An interesting analogy to an association step like

$$(Cp)_2Mo_2(CO)_6 \xrightarrow{+h\nu} 2(Cp)Mo(CO)_3$$

$$(Cp)Mo(CO)_3 + L \rightarrow (Cp)Mo(CO)_3(L) \quad (68)$$

$$(Cp)Mo(CO)_3(L) + (Cp)Mo(CO)_3 \rightarrow$$
$$(Cp)Mo(CO)_3(L)^+ + (Cp)Mo(CO)_3^-$$

prising since the lower coordinate intermediates are expected to be somewhat electron deficient. In this regard, the associative substitution of PR_3 for CO in $Mn(CO)_5$ comes to mind. An interesting analogy to an association step like

$$(\eta^5-C_5H_5)Mo(CO)_3 + Br^- \rightarrow (\eta^5-C_5H_5)Mo(CO)_3Br^-$$

is to the known affinity of halogen atoms for halide ions, for example,

$$I + I^- \rightarrow I_2^-$$

In fact, in some ways, the monomers can be regarded as pseudohalogen atoms.

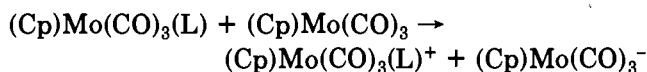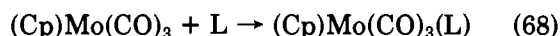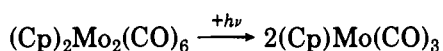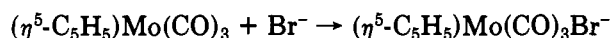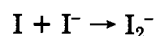Recall (Figure 8) that there is a clear advantage to preassociation of Br^- or of a solvent molecule prior to electron transfer in order to avoid the dilemma of forming the coordinatively unsaturated cation $(\eta^5-C_5H_5)Mo(CO)_3^+$ via eq 69.

$$2(\eta^5-C_5H_5)Mo(CO)_3 \rightarrow$$
$$(\eta^5-C_5H_5)Mo(CO)_3^+ + (\eta^5-C_5H_5)Mo(CO)_3^- \quad (69)$$
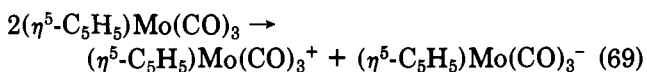
As suggested by Stiegman and Tyler[36,40] based on earlier proposals by Brown et al.,[47-49] the appearance of $\phi > 1$ for disproportionation and evidence for radical-chain behavior can also be accounted for by electron-transfer steps. In particular, electron transfer to the starting dimer represents a propagating step because of the reappearance of $(\eta^5-C_5H_5)Mo(CO)_3$ which reenters the electron-transfer cycle, eq 70.

$$(\eta^5-C_5H_5)Mo(CO)_3(L) + (\eta^5-C_5H_5)_2Mo_2(CO)_6 \rightarrow$$
$$(\eta^5-C_5H_5)Mo(CO)_3(L)^+ + (\eta^5-C_5H_5)Mo(CO)_3^- +$$
$$(\eta^5-C_5H_5)Mo(CO)_3 \quad (70)$$
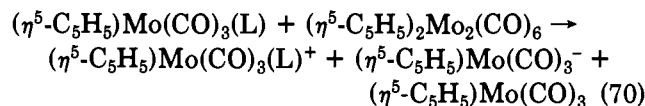
Electron transfer to the dimer would give initially the dimeric anion, $(\eta^5-C_5H_5)_2Mo_2(CO)_6^-$, followed by separation into $(\eta^5-C_5H_5)Mo(CO)_3$ and $(\eta^5-C_5H_5Mo(CO)_6^-$. The situation here may be somewhat analogous to halocarbons where radical anions like $CCl_4^-\cdot$ are known to be unstable and rapidly breakdown into the corresponding halide ion and carbon-based radical.[76] An interesting observation on this point was made by Meckstroth et al., who report that upon pulse radiolysis of ethanol solutions containing $Re_2(CO)_{10}$ an intermediate forms which may be $Re_2(CO)_{10}^-$.[12] The intermediate absorbs at 415 and 515 nm and is unstable with respect to decomposition, perhaps through an intermediate hydride.

Given the electron-transfer steps in eq 68 and 70, an important factor determining quantum yields for disproportionation must be the relative rates of electron transfer from $(\eta^5-C_5H_5)Mo(CO)_3(L)$ to $(\eta^5-C_5H_5)Mo(CO)_3$ or $(\eta^5-C_5H_5)_2Mo_2(CO)_6$. The monomer is always present in a low steady-state concentration but is presumably considerably more reactive toward electron transfer than the dimer which allows it to compete with the dimer for $(\eta^5-C_5H_5)Mo(CO)_3(L)$. Although values for $\phi_{dis} > 1$ may signal the importance of the radical-chain component through eq 70, it should be realized that the converse is also true. The observation of ϕ_{dis} values equal to the sum of the appearance efficiencies for $(\eta^5-C_5H_5)Mo(CO)_3$ and $(\eta^5-C_5H_5)_2Mo_2(CO)_5$ in the limit of high added ligand concentrations, provides strong evidence for the *absence* of an electron-transfer chain component.

Disproportionation in the presence of added phosphine and phosphites presumably involves many of the same features, note, for example, Scheme IV. However, an interesting feature here is the apparent necessity for the addition of two phosphine or phosphite groups to the monomer to give $CpMo(CO)_2(L)_2$ before disproportionation can occur. Presumably, an intermediate like $CpMo(CO)_3(L)$, if present in appreciable concentrations, is insufficiently strong as a reducing agent to initiate the electron-transfer reactions needed for disproportionation to occur, e.g.,

$$(Cp)Mo(CO)_3(PR_3) + (Cp)_2Mo_2(CO)_6 \xrightarrow{(slow)}$$
$$(Cp)Mo(CO)_3(PR_3)^+ + (Cp)_2Mo_2(CO)_6^-$$

$$(Cp)Mo(CO)_3(PR_3) + (Cp)Mo(CO)_3 \xrightarrow{(slow)}$$
$$(Cp)Mo(CO)_3(PR_3)^+ + (Cp)Mo(CO)_3^-$$
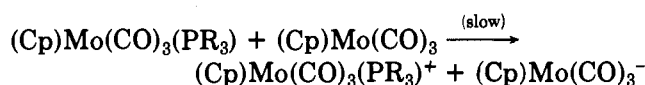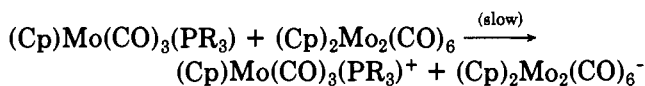
The contribution of monomers to the photochemically induced disproportionation of $Mn_2(CO)_{10}$ in the presence of nitrogen bases presumably occurs by a similar mechanism.[47,58] However, recall that photolysis

of $Mn_2(CO)_{10}$ in acetonitrile gives $Mn_2(CO)_9(CH_3CN)$ which by direct observation arises solely from $Mn_2(CO)_9$.[14] Also, in pyridine (py) solution, $Mn_2(CO)_9(py)$ is an initial product but $Mn_2(CO)_8(py)_2$ is not. $Mn_2(CO)_8(py)_2$ undergoes further photolysis to give $Mn_2(CO)_{10}$, $[Mn(CO)_3(py)_3]^+$ and $Mn(CO)_5^-$. These observations suggest that an important contribution to disproportionation may come from initial photosubstitution to give $Mn_2(CO)_9(py)$ via $Mn_2(CO)_9$ followed by the expected sequence of events in Scheme XIII (also note Scheme VI). One feature of note in the scheme is the implication that substitution of pyridine for CO to give $Mn(CO)_4(py)$ leads to further labilization of CO in the monomers. Another, as always, is that energetic considerations nearly demand the prior association of an additional ligand to give $Mn(CO)_3(py)_3$ *prior* to electron transfer. A third is the implied necessity of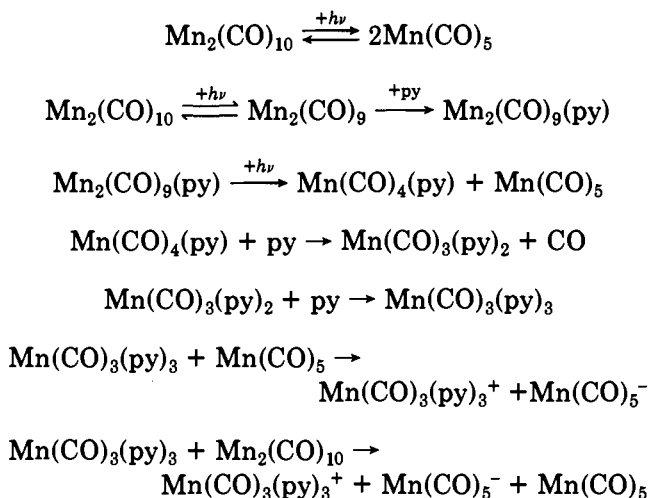 substitution of two CO groups before electron transfer can occur. An additional point of interest in the scheme is the suggestion that *both* the monomeric and CO-loss dimeric intermediates may intervene in the net reaction although in sequential steps.

SCHEME XIII

$$Mn_2(CO)_{10} \overset{+h\nu}{\rightleftharpoons} 2Mn(CO)_5$$

$$Mn_2(CO)_{10} \overset{+h\nu}{\rightleftharpoons} Mn_2(CO)_9 \overset{+py}{\longrightarrow} Mn_2(CO)_9(py)$$

$$Mn_2(CO)_9(py) \overset{+h\nu}{\longrightarrow} Mn(CO)_4(py) + Mn(CO)_5$$

$$Mn(CO)_4(py) + py \rightarrow Mn(CO)_3(py)_2 + CO$$

$$Mn(CO)_3(py)_2 + py \rightarrow Mn(CO)_3(py)_3$$

$$Mn(CO)_3(py)_3 + Mn(CO)_5 \rightarrow$$
$$Mn(CO)_3(py)_3^+ + Mn(CO)_5^-$$

$$Mn(CO)_3(py)_3 + Mn_2(CO)_{10} \rightarrow$$
$$Mn(CO)_3(py)_3^+ + Mn(CO)_5^- + Mn(CO)_5$$

5. Electron Transfer

As pointed out by Hepp and Wrighton, compared to the parent metal–metal-bonded dimers, the photochemically produced monomeric intermediates are thermodynamically both better oxidants and reductants than are the dimers themselves.[34] The situation is entirely analogous to excited states where, for example, experimental estimates are available for redox potentials for the MLCT excited state of $Ru(bpy)_3^{2+}$, $(bpy)_2Ru^{III}(bpy^-)^{2+*}$, acting as either an oxidant (0.8 V vs. the saturated calomel electrode in CH_3CN) or reductant (−0.8 V vs. SCE).[107,108]

For monomeric intermediates like $Mn(CO)_5$, such a conclusion is clearly justified on electronic grounds. Note from Scheme IX that in $Mn(CO)_5$ there is a single electron in the d_{z^2} orbital which is $d\sigma^*$ in character. Compared to the σ^2 configuration of the metal–metal bond, $Mn(CO)_5$ has a higher energy electron $(d_{z^2} > \sigma)$ and is a better reducing agent. At the same time $Mn(CO)_5$ has an electron hole at higher energy $(d_{z^2} < \sigma^*)$ making it a better oxidant than the dimer.

The point is developed further in the thermodynamic

SCHEME XIV
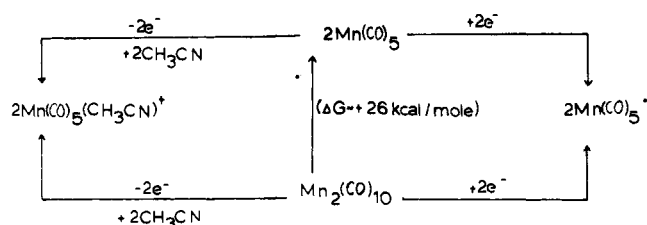
cycle in Scheme XIV. The cycle illustrates the redox couples involved in the oxidation or reduction of $Mn_2(CO)_{10}$ or $Mn(CO)_5$ in the polar organic solvent acetonitrile to give either $Mn(CO)_5(CH_3CN)^+$ or $Mn(CO)_5^-$. The value of ΔG for dissociation of the Mn–Mn bond comes from the combination of thermal and flash-photolysis kinetics data in hydrocarbon solvents mentioned in an earlier section.[53] From the cycle, photochemical excitation to give $Mn(CO)_5$ enhances the oxidizing and reducing ability of the system by ~ 26 kcal/mol (1.1 V). Redox potentials are not available for the dimer couples by electrochemical measurements because both are electrochemically irreversible.

It is apparent from reactions like those shown in eq 1 and 44 that metal–metal-bond photolysis can lead to typical electron-transfer products. Although both the monomeric and dimeric intermediates may be involved, it seems clear that monomers like $Mn(CO)_5$ can undergo inner-sphere electron transfer as shown in eq 71 and by the observation of the expected products in eq 72.

(71)[109]

$$2Ru(bpy)_2Cl_2^+ + Mn_2(CO)_{10} + 2CH_3CN \overset{+h\nu}{\longrightarrow}$$
$$2Ru(bpy)_2(CH_3CN)Cl^+ + 2Mn(CO)_5Cl \quad (72)^{110}$$
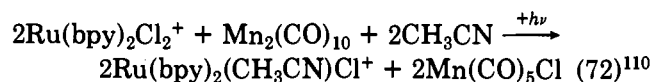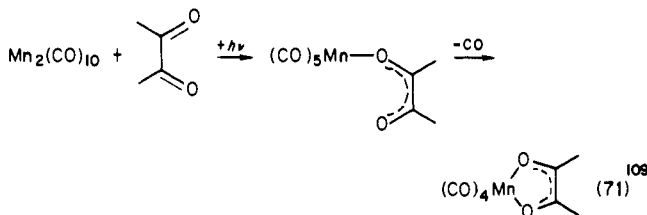
The results of an interesting electron-transfer study have been reported by Hepp and Wrighton.[34] They photolyzed $M_2(CO)_{10}$ (M = Mn, Re) and $(\eta^5\text{-}C_5H_5)_2W_2(CO)_6$ in CH_2Cl_2 or CH_3CN in the presence of both CCl_4 and potential 1-electron oxidants like Fe-$(\eta^5\text{-}C_5H_5)_2^+$ or $(4,4'\text{-}Me\text{-}^+NC_5H_4C_5H_4N^+\text{-}Me)(PQ^{2+})$. In dichloromethane solution in the presence of (N-n-Bu_4)(ClO_4)$, product analysis by infrared showed that a competition existed between one-electron oxidation and capture by CCl_4 to give as products $Mn(CO)_5(ClO_4)$ or $Mn(CO)_5Cl$. In the coordinating solvent acetonitrile, the photolysis products became $Mn(CO)_5(CH_3CN)^+$ or $Mn(CO)_5Cl$. Although the quantitative details of their results may be somewhat obscured by contributions from $Mn_2(CO)_9(CH_3CN)$ or $Mn_2(CO)_9$, they were able to obtain some useful information. By using known values for rate constants with CCl_4 obtained in earlier work, they calculated rate constants for reactions 73 and 74 in 0.1 M (N-n-Bu_4)(ClO_4)–CH_3CN$ at room temperature.

$$(Cp)W(CO)_3 + CH_3CN + Fe(Cp)_2^+ \overset{k = 1.4 \times 10^6 \text{ M}^{-1} \text{ s}^{-1}}{\longrightarrow}$$
$$(Cp)W(CO)_3(CH_3CN)^+ + Fe(Cp)_2 \quad (73)$$

$$Mn(CO)_5 + CH_3CN + Fe(Cp)_2^+ \xrightarrow{k = 7.0 \times 10^6 \text{ M}^{-1} \text{s}^{-1}}$$
$$Mn(CO)_5(CH_3CN)^+ + Fe(Cp)_2 \quad (74)$$
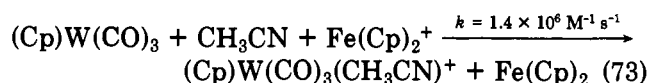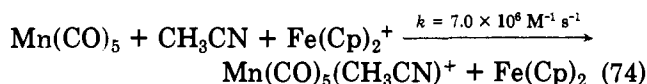
They were also able to show that for a given radical, the one-electron-transfer pathway became more competitive as the oxidizing strength of the added oxidant increased and that there were systematic variations in the reactivities of the various monomeric intermediates toward 1-electron transfer. Recall, once again, the advantage of binding a solvent molecule *before* outer-sphere electron transfer occurs.

$$Mn(CO)_5 + CH_3CN \rightleftharpoons Mn(CO)_5(CH_3CN)$$

$$Mn(CO)_5(CH_3CN) + Fe(\eta^5\text{-}C_5H_5)_2^+ \rightarrow$$
$$Mn(CO)_5(CH_3CN)^+ + Fe(\eta^5\text{-}C_5H_5)_2 \quad (75)$$
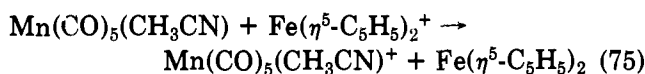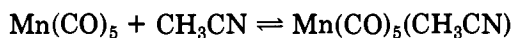
In a related experiment, rate constants were obtained directly for the oxidation of $Mn(CO)_5$ by a series of pyridinium ions in acetonitrile by flash photolysis.[110]
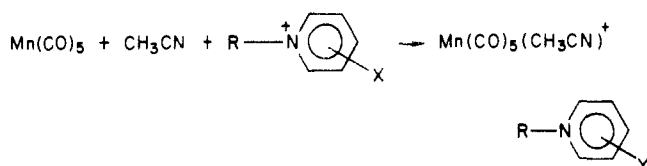
In Table VII are listed both the second-order rate constants from the flash photolysis study and reduction potentials for the pyridinium couples. The data show that even with the least strongly oxidizing pyridinium ion, electron transfer is still quite rapid. Consequently, it is possible to estimate that for the couple $Mn(CO)_5(CH_3CN)^+/Mn(CO)_5$ or $Mn(CO)_5(CH_3CN)^+/Mn(CO)_5(CH_3CN)$, $E° < -0.8$ V vs. SCE or $E° < -0.6$ V vs. NHE (normal hydrogen electrode). With this value and the cycle in Scheme XIV, it is possible to estimate that for the dimer couple, $Mn(CO)_5(CH_3CN)^+/Mn_2(CO)_{10}$, $E° < -0.2$ V vs. SCE, or $E° < 0.0$ V vs. NHE. To help put the redox potential values into perspective, they show that both $Mn(CO)_5$ and $Mn_2(CO)_{10}$ are at least mild reducing agents, and further, that $Mn(CO)_5$ is *at least* a stronger reducing agent than is Cr^{2+} in water, $E°$ $(Cr(H_2O)_6^{3+/2+}) = -0.4$ V vs. NHE.

Heretofore, there appear to be no reported examples of reduction of the monomers, as for example in

$$Mn(CO)_5 + D \rightarrow Mn(CO)_5^- + D^+$$
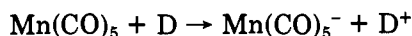
where D is an electron-transfer donor. Such a study with a series of closely related reducing agents like $Me_2NC_6H_4X$ where X is a substituent on the aromatic ring, could be of real value in estimating redox potentials for couples like $Mn(CO)_5/Mn(CO)_5^-$. This approach has proven to be of value in estimating redox potentials of excited states.[107,108]

6. Substitution

A common mechanistic feature proposed for substitution reactions of the monomeric intermediates produced either thermally or photochemically involves initial loss of CO to give lower coordinate intermediates,[59,60] for example, eq 76. However, as noted in a

$$Mn(CO)_5 \underset{+CO}{\overset{-CO}{\rightleftharpoons}} Mn(CO)_4 \xrightarrow{+PBu_3} Mn(CO)_4(PBu_3) \rightarrow$$
$$1/2 Mn_2(CO)_8(PBu_3)_2 \quad (76)$$
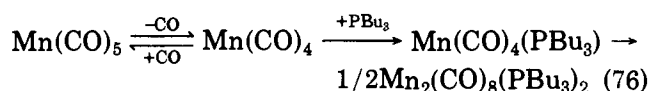
TABLE VII. Electron-Transfer Rate Constants for the Reaction $P^+ + Mn(CO)_5 + CH_3CN \rightarrow P + Mn(CO)_5(CH_3CN)^+$ at 22 ± 2 °C[110]

P^+ or P^{2+}	$E°'$ (P^+/P) or $E°'$ (P^{2+}/P^+), V^a	k, M^{-1} s^{-1}
[PhCH₂N⟨⟩—⟨⟩NCH₂Ph]²⁺	0.36	1.5×10^6
[CH₃N⟨⟩—⟨⟩NCH₃]²⁺	0.45	6.8×10^5
[CH₃N⟨⟩—CN]⁺	0.66	5.5×10^5
[CH₃N⟨⟩—C(O)CH₃]⁺	0.78	3.0×10^5

^{a} Formal potentials in 0.1 M ($^+NEt_4$)(ClO_4^-) vs. the saturated calomel electrode (SCE).

previous section, the available mechanistic evidence suggests that this assumption may not be valid.[55,61-64] It appears that in some cases photochemically induced susbtitution may not occur via the monomeric intermediates and even when it does, the details of the mechanistic step may be associative rather than dissociative in detail. A particular case in point came in the photolysis of $Mn_2(CO)_{10}$ in hydrocarbon solvents in the presence of phosphines where at low concentrations of added PR_3, substitution occurs via the intermediate $Mn_2(CO)_9$ to give $Mn_2(CO)_9(PPh_3)$. At higher concentrations, a reaction between $Mn(CO)_5$ and PPh_3 appears but apparently proceeds by an associative mechanism.

D. Reactivity and Properties of the Dimeric Intermediates

1. Molecular and Electronic Structure

In all of the systems discussed, clear evidence has been obtained from transient absorbance experiments for relatively long-lived intermediates in addition to the monomers. Some of their properties, as obtained by flash photolysis of the dimers or in low-temperature matrices, are summarized in Table VIII. As noted in earlier sections, there is good evidence in all cases that the second intermediate is a CO-loss dimer.

There are analogies and possible structural precedences in related systems. For example, photochemically induced loss of CO from the Co and Rh monomers $(\eta^5\text{-}C_5H_5)M(CO)_2$ (M = Co, Rh) leads to loss of CO and metal–metal bond formation as shown in eq 77.[111]
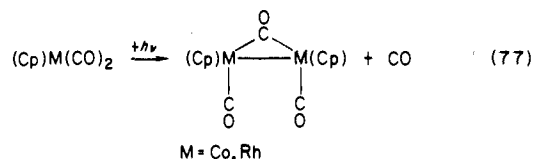
An interesting structure which may represent a stabilized form of a CO-loss intermediate appears in $Mn_2(CO)_5(Ph_2PCH_2PPh_2)_2$.[112] As portrayed in Figure 9, the salient features of the structure include the presence of the bridging diphosphine ligands and a semibridging CO group. Note the direct analogy in terms of ligand composition between the diphosphine-based dimer and the proposed intermediate $Mn_2(CO)_9$.

Another structure of interest is the cyano-bridged dimer, $[(\eta^5\text{-}C_5H_5)_2Mo_2(CO)_4(CN)]^-$, obtained by Curtis

TABLE VIII. Properties of the Dimeric Intermediates in Cyclohexane at 22 ± 2 °C; ν (CO) in Low-Temperature Glasses or Matrices

starting dimer/suggested intermediate	λ_{max}, nm	ν (CO), cm^{-1}	decay characteristics[a]
$(\eta^5\text{-}C_5H_5)_2Fe_2(CO)_4/(\eta^5\text{-}C_5H_5)_2Fe_2(CO)_3$	510	1812[17a,22,24]	first order, also a photochemical path[32]
$[\eta^5\text{-}C_5H_5)_2Mo_2(CO)_6/(\eta^5\text{-}C_5H_5)_2Mo_2(CO)_5$	360–380	1978, 1933,[23] 1895, 1665	$k = 1.2\text{-}17 \times 10^7$ M^{-1} s^{-1} [45]
$Mn_2(CO)_{10}/Mn_2(CO)_9$	495	1760[b,21]	second order + CO, $k \leq 1.2 \times 10^5$ M^{-1} s^{-1} [14]
$Re_2(CO)_{10}/Re_2(CO)_9(?)$	550 (375 ± 10)		$t_{1/2} = \sim 100$ ms[15]

[a] For return to the starting dimer. [b] ν(CO) for the bridging CO group only.
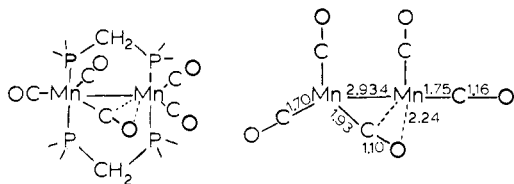
Figure 9. Structure of $Mn_2(CO)_6(Ph_2PCH_2PPh_2)_2$.

et al. by the addition of one equivalent of CN$^-$ to $(\eta^5\text{-}C_5H_5)(CO)_2Mo\equiv\equiv Mo(CO)_2(\eta^5\text{-}C_5H_5)$.[113] Two features of note in the structure
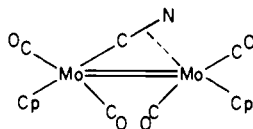
are the appearance of a semibridged cyano group and multiple metal-metal bonding between the molybdenum atoms.[113] There is obviously a close connection, at least in a formal sense, between the cyano-bridged dimer and the proposed intermediate $(\eta^5\text{-}C_5H_5)_2Mo_2$-$(CO)_5$.

As noted in earlier sections, CO-bridged structures have been proposed for the intermediates $(\eta^5\text{-}C_5H_5)_2Fe_2(CO)_3$[22,24] and $(\eta^5\text{-}C_5H_5)_2Mo_2(CO)_5$[23] in low-temperature matrices, based on the pattern of ν(CO) bands in the infrared. The structures in the low-temperature experiments probably exist in hydrocarbon solvents at room temperature as well as shown by the coincidence of λ_{max} and ν(CO) values for $(\eta^5\text{-}C_5H_5)_2Fe_2(CO)_3$ produced at low temperatures in poly-(vinyl chloride) with λ_{max} and ν(CO) values obtained by flash photolysis at room temperature in cyclohexane. However, in potentially coordinating solvents, the electron-deficiency problems associated with CO loss can be solved by ligand binding, e.g., to give $Mn_2(C-O)_9(S)$, rather than by the formation of bridging or semibridging groups, and the situation may be quite different.

Another revealing feature about the dimeric intermediates is the nature of the decay process by which they return to the starting dimers. For $(\eta^5\text{-}C_5H_5)_2Mo_2(CO)_5$ and $Mn_2(CO)_9$, the return of the intermediate to the starting dimer is first order in both intermediate and in CO. From the kinetics, the processes being observed appear to involve the addition of CO to the CO-bridged, dimeric intermediates in hydrocarbon solvents or perhaps by displacement of a coordinated solvent molecule from an intermediate like $(\eta^5\text{-}C_5H_5)_2Mo_2(CO)_5(THF)$ in potentially coordinating solvents. On the other hand, the return of the dimeric iron intermediate to the parent dimer occurs by a first-order process. The process is independent of the concentration of CO under conditions, e.g., in cyclohexane, where the CO-bridged structure appears to

prevail. One inference that can be drawn from the kinetics data is that in order for further chemistry to occur, an intramolecular rearrangement process involving the intermediate to give a more reactive form must occur. Although no information is available concerning such "reactive forms" the processes involved may occur by opening of a bridging or semibridging ligand to give a coordinatively unsaturated site at the metal-metal bond.

2. Redox Chemistry. Halocarbons

At least in some cases, the CO-loss intermediates also have a net redox chemistry with halocarbons. Reactions between $(\eta^5\text{-}C_5H_5)_2Fe_2(CO)_3$ and CCl_4 in cyclohexane (k (22 °C) = 4×10^3 M^{-1} s^{-1})[32] and between $Mn_2(CO)_9$ and CCl_4 in CCl_4 ($k = (2.1 \pm 0.4) \times 10^2$ s^{-1})[14] have been observed directly by flash photolysis. The data in Table III suggest that, depending on conditions, the dimeric intermediates are produced at a level of 20–40% of the monomers. As a consequence, it is important to realize that the dimeric intermediates may account for an appreciable fraction of the net photochemistry observed with halocarbons and perhaps in other photoredox processes as well.

As was true for the monomers, the thermodynamic strength of the dimeric intermediates both as oxidants and as reductants are necessarily enhanced compared to the parent dimers. For $(\eta^5\text{-}C_5H_5)_2Fe_2(CO)_3$, the initial redox step most likely involves initial Cl-atom transfer

$$(\eta^5\text{-}C_5H_5)_2Fe_2(CO)_3 + CCl_4 \rightarrow$$
$$(\eta^5\text{-}C_5H_5)_2Fe_2(CO)_3Cl + CCl_3^- \quad (78)$$
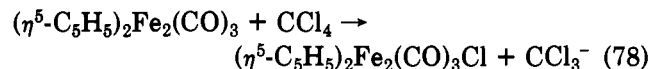
perhaps followed by a more facile reaction between the partially oxidized dimer and a second molecule of CCl_4

$$(\eta^5\text{-}C_5H_5)_2Fe_2(CO)_3Cl + CO + CCl_4 \rightarrow$$
$$2(\eta^5\text{-}C_5H_5)Fe(CO)_2Cl + CCl_3$$
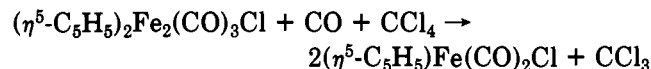
Alternatively, the oxidized dimer may be unstable toward dissociation leading to cleavage with the subsequent chemistry carried by monomeric fragments
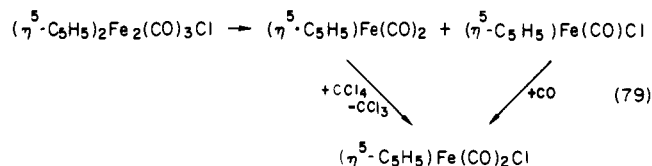
3. Disproportionation

From flash-photolysis studies at low [Br$^-$], evidence has been obtained for a rapid reaction between $(\eta^5\text{-}C_5H_5)_2Mo_2(CO)_5$ and Br$^-$.[45] Presumably the first step involves Br$^-$ addition. A possible mechanistic scheme to explain the subsequent steps leading to the observed disproportionation products is shown in eq 80. One

$$(Cp)_2Mo_2(CO)_5 + Br^- (10^{-4} M) \longrightarrow [(Cp)(CO)_2\underset{\underset{Br}{|}}{Mo}\text{---}Mo(CO)_3(Cp)]^-$$

$$(Cp)Mo(CO)_2Br_2^- \quad\underset{+Br^-}{\diagdown}$$

$$(Cp)Mo(CO)_2Br + (Cp)Mo(CO)_3^- \qquad (80)$$

$$(Cp)Mo(CO)_3Br \quad\underset{+CO}{\diagup}$$

of the keys in eq 80 is the heterolytic cleavage of the proposed intermediate $(\eta^5\text{-}C_5H_5)_2Mo(\mathring{C}O)_5Br^-$. Presumably the role of electron-donating anions like Br^- may be to polarize the Mo–Mo bond sufficiently to help stabilize the initial disproportionation products. Competitive capture of $(\eta^5\text{-}C_5H_5)Mo(CO)_2Br$ by CO or Br^- is not unreasonable, $(\eta^5\text{-}C_5H_5)Mo(CO)_2Br_2^-$ has been observed as a photoproduct in relatively high concentrations of Br^-.[34]

However, as noted by Stiegman and Tyler[51] other pathways may be available for disproportionation. Recall their observation that $(\eta^5\text{-}C_5H_5)_2Mo_2(CO)_5(PPh_3)$ does undergo disproportionation in the presence of PPh_3 to give $(\eta^5\text{-}C_5H_5)Mo(CO)_3^- + (\eta^5\text{-}C_5H_5)Mo(CO)_2\text{-}(PPh_3)_2^+$, but only for photolysis wavelengths, $\lambda > 290$ nm. They suggested as an origin for the high energy pathway for formation of a CO-bridged intermediate

$$(\eta^5\text{-}C_5H_5)(CO)_3Mo\text{-}\overset{\overset{\displaystyle O}{\|}}{C}\text{-}Mo(CO)_2(\eta^5\text{-}C_5H_5)$$

They also suggested a second possibility which is based on the potential energy curves shown in Figure 4 where the transition, $^1(\sigma^2) \xrightarrow{+h\nu} {}^1(\sigma\sigma^*)$, is illustrated. They note that at high photolysis energies, vibrational levels above the dissociation level for the $^1(\sigma\sigma^*)$ state may be populated leading to dissociation before crossing to $^3(\sigma\sigma^*)$ can occur. If such were the case, it should be reflected in the band shape on the high energy side of the $\sigma \to \sigma^*$ transition, and given the fact that the disproportionation products are ions, in profound solvent effects.

In the context of the disproportionation reaction, it may be useful to recall the results of picosecond emission experiments on $(\eta^5\text{-}C_5H_5)_2M_2(CO)_6$ (M = Mo, W).[46] In that work, ultraviolet photolysis resulted in the appearance of both short- and long-lived emissions which were assigned to MLCT excited states. Although the exact nature of the emitting excited states was not well established, a charge-transfer description is reasonable in these and related organometallic complexes containing CO and cyclopentadienyl ligands.[1] Since these states are only accessible following ultraviolet photolysis they may be the states responsible for the disproportionation observed by Stiegman and Tyler. Disproportionation would not be unexpected given the electronic structures involved, eq 81.

$$(Cp)(PPh_3)(CO)_2Mo^I\text{-}Mo^I(CO)_3(Cp) \xrightarrow{UV}$$

$$(Cp)(PPh_3)(CO^-)(CO)Mo^{II}\text{-}Mo^I(CO)_3(Cp) \xrightarrow{+PPh_3}$$

$$(Cp)Mo(CO)_2(PPh_3)_2^+ + (Cp)Mo(CO)_3^- \quad (81)$$

4. Substitution

It is clear both by direct observation and by inference based on product studies that the dimeric intermediates

undergo reactions with added ligands to undergo net photochemical substitution for CO. By flash photolysis in cyclohexane, the intermediate, $(\eta^5\text{-}C_5H_5)_2Fe_2(CO)_3$, was observed to undergo reactions with added PPh_3 ($k = 1.5 \times 10^5 \ M^{-1} \ s^{-1}$) and with CO ($k[CO] = 280 \ s^{-1}$).[32] As noted in previous sections, in some cases the CO-loss intermediates may be the *only* source of substitutional photochemistry. In addition, it is important to keep in mind the possible role of the CO-loss intermediates in secondary photochemical reactions leading to further substitution, eq 41.

IV. Conclusion

In concluding this account, it seems useful to review some of the overall conclusions deduced from the mechanistic studies. (1) In order to establish unequivocally the details of a photochemical mechanism, it is essential to utilize a full array of time-resolution capabilities from picosecond spectroscopy to product analysis. Perhaps the most insightful and, unfortunately, the most difficult type of experiment is the direct observation of transients and of their reactions with added substrates. (2) In the systems that have been studied in detail, the observed photochemistry can be accounted for largely by the appearance of two different intermediates. The two intermediates appear to be primary photoproducts which may have their origin in a single excited state or in different excited states between which an intersection exists as suggested by the appearance of wavelength-independent photochemistry. (3) In accounting for the observed photochemistry, it is necessary to take into account the reactions of *both* intermediates. In some cases, e.g., for $Mn_2(CO)_{10}$ with added CCl_4 or for $(\eta^5\text{-}C_5H_5)_2Mo_2(CO)_6$ in THF with added Br^-, both intermediates appear to lead to the observed photoproducts. In others, e.g., $Mn_2(CO)_{10}$ in CH_3CN or $(\eta^5\text{-}C_5H_5)_2Fe_2(CO)_4$ with PPh_3, only one of the intermediates may be involved. In still others, e.g., disproportionation of $Mn_2(CO)_{10}$ in pyridine, complex reaction sequences involving both types of intermediates may play a role in the net photochemistry. (4) Because of the different transient decay and reactivity patterns for the two types of intermediates, different results can be obtained under different conditions. For example, at low concentrations of an added reactant, recombination of photochemically produced monomers may be too rapid for them to be intercepted and the dimeric intermediates may dominate the photochemistry. As a consequence, a full picture of photochemical reactivity must include concentration-dependent studies or the direct observation of the intermediates. (5) In some cases different intermediates may begin to play a role or higher excited states come to dominate the photochemistry as in the disproportionation of $(\eta^5\text{-}C_5H_5)_2Mo_2(CO)_5(PPh_3)$.

Before further progress can be made in this area, it seems clear that, as in much of organimetallic chemistry, there is far too little detailed information concerning electronic structure. In the mechanistic area, it appears that the real challenges involve bringing new techniques to bear on observing and characterizing photochemical intermediates and their reactions. Finally, it should be appreciated that every metal–metal-bonded compound represents what could potentially

be a new adventure mechanistically and if it fails to behave in accordance with the patterns described here, it is not the fault of the authors.

V. References

(1) Geoffroy, G. L.; Wrighton, M. S. "Organometallic Photochemistry"; Academic Press: New York, 1979.
(2) (a) Wrighton, M. S. *Top. Curr. Chem.* **1976**, *65*, 37. (b) Wrighton, M. S. *Chem. Rev.* **1974**, *74*, 401.
(3) Stiegman, A. E.; Tyler, D. R. *Acc. Chem. Res.* **1984**, *17*, 61.
(4) Meyer, T. J. *Prog. Inorg. Chem.* **1975**, *19*, 1.
(5) Levenson, R. A.; Gray, H. B. *J. Am. Chem. Soc.* **1975**, *97*, 6042.
(6) Wilson, R. B.; Solomon, E. I. *J. Am. Chem. Soc.* **1980**, *102*, 4085.
(7) (a) Ballhausen, C. J. "Introduction to Ligand Field Theory"; McGraw-Hill: New York, 1962. (b) Ballhausen, C. J. "Molecular Electronic Structures of Transition Metal Complexes"; McGraw-Hill: New York, 1979. (c) Figgis, B. N. "Introduction to Ligand Fields"; Wiley: New York, 1966. (d) Griffith, J. S. "The Theory of Transition Metal Ions"; Cambridge University Press: London, 1961.
(8) Hudson, A.; Lappert, M. F.; Nicholson, B. K. *J. Chem. Soc., Dalton Trans.* **1977**, 551.
(9) (a) Wrighton, M. S.; Bredesen, D. *J. Organomet. Chem.* **1973**, *50*, C35. (b) Wrighton, M. S.; Ginley, D. S. *J. Am. Chem. Soc.* **1975**, *97*, 2065.
(10) Wrighton, M. S.; Ginley, D. S. *J. Am. Chem. Soc.* **1975**, *97*, 4246.
(11) Waltz, W. L.; Hackelberg, O.; Dorfman, L. M.; Wojcicki, A. *J. Am. Chem. Soc.* **1978**, *100*, 7259.
(12) Meckstroth, W. M.; Walters, R. T.; Waltz, W. L.; Wojcicki, A.; Dorfman, L. M. *J. Am. Chem. Soc.* **1982**, *104*, 1842.
(13) Kidd, D. R.; Brown, T. L. *J. Am. Chem. Soc.* **1978**, *100*, 4095.
(14) Yesaka, H.; Kobayashi, T.; Yasufuku, K.; Nagakura, S. *J. Am. Chem. Soc.* **1983**, *105*, 6249.
(15) Caspar, J. V.; Meyer, T. J., unpublished results.
(16) Rothberg, L. J.; Cooper, N. J.; Peters, K. S.; Vaida, V. *J. Am. Chem. Soc.* **1982**, *104*, 3536.
(17) (a) Moore, B. D.; Simpson, M. B.; Poliakroff, M.; Turner, J. J. *J. Chem. Soc., Chem. Commun.* **1984**, 972. (b) Hermann, H.; Grevels, F.·W.; Henne, A.; Schaffner, K. *J. Phys. Chem.* **1982**, *86*, 5151. (c) Bridoux, M.; Delhaye, M. *Adv. Infrared Raman Spectrosc.* **1976**, *2*, Chapter 4. (d) Woodruff, W. H.; Farqharson, S. In "New Applications of Lasers in Chemistry"; Hieftje, G., Ed.; American Chemical Society: Washington, D.C., 1978.
(18) Laine, R. M.; Ford, P. C. *Inorg. Chem.* **1977**, *16*, 388.
(19) Fox, A.; Poë, A. *J. Am. Chem. Soc.* **1980**, *102*, 2497.
(20) Church, S. P.; Poliakoff, M.; Timney, J. A.; Turner, J. J. *J. Am. Chem. Soc.* **1981**, *103*, 7515.
(21) Hepp, A. F.; Wrighton, M. S. *J. Am. Chem. Soc.* **1983**, *105*, 5934.
(22) Hooker, R. H.; Mahmoud, K. A.; Rest, A. J. *J. Chem. Soc., Chem. Commun.* **1983**, 1022.
(23) Hooker, R. H.; Rest, A. J. *J. Organomet. Chem.* **1983**, *249*, 127.
(24) Hepp, A. F.; Blaha, J. P.; Lewis, C.; Wrighton, M. S. *Organometallics* **1984**, *3*, 174.
(25) (a) Bullitt, J. G.; Cotton, F. A.; Marks, T. J. *Inorg. Chem.* **1972**, *11*, 671. (b) Bullitt, J. G.; Cotton, F. A.; Marks, T. J. *J. Am. Chem. Soc.* **1970**, *92*, 2155.
(26) (a) Fischer, R. D.; Vogler, A.; Noack, K. *J. Organomet. Chem.* **1967**, *7*, 135. (b) Noack, K. *J. Organomet. Chem.* **1967**, *7*, 151.
(27) McArdle, P.; Manning, A. R. *J. Chem. Soc. A* **1970**, 2120.
(28) Abrahamson, H. B.; Palazotto, M. C.; Reichel, C. L.; Wrighton, M. S. *J. Am. Chem. Soc.* **1979**, *101*, 4123.
(29) Giannoti, C.; Merle, G. *J. Organomet. Chem.* **1976**, *105*, 97.
(30) Tyler, D. R.; Schmidt, M. A.; Gray, H. B. *J. Am. Chem. Soc.* **1979**, *101*, 2753.
(31) Tyler, D. R.; Schmidt, M. A.; Gray, H. B. *J. Am. Chem. Soc.* **1983**, *105*, 6018.
(32) Caspar, J. V.; Meyer, T. J. *J. Am. Chem. Soc.* **1980**, *102*, 7794.
(33) Haines, R. J.; duPreez, A. L. *Inorg. Chem.* **1969**, *8*, 1459.
(34) Hepp, A. F.; Wrighton, M. S. *J. Am. Chem. Soc.* **1981**, *103*, 1258.
(35) King, R. B.; Pannell, K. H. *Inorg. Chem.* **1968**, *7*, 2356.
(36) Stiegman, A. E.; Stieglitz, M.; Tyler, D. R. *J. Am. Chem. Soc.* **1983**, *105*, 6032.
(37) Haines, R. J.; Nyholm, R. S.; Stiddard, M. C. B. *J. Chem. Soc. A* **1968**, 43.
(38) Burkett, A. R.; Meyer, T. J.; Whitten, D. G. *J. Organomet. Chem.* **1974**, *67*, 67.
(39) Hughey, J. L.; Meyer, T. J. *Inorg. Chem.* **1975**, *14*, 947.
(40) Stiegman, A. E.; Tyler, D. R. *J. Am. Chem. Soc.*, in press.
(41) Allen, P. M.; Cox, A.; Kemp, T. J.; Sultana, Q.; Pitts, R. B. *J. Chem. Soc., Dalton Trans.* **1976**, 1189.
(42) Ginley, D. S.; Bock, C. R.; Wrighton, M. S. *Inorg. Chim. Acta* **1977**, *23*, 85.
(43) Ginley, D. S.; Wrighton, M. S. *J. Am. Chem. Soc.* **1975**, *97*, 4908.
(44) Hughey, J. L.; Bock, C. R.; Meyer, T. J. *J. Am. Chem. Soc.* **1975**, *97*, 4440.
(45) Hughey, J. L. Ph.D. Dissertation, University of North Carolina, Chapel Hill, 1975.
(46) Morgante, C. G.; Struve, N. S. *Chem. Phys. Lett.* **1980**, *69*, 56.
(47) McCullen, S. B.; Brown, T. L. *Inorg. Chem.* **1981**, *20*, 3528.
(48) Forbus, N. P.; Oteiza, R.; Smith, S. C.; Brown, T. L. *J. Organomet. Chem.* **1980**, *193*, C71.
(49) Absi-Halabi, M.; Brown, T. L. *J. Am. Chem. Soc.* **1977**, *99*, 2982.
(50) Stiegman, A. E.; Tyler, D. R. *J.Photochem.* **1984**, *24*, 311.
(51) Stiegman, A. E.; Tyler, D. R. *J. Am. Chem. Soc.* **1982**, *104*, 2944.
(52) Allen, D. M.; Cox, A.; Kemp, T. J.; Sultana, Q.; Pitts, R. B. *J. Chem. Soc., Dalton Trans.* **1976**, 1189.
(53) Hughey, J. L.; Anderson, C. P.; Meyer, T. J. *J. Organomet. Chem.* **1977**, *125*, C49.
(54) Wegman, R. W.; Olsen, R. J.; Gard, D. R.; Faulkner, L. R.; Brown, T. L. *J. Am. Chem. Soc.* **1981**, *103*, 6089.
(55) Walker, H. W.; Herrick, R. S.; Olsen, R. J.; Brown, T. L. *Inorg. Chem.*, in press.
(56) Huber, H.; Kundig, E. P.; Ozin, G. A. *J. Am. Chem. Soc.* **1974**, *96*, 5585.
(57) Haines, L. I. B.; Hopgood, D.; Poë, A. J. *J. Chem. Soc. A* **1968**, 421.
(58) Stiegman, A. E.; Tyler, D. R. *Inorg. Chem.* **1984**, *23*, 527.
(59) Byers, B. H.; Brown, T. L. *J. Am. Chem. Soc.* **1977**, *99*, 2527.
(60) Hoffman, N. W.; Brown, T. L. *Inorg. Chem.* **1978**, *100*, 4095.
(61) Poë, A. *Transition Met. Chem. (Weinheim, Ger.)* **1982**, *7*, 65 and references therein.
(62) Fox, A.; Malito, J.; Poë, A. *J. Chem. Soc., Chem. Commun.* **1981**, 1052.
(63) (a) Fawcett, J. P.; Jackson, R. A.; Poë, A. *J. Chem. Soc., Chem. Commun.* **1975**, 733. (b) Fawcett, J. P.; Jackson, R. A.; Poë, A. *J. Chem. Soc., Dalton Trans.* **1978**, 789.
(64) Herrick, R. S.; Herrington, T. R.; Walker, H. W.; Brown, T. L., submitted for publication in *Organometallics*.
(65) Shaik, S.; Hoffmann, R.; Fisel, C. R.; Summerville, R. H. *J. Am. Chem. Soc.* **1980**, *102*, 4555.
(66) Higginson, B. R.; Lloyd, D. R.; Evans, S.; Orchard, A. F. *Trans. Faraday Soc.* **1975**, 1913.
(67) Coulson, C. A.; Fischer, I. *Philos. Mag.* **1949**, *40*, 386.
(68) Tinkham, M. "Group Theory and Quantum Mechanics"; McGraw-Hill: New York, 1964; p 223.
(69) Junk, G. A.; Svec, H. J. *J. Chem. Soc. A* **1970**, 471.
(70) Freedman, A.; Bersohn, R. *J. Am. Chem. Soc.* **1978**, *100*, 4116.
(71) Mitschler, A.; Rees, B.; Lehmann, M. S. *J. Am. Chem. Soc.* **1978**, *102*, 3340.
(72) Jemmis, E. D.; Pinhas, A. R.; Hoffman, R. *J. Am. Chem. Soc.* **1980**, *102*, 2576.
(73) Benard, M. *Inorg. Chem.* **1979**, *18*, 2782.
(74) Bock, C. R.; Wrighton, M. S. *Inorg. Chem.* **1977**, *16*, 1309.
(75) Ferguson, J. A.; Meyer, T. J., *J. Am. Chem. Soc.* **1972**, *94*, 3409.
(76) Infelta, P. P.; Schuler, R. H. *J. Phys. Chem.* **1972**, *76*, 987.
(77) Malouf, G.; Ford, P. C. *J. Am. Chem. Soc.* **1977**, *99*, 7213.
(78) Malouf, G.; Ford, P. C. *J. Am. Chem. Soc.* **1974**, *96*, 601.
(79) Figard, J. E.; Petersen, J. D. *Inorg. Chem.* **1978**, *17*, 1059.
(80) Wrighton, M. S.; Abrahamson, H. B.; Morse, D. L. *J. Am. Chem. Soc.* **1976**, *98*, 4105.
(81) Wrighton, M. S.; Morse, D. L.; Gray, H. B.; Ottesen, D. K. *J. Am. Chem. Soc.* **1976**, *98*, 1111.
(82) Alway, D. G.; Barnett, K. W. *Adv. Chem. Ser.* **1978**, *168*, 115.
(83) Wrighton, M. S.; Morse, D. L. *J. Am. Chem. Soc.* **1974**, *96*, 998.
(84) Luong, J. Ph.D. Dissertation, M.I.T., Cambridge, 1981.
(85) Caspar, J. V.; Meyer, T. J. *J. Phys. Chem.* **1983**, *87*, 952.
(86) (a) Crosby, G. A. *Acc. Chem. Res.* **1975**, *8*, 231. (b) Meyer, T. J. *Prog. Inorg. Chem.* **1983**, *30*, 389.
(87) (a) Carlin, C. M.; DeArmond, M. K. *Chem. Phys. Lett.* **1982**, *89*, 297. (b) Hager, G. D.; Crosby, G. A. *J. Am. Chem. Soc.*

1975, 97, 7031. (c) Felix, F.; Ferguson, J.; Gudel, H. U.; Ludi, A. *J. Am. Chem. Soc.* **1980**, *102*, 4096. (d) Bradley, P. G.; Kress, N.; Hornberger, B. A.; Dallinger, R. F.; Woodruff, W. H. *J. Am. Chem. Soc.* **1981**, *103*, 744.

(88) (a) Kober, E. M.; Meyer, T. J. *Inorg. Chem.* **1982**, *21*, 371. (b) Ferguson, J.; Herren, F. *Chem. Phys. Lett.* **1982**, *89*, 371.

(89) (a) Caspar, J. V.; Kober, E. M.; Sullivan, B. P.; Meyer, T. J. *J. Am. Chem. Soc.* **1982**, *104*, 630. (b) Caspar, J. V.; Meyer, T. J. *Inorg. Chem.* **1983**, *22*, 2444.

(90) Morse, D. L.; Wrighton, M. S. *J. Am. Chem. Soc.* **1976**, *98*, 3931.

(91) (a) VanHouten, J.; Watts, R. J. *Inorg. Chem.* **1978**, *17*, 3381. (b) Durham, B.; Caspar, J. V.; Nagle, J. K.; Meyer, T. J. *J. Am. Chem. Soc.* **1982**, *104*, 4803.

(92) King, R. B.; Pannell, K. H. *Inorg. Chem.* **1968**, *7*, 2356.

(93) Adamson, A. W.; Waltz, W. L.; Zinato, E.; Watts, D. W.; Fleischauer, P. D.; Lindholm, R. D. *Chem. Rev.* **1968**, *68*, 541.

(94) Purcell, K. F.; Clark, S. F.; Petersen, J. D. *Inorg. Chem.* **1980**, *19*, 2183.

(95) Alexander, J. J.; Gray, H. B. *J. Am. Chem. Soc.* **1967**, *89*, 3356.

(96) McCullen, S. B.; Brown, T. L. *J. Am. Chem. Soc.* **1982**, *104*, 7496.

(97) Noyes, R. M. *Prog. React. Kinet.* **1961**, *1*, 129.

(98) Lorand, J. P., *Prog. Inorg. Chem.* **1972**, *17*, 203.

(99) (a) Abrahamson, H. B.; Wrighton, M. S. *Inorg. Chem.* **1978**, *17*, 1003. (b) Abrahamson, H. B.; Wrighton, M. S. *J. Am. Chem. Soc.* **1977**, *99*, 5510.

(100) Halpern, J.; Maher, J. P., *J. Am. Chem. Soc.* **1964**, *86*, 2311; **1965**, *87*, 5361.

(101) (a) Salem, L.; Leforestier, C.; Wetmore, R. *J. Am. Chem. Soc.* **1975**, *97*, 479. (b) Pullman, A.; Salem, L.; Veillard, A. In "Quantum Theory of Chemical Reactions"; Daudel, R., Ed.; Reidel: Dordrecht, 1979.

(102) (a) Brown, L. D.; Raymond, K. N.; Goldberg, S. B. *J. Am. Chem. Soc.* **1972**, *94*, 7664. (b) Simon, G. L.; Adamson, A. W.; Dahl, L. F. *J. Am. Chem. Soc.* **1972**, *74*, 7654.

(103) Sacco, A.; Freni, M. *Gazz. Chim. Ital.* **1959**, *89*, 1800.

(104) Kidd, D. R.; Cheng, C. P.; Brown, T. L. *J. Am. Chem. Soc.* **1978**, *100*, 4103.

(105) McCullen, S. B.; Walker, H. W.; Brown, T. L. *J. Am. Chem. Soc.* **1982**, *104*, 4007.

(106) Wender, I.; Sternberg, H. W.; Orchin, M. *J. Am. Chem. Soc.* **1952**, *74*, 1216.

(107) (a) Meyer, T. J. *Acc. Chem. Res.* **1978**, *11*, 1978. (b) Bock, C. R.; Connor, J. A.; Gutierrez, A. R.; Meyer, T. J.; Whitten, D. G.; Sullivan, B. P.; Nagle, J. K. *J. Am. Chem. Soc.* **1979**, *101*, 4815.

(108) (a) Kalyanasundaram, K. *Coord. Chem. Rev.* **1982**, *46*, 159. (b) Balzani, V.; Bolletta, F.; Gandolfi, M. T.; Maestri, M. *Top. Curr. Chem.* **1978**, *79*, 1.

(109) (a) Alberti, A.; Camaggi, C. M. *J. Organomet. Chem.* **1979**, *107*, 355. (b) Posimeni, L.; Zanonato, P. L.; Corvaja, C. *Inorg. Chim. Acta* **1979**, *37*, 241.

(110) Caspar, J. V.; Meyer, T. J., unpublished results.

(111) Volhardt, K. P. C.; Bercaw, J. E.; Bergman, R. G. *J. Organomet. Chem.* **1975**, *97*, 283.

(112) Commons, C. J.; Hoskins, B. F. *Aust. J. Chem.* **1975**, *28*, 1668.

(113) Curtis, M. D.; Han, K. R.; Butler, W. M. *Inorg. Chem.* **1980**, *19*, 2096.